Alma Mater Studiorum - Università di Bologna

DOTTORATO DI RICERCA IN

SCIENZE DELLA TERRA, DELLA VITA E DELL'AMBIENTE

Ciclo 34

Settore Concorsuale: 04/A3 - GEOLOGIA APPLICATA, GEOGRAFIA FISICA E GEOMORFOLOGIA

Settore Scientifico Disciplinare: GEO/05 - GEOLOGIA APPLICATA

TESTING THE EFFECTIVENESS OF PHYTOSCREENING TO MONITOR SHALLOW GROUNDWATER CONTAMINATION BY CHLORINATED ETHENES

Presentata da: Carlotta Leoncini

Coordinatore Dottorato

Maria Giovanna Belcastro

Supervisore

Alessandro Gargini

Co-supervisore

Juri Nascimbene

Maria Filippini

Esame finale anno 2022

ABSTRACT

The research presented herein aims to investigate the strengths and weaknesses of a relatively new technique called phytoscreening. Parallel to the well-known phytoremediation, it consists of exploiting the absorbing potential of trees to delineate groundwater contamination plumes, especially for chlorinated ethenes (i.e., PCE, TCE, 1,2-cis DCE, and VC). The latter are indeed prevalent contaminants in groundwater but their fate and transport in surface ecosystems, such as trees, are still poorly understood and subjected to high variability. Moreover, the analytical validity and trustability of tree-coring are still limited in many countries possibly due to a lack of knowledge of its application opportunities. Tree-cores are extracted from trunks and generally analyzed by gas chromatography/mass spectrometry. A systematic review of former literature on phytoscreening for chlorinated ethenes is presented in this PhD thesis to evaluate the factors influencing the effectiveness of the technique. Besides, we tested the technique by probing eight sites contaminated by chlorinated ethenes in Italy (Emilia-Romagna) in different hydrogeological and seasonal settings. We coupled the technique with the assessment of gaseous-phase concentrations directly on-site, inserting detector tubes or a photoionization detector in the tree-holes left by the coring tool. Finally, we applied rank order statistic analysis on our field data along with data retrieved from literature to assess under which conditions phytoscreening should be applied to either screen or monitor environmental contamination issues. A significant and relatively high correlation exists between tree-core and groundwater concentrations (Spearman's $\rho > 0.6$), being higher for compounds with higher sorption, for sites with shallower and thinner aquifers, and when sampling specific tree types with standardized sampling and extraction protocols. These results indicate the opportunities for assessing the occurrence, type, and concentration of solvents directly from the stem of trees. This can reduce the costs of characterization surveys, allowing rapid identification of hotspots and plume direction and thus optimizing the drilling of boreholes.

Key-words: phytoscreening, chlorinated ethenes, meta-analysis

ACKNOWLEDGEMENTS

During these crazy years, many people have crossed my path and every one of them has taught me something precious. Firstly, I would like to thank my academic advisor, Prof. Alessandro Gargini, for allowing me to dive into the academic world and for being there until the very end of this period, especially in the not-so-bright moments. A big “thank you” also goes to my co-advisors, Prof. Juri Nascimbene and Dr. Maria Filippini, who are wells of knowledge from which I extracted as much as I could. An immense thanks to all the ARPAE group, especially to Renata and Emanuela, who have literally always been there, on the field, in the mud, inside the thicker forests, under winter rains or heavy summer mugginess. Thanks also to Simona, our lab analyst, without whom nothing would have ever been discovered.

Thanks to my first mentees, Maxime and Sakinat, for tolerating my teaching style and showing gratitude anyway.

Unconditioned support came from my parents, and I will never thank them enough. They always showed appreciation and wonder for what I was doing, and this kept me focused and self-motivated on the gloomiest days. A huge “thank you” to my brother Jacopo and my sister-in-law Ester, because of their permanent positivity and their sunny and funny advice and support. A special thanks to my grandparents Mara and Fernando, whose memory, jokes, and recipes still live.

Thanks to my oldest friends, Gemma and Francesco, for following me in many adventures and long talks and for being my best buddies no matter what.

I will never forget these years in the red Bologna, not for the walls or the buildings, but for the people I met. Miriana with her lovely pessimism, Giulia and Elena with their incurable optimism. Leonardo for being the most amazing roommate. Matteo, Andrea, and Greta for being the craziest geologist in the world. Francesca, the most smiling person I know, and her kids for calling me auntie and being incredibly cute.

Finally, I thank Gabriele, for being such a wonderful friend, amazing partner, and relentless reviewer. Like a stone…

PREFACE

The research presented in this dissertation was carried out within the framework of a three-year Ph.D. scholarship funded by the *Alma Mater Studiorum* - Università di Bologna. The general aim of the project has been to address and test the effectiveness of phytoscreening, i.e., the use of trees as screening tools for underground contamination, specifically for chlorinated ethenes.

This short outline is meant to help the reader to navigate through the underpinning research questions discussed in the dissertation. The thesis starts with an Introduction (Chapter 1) to provide the rationale of the research, an overview of the relevant literature, the scientific background of the research along with the research goals. The bulk of this thesis consists of the comparison between data collected in one systematic review paper (Chapters 2) published in a relevant peer-reviewed international journal, and data collected on the field in eight contaminated sites (Chapter 3). The results of this comparison are then reported in terms of optimal conditions for the application of phytoscreening (Chapter 4). Conclusions are then made on the effectiveness of the technique to either screen for contamination in poorly investigated areas or monitor existing contamination (Chapter 5). As several chapters are meant as stand-alone contributions on related topics, there is some overlap among the different sections of this dissertation.

Through my Ph.D., I had the unique opportunity for developing and honing several skills, which include research project management, sampling design, field sampling, spatial and statistical analysis, team leading, mentoring, and scientific writing. Moreover, I was able to broaden my knowledge in several research topics, such as contaminant hydrogeology, plant physiology, plant taxonomy, phytoscreening measurements, laboratory analysis of solid samples, and univariate and bivariate statistics.

This work represents my research contribution which is compiled into five chapters. My advisors Alessandro Gargini, Juri Nascimbene, and Maria Filippini have provided guidance and focus during the development of this project. In the following, the main contents of each chapter are described along with the contributions that I benefited from.

Chapter 1. "Introduction" presents the scientific research background of phytoscreening explaining the basics of the sampling technique, the main application opportunities, and a discussion of the factors limiting the effectiveness of the results. A brief statement of the scope of this work is then presented through the clarification of the aspects considered to assess the quantification and detectability potential of phytoscreening.

Chapter 2. "Literature review" reports a review paper:

> Leoncini, C., Filippini, M., Nascimbene, J., Gargini, A., 2022. A quantitative review and meta-analysis on phytoscreening applied to aquifers contaminated by chlorinated ethenes. Sci. Total Environ. 817, 153005. doi.org/10.1016/j.scitotenv.2022.153005

that identifies, via a metanalysis of literature data, the major drivers of variability in tree-core concentration data. The conclusions of the paper reflect on the optimal conditions under which phytoscreening can be used to monitor contaminant plumes and screen for uninvestigated groundwater contaminations by chlorinated ethenes. The initiative for this research was taken by myself and conceptual modeling was achieved thanks to the co-authors Alessandro Gargini, Maria Filippini, and Juri Nascimbene that have provided useful suggestions for the improvement of the manuscript. Moreover, they contributed to discussing the results and provided careful editing of the manuscript. My contributions include data collection, analysis, manuscript writing and revision, and figure preparations and editing.

Chapter 3. "Fieldwork results" introduces the data collected on 8 contaminated sites in Emilia-Romagna (Italy). A concise overview of the hydrogeological settings of the sites is presented and the interpretation and discussion of the results follow. Concentration data were obtained through analyses of tree-cores via Gas Chromatography/Mass spectrometry and the use of colorimetric vials and a photoionization detector. This fieldwork is part of an agreement between the Department BiGeA (Biological, Geological, and Environmental Sciences) of the University of Bologna and the regional environmental authority (ARPAE - Agenzia Regionale Prevenzione Ambiente e Energia Emilia-Romagna). ARPAE granted access to the contaminated sites, participated in the field data collection, and run the chemical analysis on tree-core samples. Alongside fieldwork activities, my contribution stands in the interpretation and presentation of the results carried out with the supervision of my advisor and co-advisors. ARPAE's collaboration features Emanuela Fabbrizi, Renata Emiliani, and Giacomo Zaccanti in the fieldwork activities and Simona Gagni as lab analyst. At the end of this project, a report named "Guide-lines for phytoscreening application" will be developed together with the ARPAE group to effectively promote a standardized and practitioner-oriented use of this technique on contaminated sites in Italy.

Chapter 4. "Comparison between literature and field data" presents the similarities and the divergences that emerged from the analysis of data collected from the literature and our field investigations. A focus on the optimal conditions to apply phytoscreening is given in terms of using the technique to either screen a poorly investigated area or monitor the contaminant's fate and transport.

Chapter 5. "Conclusions" features the main results and conclusions of the research, such as its implications, and possible future research scenarios.

The Appendix (SM) include the supplementary materials related to chapter 2 and 3 and contains supplementary data which are useful to support the discussion in the main text. All references cited in the text are listed in the Reference list at the end of each Chapter.

CONTENTS

1
Introduction

1.1 Scientific background

Parallelly to the basic removal of contaminants by direct uptake and degradation (phytoremediation), the use of trees in hydrogeology as sentinels of the qualitative state of groundwater (gw) has been adopted for different applications and with various sampling protocols. From screening and monitoring concentrations for plume tracking or natural attenuation evaluation (e.g., Larsen et al., 2008) to assessing soil vapor intrusion up to the ground surface (e.g. Wilson et al., 2017), and date back contamination events with dendroecology (Balouet et al., 2007), phytoscreening demonstrated to be able to assess plume occurrence, area, magnitude, and average migration direction. Phytoscreening has been considered as an ecohydrogeological application (Cantonati et al., 2020) which is particularly scientifically attractive because probing and analysis protocols are time-saving and cost-effective.

Plant roots can carry contaminants dissolved in water through the xylem until the leaf sector. This transport is due to direct contact of the roots with groundwater (gw), capillary water, or soil water. Few studies demonstrated that the detection in trees could also be associated with soil gas contaminations (Algreen et al., 2015; Struckhoff et al., 2005; Wilson et al., 2017). In particular, Struckhoff et al. (2005) asserted that because vapor-phase volatile organic compounds (VOCs) and aqueous-phase VOCs in the subsurface are typically related through steady-state interactions and Henry's law, concentrations of contaminants in tree-cores, observed to be correlated to gw concentration, were likely related to vapor-phase concentrations, assumed to be in equilibrium with gw concentrations. Due to this statement and the general paucity of data on soil and soil gas

concentrations, this work is mainly focused on the correlation between tree-core and gw concentration.

Phytoscreening sampling consists of drilling micro-cores of mature tree stems with a tree-coring tool (FIGURE 1.1). The tree-coring tool consists of an increment borer and a core extractor. Increment borers are available in various lengths and diameters depending on the amount of desired drilling depth. Usually, an increment borer of 15 to 25 cm and a diameter of 0.45 cm are adopted for phytoscreening applications (Vroblesky, 2008). The core extractor consists of an aluminum tray, which is inserted in the hollow borer to extract the core from the tree. The tree tissue to be analyzed is generally the outer fringe of the trunk. The water transport indeed takes place inside the outermost tree rings (Ellmore and Ewers, 1986), thus tree-cores are generally less than 10 cm long (Holm & Rotard, 2011). The bark is removed to avoid atmospheric influence and since it is not involved in the transpiration flow (Algreen et al., 2015; Vroblesky, 2008).

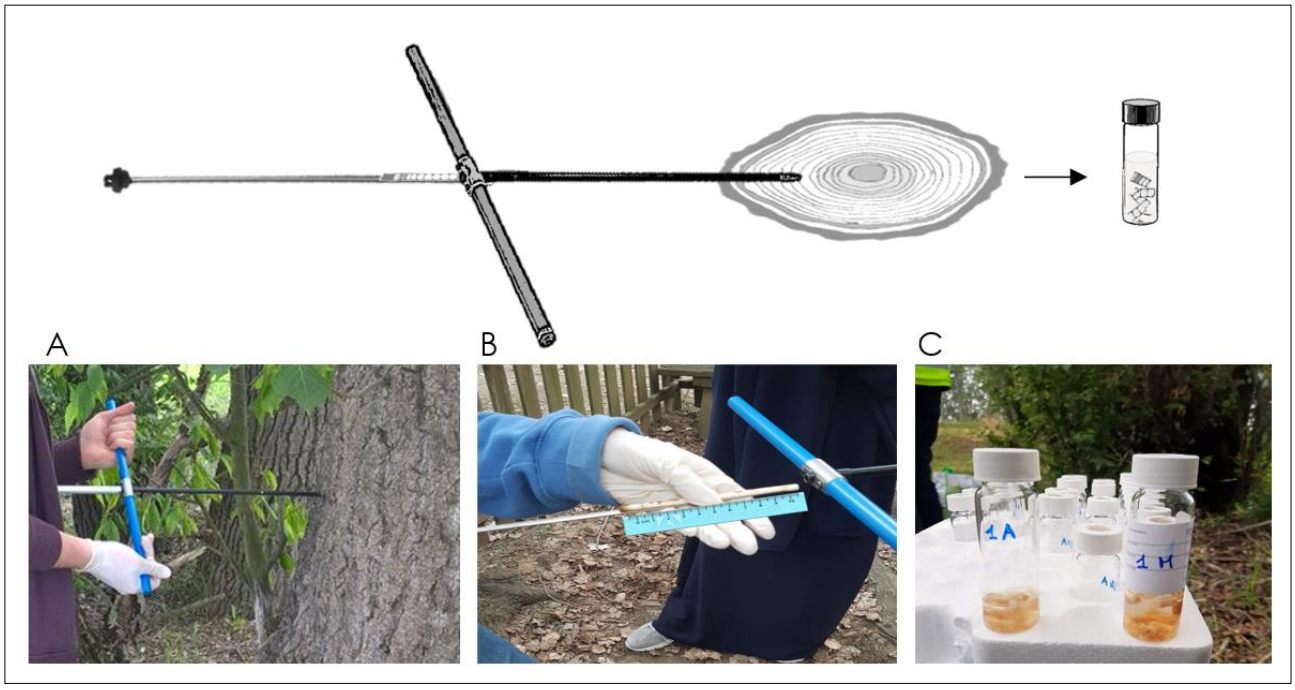

FIGURE 1.1. Process of drilling tree-cores (A) and extracting the sample (B), which is cut down and stored in 40 mL vials (C).

A few authors searched for volatile organic compounds (VOCs) also in different plant matrices: for example, Gopalakrishnan et al. (2011) and Duncan et al. (2017) detected chlorinated ethenes (CEs)

in tree branches and leaves albeit the results were poorly correlated with subsurface concentrations. Samples are placed in a vial and immediately capped to avoid volatilization loss of volatile compounds. The time used for extraction usually varies from 24 to 48 h before analysis (e.g., Vroblesky et al., 2004). The analysis is then conducted similarly to that used for soil or solid waste, in most cases through the application of Gas Chromatography followed by Mass Spectrometry (GC/MS; e.g., Rein et al., 2015).

Vroblesky et al. (1999) detected for the first time trichloroethene (TCE) and 1,2 cis-dichloroethene (cDCE) in tree-cores through headspace analysis of tree-cores. Subsequently, numerous researchers included also tetrachloroethene (PCE) among the detected compounds (Duncan et al., 2017; Larsen et al., 2008; Shetty et al., 2014). Later, Ottosen et al. (2018) detected for the first and unique time traces of Vinyl Chloride (VC) in tree-cores. Besides, phytoscreening was applied not only on CEs, but also for BTEX (e.g., Wilson et al., 2013), heavy metals (e.g., Algreen et al., 2014), and other organic compounds, although most of the studies focused on the comparison of CEs concentration in gw and tree-cores. Gw contamination by CEs was selected for our research too, due to their ubiquity, persistence, and toxicity at a global scale of these compounds. Also, CEs plumes characterization and monitoring are challenging in terms of technological and money efforts, thus the integration of a timesaving and cost-effective technique like phytoscreening could relevantly ease the assessment of contaminated sites conditions.

Numerous factors potentially affect the degree of correlation between CEs concentration in tree-core and gw. The physicochemical properties of CEs have been cited by many researchers as the main factor controlling the efficacy of phytoscreening as a robust method of contaminated sites' characterization. The slightly higher Henry's constant (H_c) of TCE compared to cDCE was hypothesized to be responsible for the higher loss of the first compound through the bark (Vroblesky et al., 1999). Baduru et al. (2008) stated that diffusional loss of VOCs from trees is inversely related to their molecular weight (M_w), with higher chlorinated compounds, such as PCE and TCE, having a lower tendency to diffuse compared to lower chlorinated DCE isomers and VC. Based on these

observations, Ottosen et al. (2018) sampled tree cores just above the terrain in the attempt of increasing the detectability of cDCE and VC, as characterized by the highest H_c and lowest M_w among CEs. However, they did not distinguish a clear advantage from this sampling strategy. Moreover, Larsen et al. (2008) found better correlations for cDCE compared to the ones for TCE and PCE. Trapp (2007) developed a mathematical model to predict the uptake of organic contaminants. He stated that the uptake process is regulated by partition coefficients among soil mineral phase, roots, and soil water with a key role played by the $\log K_{ow}$ (octanol-water partition coefficient): more hydrophobic compounds (higher $\log K_{ow}$) are less eager to be translocated in the tree transpiration stream due to their tendency of bounding to plant roots. On the other hand, Schnoor et al. (1995) found that very soluble and low retarded organic compounds are not absorbed by roots as much as lower solubility ones.

Besides the intrinsic properties of CEs, Duncan & Brusseau (2018) assessed for the first time how the depth to water table (DWT) could affect the correlation between VOCs concentration in tree tissues and gw (based on 100 measurements). They observed a higher correlation of samples from sites with a limited DWT, concluding that a low thickness of unsaturated zone, specifically when DWT was lower than 4 m below ground level (b.g.l.), does significantly affect phytoscreening effectiveness. To date, no other site-specific aquifer or groundwater parameters have been analyzed in terms of impacts on the degree of correlation between tree-core and gw concentration.

Furthermore, tree taxonomy was the main concern for most of previous studies (e.g. Duncan et al., 2017). Vroblesky et al. (2004), asserted that, within an individual tree species, higher gw concentrations can produce higher tree-core concentrations and that the uptake capacity of CEs by the tree depends on the genus. Trapp et al. (2007) stated that conifers are best suited for phytoscreening because they have a broad sapwood zone (the active portion of the stem), and transpire throughout the whole year, resulting in continuous uptake of groundwater. Different species indeed react differently to contamination because of different physiological mechanisms and sensitivity to toxins (Smith & Shortle, 1996). For example, the process of phytoaccumulation can fix

contaminants in tree tissues at much higher concentrations than the corresponding concentrations in soil or water (Balouet et al., 2007). Meanwhile, phytodegradation can take place inside the xylem (where the water flow takes place) or within the rhizosphere (Newman and Reynolds, 2004). All these mechanisms may also largely depend on the tree anatomy (xylem structure or tree diameter). In trees with ring-porous xylem, over 90 percent of water is transported in the outermost growth ring whereas in diffuse-porous and coniferous trees the water flow is more equally distributed among the xylem rings (Ellmore and Ewers, 1986). Several studies suggest that tree diameter has a little measurable effect on tree-core concentrations (Limmer & Burken, 2015; Wahyudi et al., 2012) while others demonstrated experimentally that diffusional loss in small trees (2 cm in diameter) occurs at a rate 10 times higher than in trees 15 cm in diameter (Schumacher et al., 2004; Struckhoff, 2003).

Concerning the sampling protocols, Vroblesky (2008) suggests that a core of 7-8 cm (not including the bark) is sufficient to detect VOCs. In ring-porous trees, the inclusion of the outermost growth ring is particularly important because it is where the transport takes place, while in non- and diffuse-porous trees the VOCs concentrations decrease from the inner to outer parts of the stem (xylem), possibly due to volatilization loss through the bark (Ma and Burken, 2003). Vroblesky (2008) also stated that a core collected near the ground usually provides higher VOCs concentrations than a core collected higher up the stem because of possible diffusional loss but, as stated before Ottosen et al. (2018) found no advantage in this evidence. Finally, several approaches to extract CEs from collected samples have been used: “dry” extraction (sample collected ‘as is’; e.g., Larsen et al., 2008), methanol extraction (e.g., Duncan et al., 2017), organic-free water extraction (e.g., Wittlingerova et al., 2013), Solid Phase Micro-Extraction (SPME) through the use of a fiber inserted in the residual tree-hole after the drilling (e.g., Holm & Rotard, 2011). To date, no major considerations were made above the differences among these extraction methods.

1.2 Research scope

The employment of plants in environmental hydrogeology has risen attention during the last decades in academic and non-academic research due to the abundance of application purposes. In order to give to this underused, green technique a valid and standardized application, it is necessary to define the main factors influencing the quality of the results. Most previous studies concluded that this technique is qualitatively reliable, but little has been done to assess which conditions limit the quantification of contaminants' concentration. The focus on the limitations was posed on the variety of parameters coming at stake when dealing with living organisms (trees) to signal the state of contamination of an environmental matrix (gw) with which plants are involved in a complex partitioning mechanism mediated by various chemical, biological, hydrological, and climatic factors. Some synthesis efforts were directed to outlining a practical and standardized field protocol based on the existing knowledge on phytoscreening (Vroblesky, 2008). Duncan & Brusseau (2018) evaluated 11 previous studies, focusing on the variability of correlation between gw and tree tissues concentrations associated with increasing DWT; Trapp (2007) proposed a complex theoretical model for the prediction of chemical uptake in trees. The model was based on more than 30 parameters, both hydrogeological and ecological, thus highlighting the complexity of quantitative phytoscreening.

Here, we provide a collection and discussion of literature and field data that aims to evaluate which factors affect the performance of the technique. To do so, we rely on the quantification of the correlation between gw and tree-core CEs concentrations and on the assessment of the detectability potential of each factor associated with the technique. Among these factors, we made inferences on the effect of 1) physicochemical properties of CEs, 2) hydrogeological features of the contaminated aquifer, 3) tree identity and anatomy, 4) methodological protocols, and 5) meteorological conditions. We present a systematic analysis of the factors that affect a) the correlation degree between CEs concentration in tree-cores and gw, and b) CEs detectability potential. The aim is to lead future users

to an easier and more accurate application and interpretation of the data collected with tree coring for indirect characterization of gw contaminations.

REFERENCES

Algreen, M., Trapp, S., Jensen, P.R., Broholm, M.M., 2015. Tree Coring as a Complement to Soil Gas Screening to Locate PCE and TCE Source Zones and Hot Spots. Groundw. Monit. Remediat. 35, 57–66. https://doi.org/10.1111/gwmr.12133

Algreen, M., Trapp, S., Rein, A., 2014. Phytoscreening and phytoextraction of heavy metals at Danish polluted sites using willow and poplar trees. Environ. Sci. Pollut. Res. 21, 8992–9001. https://doi.org/10.1007/s11356-013-2085-z

Baduru, K.K., Trapp, S., Burken, J.G., 2008. Direct measurement of VOC diffusivities in tree tissues: Impacts on tree-based phytoremediation and plant contamination. Environ. Sci. Technol. 42, 1268–1275. https://doi.org/10.1021/es071552l

Balouet, J.C., Oudijk, G., Smith, K.T., Petrisor, I., Grudd, H., Stocklassa, B., 2007. Applied dendroecology and environmental forensics. Characterizing and age dating environmental releases: Fundamentals and case studies. Environ. Forensics 8, 1–17. https://doi.org/10.1080/15275920601180487

Cantonati, M., Stevens, L.E., Segadelli, S., Springer, A.E., Goldscheider, N., Celico, F., Filippini, M., Ogata, K., Gargini, A., 2020. Ecohydrogeology: The interdisciplinary convergence needed to improve the study and stewardship of springs and other groundwater-dependent habitats, biota, and ecosystems. Ecol. Indic. 110. https://doi.org/10.1016/j.ecolind.2019.105803

Duncan, C.M., Brusseau, M.L., 2018. An assessment of correlations between chlorinated VOC concentrations in tree tissue and groundwater for phytoscreening applications. Sci. Total Environ. 616–617, 875–880. https://doi.org/10.1016/j.scitotenv.2017.10.235

Duncan, C.M., Mainhagu, J., Virgone, K., Ramírez, D.M., Brusseau, M.L., 2017. Application of phytoscreening to three hazardous waste sites in Arizona. Sci. Total Environ. 609, 951–955. https://doi.org/10.1016/j.scitotenv.2017.07.236

Ellmore, G.S., Ewers, F.W., 1986. Fluid flow in the outermost xylem increment of a ring-porous tree, ulmus americana. Am. J. Bot. 73, 1771–1774. https://doi.org/10.1002/j.1537-2197.1986.tb09709.x

Gopalakrishnan, G., Negri, M.C., Minsker, B.S., Werth, C.J., 2007. Monitoring Subsurface Contamination Using Tree Branches. Ground Water Monit. Remediat. 27, 65–74. https://doi.org/10.1111/j.1745-6592.2006.00124.x

Holm, O., Rotard, W., 2011. Effect of Radial Directional Dependences and Rainwater Influence on CVOC Concentrations in Tree Core and Birch Sap Samples Taken for Phytoscreening Using HS-SPME-GC/MS. Environ. Sci. Technol. 45, 9604–9610. https://doi.org/10.1021/es202014h

Larsen, M., Burken, J., Machackova, J., Karlson, U.G., Trapp, S., 2008. Using tree core samples to monitor natural attenuation and plume distribution after a PCE spill. Environ. Sci. Technol. 42, 1711–1717. https://doi.org/10.1021/es0717055

Limmer, M., Burken, J., 2015. Phytoscreening with SPME: Variability Analysis Article in. Int. J. Phytoremediation. https://doi.org/10.1080/15226514.2015.1045127

Ma, X., Burken, J.G., 2003. TCE diffusion to the atmosphere in phytoremediation applications. Environ. Sci. Technol. 37, 2534–2539. https://doi.org/10.1021/es026055d

Newman, L.A., Reynolds, C.M., 2004. Phytodegradation of organic compounds. Curr. Opin. Biotechnol. 15, 225–230. https://doi.org/10.1016/j.copbio.2004.04.006

Ottosen, C.B., Rønde, V., Trapp, S., Bjerg, P.L., Broholm, M.M., 2018. Phytoscreening for Vinyl Chloride in Groundwater Discharging to a Stream. Groundw. Monit. Remediat. 38, 66–74. https://doi.org/10.1111/gwmr.12253

Rein, A., Holm, O., Trapp, S., Popp-Hofmann, S., Bittens, M., Leven, C., Dietrich, P., 2015. Comparison of Phytoscreening and Direct-Push-Based Site Investigation at a Rural Megasite

Contaminated with Chlorinated Ethenes. Groundw. Monit. Remediat. 35, 45–56. https://doi.org/10.1111/gwmr.12122

Schumacher, J.G., Struckhoff, G.C., Burken, J.G., 2004. Assessment of subsurface chlorinated solvent contamination using tree cores at the front street site and a former dry cleaning facility at the Riverfront Superfund site, New Haven, Missouri, 1999-2003, U.S. Geological Survey Scientific Investigations Report 2004-5049. https://doi.org/https://doi.org/10.3133/sir20045049

Shetty, M.K., Limmer, M.A., Waltermire, K., Morrison, G.C., Burken, J.G., 2014. In planta passive sampling devices for assessing subsurface chlorinated solvents. Chemosphere 104, 149–154. https://doi.org/10.1016/j.chemosphere.2013.10.084

Smith, K.T., Shortle, W.C., 1996. Tree biology and dendrochemistry, in: Dean, J.S., Meko, M.D., Swetnam, T.. (Eds.), Tree Rings, Environment and Humanity. Radiocarbon Dept. of Geosciences University, pp. 629–635.

Struckhoff, G., 2003. Uptake of vapor phase PCE by plants: impacts to phytoremediation. Masters theses.

Struckhoff, G.C., Burken, J.G., Schumacher, J.G., 2005. Vapor-phase exchange of perchloroethene between soil and plants. Environ. Sci. Technol. 39, 1563–1568. https://doi.org/10.1021/es049411w

Trapp, S., 2007. Fruit tree model for uptake of organic compounds from soil and air. SAR QSAR Environ. Res. 18, 367–387. https://doi.org/10.1080/10629360701303693

Trapp, S., Larsen, M., Legind, C.N., Burken, J., Macháčková, J., 2007. A Guide to Vegetation Sampling for Screening of Subsurface Pollution, in: BIOTOOL Project GOCE 003998.

Vroblesky, D.A., 2008. User's Guide to the Collection and Analysis of Tree Cores to Assess the Distribution of Subsurface Volatile Organic Compounds, Scientific Investigations Report 2008–5088. U.S. Geological Survey. https://doi.org/https://doi.org/10.3133/sir20085088

Vroblesky, D.A., Clinton, B.D., Vose, J.M., Casey, C.C., Harvey, G.J., Bradley, P.M., 2004. Ground water chlorinated ethenes in tree trunks: Case studies, influence of recharge, and

potential degradation mechanism. Gr. Water Monit. Remediat. 24, 124–138. https://doi.org/10.1111/j.1745-6592.2004.tb01299.x

Vroblesky, D.A., Nietch, C.T., Morris, J.T., 1999. Chlorinated Ethenes from Groundwater in Tree Trunks. Environ. Sci. Technol. 33, 510–515. https://doi.org/10.1021/es980848b

Wahyudi, A., Bogaert, P., Trapp, S., MacHáčková, J., 2012. Pollutant plume delineation from tree core sampling using standardized ranks. Environ. Pollut. 162, 120–128. https://doi.org/10.1016/j.envpol.2011.11.010

Wilson, J., Bartz, R., Limmer, M., Burken, J., 2013. Plants as Bio-Indicators of Subsurface Conditions: Impact of Groundwater Level on BTEX Concentrations in Trees. Int. J. Phytoremediation 15, 257–267. https://doi.org/10.1080/15226514.2012.694499

Wilson, J.L., Samaranayake, V.A., Limmer, M.A., Schumacher, J.G., Burken, J.G., 2017. Contaminant Gradients in Trees: Directional Tree Coring Reveals Boundaries of Soil and Soil-Gas Contamination with Potential Applications in Vapor Intrusion Assessment. Environ. Sci. Technol. 51, 14055–14064. https://doi.org/10.1021/acs.est.7b03466

Wittlingerova, Z., Machackova, J., Petruzelkova, A., Trapp, S., Vlk, K., Zima, J., 2013. One-year measurements of chloroethenes in tree cores and groundwater at the SAP Mimoň Site, Northern Bohemia. Environ. Sci. Pollut. Res. 20, 834–847. https://doi.org/10.1007/s11356-012-1238-9

2

Literature review

A quantitative review and meta-analysis on phytoscreening applied to aquifers contaminated by chlorinated ethenes

Carlotta Leoncini[a], Maria Filippini[a], Juri Nascimbene[a], Alessandro Gargini[a]

[a]Department of Biological, Geological, and Environmental Sciences, Alma Mater Studiorum University of Bologna, via Zamboni 67, 40126 Bologna, Italy

Journal: Science of the Total Environment

Received at Editorial Office: 22 Oct 2021
Article revised: 3 Jan 2022
Article accepted for publication: 5 Jan 2022

GRAPHICAL ABSTRACT:

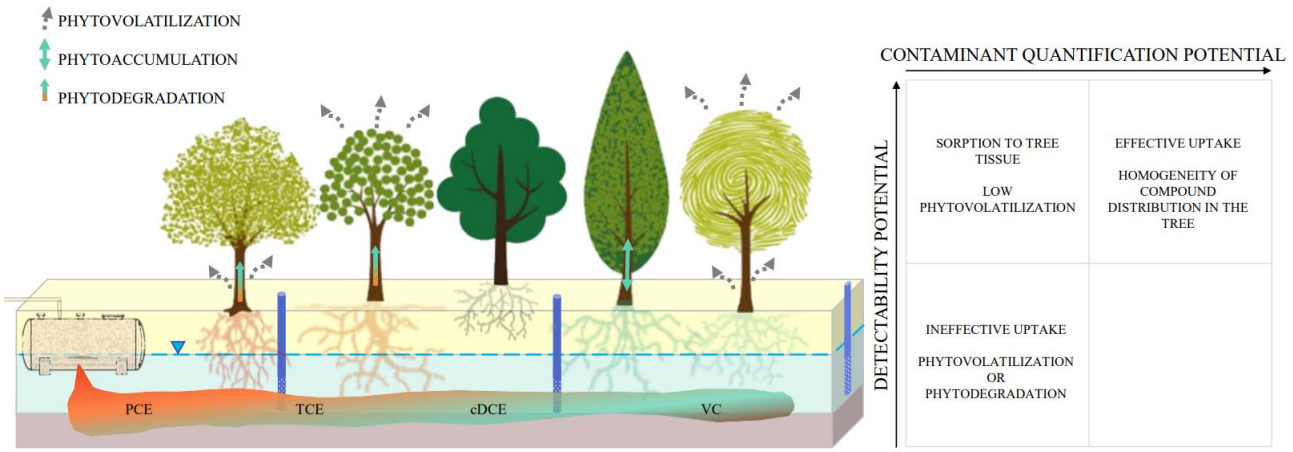

ABSTRACT

Applications and acceptance of phytoscreening, i.e., the use of trees as screening tools for underground contamination, are still limited in many countries due to the lack of awareness of application policies, the intrinsic qualitative nature of the technique, and the paucity of critical analyses on available data. To date, the conditions influencing the effectiveness of the technique have been descriptively discussed, yet rarely quantified. This review will contribute to filling this knowledge gap, shedding light on the most suitable approaches to apply phytoscreening. The focus was placed specifically on chlorinated ethene compounds since they are among the main organic contaminants in groundwater and have been the most studied in the field of phytoscreening. Chlorinated ethenes' behavior and biodegradation potential largely depend on their physicochemical properties as well as the hydrogeological features of the system in which they migrate. Besides, their fate and transport in surface ecosystems are still poorly understood. Here, phytoscreening data from sites contaminated by chlorinated ethenes were extracted from relevant literature to form a global-scale database. Data were statistically analyzed to identify the major drivers of variability in tree-cores concentration. Correlation between tree-core and groundwater concentration was quantified through Spearman's rank coefficients, whilst detectability potential was determined based on tree-cores showing non-detection of contaminants. The influence on such parameters of factors like contaminant properties, hydrogeology, tree features, and sampling/analytical protocols was assessed. Results suggest that factors controlling plant uptake and contaminant phytovolatilization regulate correlation and detectability, respectively. Conditions increasing the correlation (e.g., sites with shallow and permeable aquifers) are recommended for phytoscreening applications aimed at mapping and monitoring contaminant plumes, whereas conditions increasing detectability (e.g., sampling tree-cores near ground level) are recommended to preliminary screen underground contamination in poorly investigated areas.

KEYWORDS: groundwater**,** CEs**,** trees, quantitative phytoscreening

2.1. INTRODUCTION

Tree roots can carry contaminants dissolved in water through the trunk up to the leaves. This transport is based on direct contact of the roots with water inside the porous medium that surrounds the rhizosphere. Water can occur in different energy states: free moving gravity water in the saturated zone of the aquifer, referred to as groundwater (gw), or retention water (rw) subjected to suction and attached to soil particles as capillary or pellicular water in the unsaturated zone.

The use of plants in environmental hydrogeology has gained increasing attention during the last decades in academic research and consultant activity due to stimulating application perspectives. In parallel with contaminants removal by direct uptake and degradation (phytoremediation), Vroblesky et al. (1999) demonstrated for the first time that headspace analysis of tree-cores allows to delineate shallow gw contamination by chlorinated ethenes (CEs) such as trichloroethene (TCE) and cis 1,2-dichlorethene (cDCE). Later, Sorek et al. (2008) termed the technique "phytoscreening" and defined it as a simple, fast, non-invasive, and inexpensive screening for detecting subsurface contamination by volatile organic compounds (VOCs). Since Vroblesky et al. (1999), several comparisons between subsurface (soil, soil gas, and gw) and plant contamination were conducted, mostly by using tree-cores but also by using leaf and branch samples (e.g., Holm & Rotard, 2011; Wilcox & Johnson, 2016; Gopalakrishnan et al., 2007).

Besides screening and monitoring contaminant concentration for plume tracking or natural attenuation evaluation (e.g., Larsen et al., 2008), phytoscreening was used to assess soil vapor intrusions (e.g., Wilson et al., 2017; Algreen et al. 2015) and age-date contamination events through dendroecology (Balouet et al., 2007). Phytoscreening applicability was demonstrated for VOCs (e.g., BTEX; Wilson et al., 2013), perchlorate (e.g., Limmer et al., 2014), per- and polyfluoroalkyl substances (PFAS; Gobelius et al., 2017), or inorganic compounds like heavy metals (e.g., Algreen et al., 2014). However, CEs were the most frequent target in reported applications of phytoscreening. This review examines phytoscreening applications for CEs in groundwater, for which exist sufficient

literature information to conduct a quantitative meta-analysis. These compounds are indeed particularly responsive to uptake by plants, being relatively small and moderately hydrophobic (Burken & Schnoor, 1998). In addition to their persistence, ubiquity, and toxicity (Pankow & Cherry, 1996), characterization and monitoring of these plumes require advanced technologies and high funding, which could be mitigated by integrating a time-, and cost-effective technique like phytoscreening. The chance to determine the occurrence of subsurface volatile contaminants through trees is also important for evaluating the risks to human health such as potential ingestion and respiration from vapor intrusion into buildings, which are exposure pathways potentially associated with plant uptake. CEs detection in trees is affected by several contaminant-specific loss mechanisms (e.g., volatilization, phytodegradation) which may result in lower concentrations in plant tissues as compared to gw concentrations.

Phytoscreening of contaminated gw was considered a valuable ecohydrogeological application (Cantonati et al., 2020). However, it is necessary to identify the main factors that drive the correlation between gw and tree-core contaminant concentration as well as contaminants' detectability potential in trees in order to make this screening technique widely applicable and accepted. The correlation and detection capability can be maximized by providing directions on the standardization of sampling procedures. Several studies concluded that the technique is only qualitatively reliable due to the poor correlation observed between gw and tree-core concentration (Holm and Rotard, 2011; Larsen et al., 2008; Ottosen et al., 2018). This was attributed to multiple factors that come into play when dealing with living organisms (trees) to signal the state of contamination of an environmental matrix such as gw. Plants indeed interact with gw through complex partitioning mechanisms mediated by various chemical, biological, hydrological, and climatic factors. Synthesis efforts were directed to investigate the factors that limit the application opportunities of this technique. As a general example, Trapp (2007) proposed a theoretical model for the prediction of chemical uptake in trees based upon more than 30 parameters, either of hydrogeological or ecological nature, thus addressing the complexity of quantitative phytoscreening.

This paper provides a systematic review of former literature on the main factors that likely affect:

a) the correlation between CEs tree-core and gw concentration. Factors that determine higher correlations are favorable to apply phytoscreening to monitor, quantitatively, CEs contamination severity and degradation or natural attenuation processes.
b) the CEs detectability potential in trees. Factors that determine a lower number of contaminants non-detections in trees are favorable to preliminary screen for suspected underground contaminations by CEs in poorly investigated areas.

Several factors were selected and grouped as follows: 1) physicochemical properties of the contaminants (molecular weight, water solubility, volatility, partition coefficients); 2) hydrogeology (depth to water table, aquifer thickness, hydraulic conductivity); 3) tree identity and anatomy (genus and family, xylem structure, tree trunk diameter); 4) sampling and extraction methodology (height above ground of tree-core sampling, tree-core length, extraction method of the contaminants).

2.2. MATERIALS AND METHODS

2.2.1 Data source

A systematic search for relevant studies of phytoscreening on CEs was conducted in Scopus in January 2021. The search string was:

*TITLE-ABS-KEY (phytoscreening OR (tree AND groundwater AND (trichloroethene OR perchloroethene OR dichloroethene OR "chlorinated ethenes")))***.**

The first database search yielded 64 references. To form a global-scale database of phytoscreening data on CEs, only references containing datasets of contaminated sites that met the following criteria were selected: 1) sampling by tree trunk coring, 2) tree-core analysis of at least one compound among PCE, TCE, and cDCE, and 3) spatial proximity between a given tree and a borehole where gw

concentration analysis showed concentrations above detection limits (the distances between the locations of trees and boreholes varied from ~1 to ~10 m, or greater in few cases). When needed, we created contaminant concentration contour maps to supplement the reported gw concentration data. A total of 7 articles were identified reporting site datasets suitable for this study. The reference lists of these 7 articles were manually searched for further studies containing relevant datasets, providing 1 positive result (a technical report). Some of the final 8 selected documents contributed with more than one investigated site, providing information on a total of 11 sites. A total of 267 tree-core samples (and respective gw samples) were compiled in the global database, some of them reporting more than one compound concentration (TABLE 2.1).

The number of tree-core concentration data was 419 (see Supplementary material for the database), 118 being below the analytical detection limit (ND data hereafter). ND data represent a small fraction for most sites (below 15%; e.g., Struckhoff et al., 2005), whereas in a few sites they are almost the majority (e.g., Larsen et al., 2008; Cox, 2002). The observations above detection limits are distributed as follows: PCE - 43 observations, TCE - 194 observations, cDCE - 124 observations, and the sum of CEs - 58 observations related to one study that did not indicate single compound concentrations (Wittlingerova et al., 2013). No data were compiled for VC because only Ottosen et al. (2018) were able to detect traces of VC in trees under specific environmental conditions.

No spatial or temporal average concentrations were included in the database except for one site (Nogales site, Arizona; Duncan et al., 2017) in which only PCE average gw concentration (2 µg/L) was provided. This site was included in the database for its significance in terms of uniqueness: cores were sampled and extracted with methanol from trees of 4 different families inhabiting an arid environment with a deep aquifer table (9-10 m b.g.l.), showing PCE concentration up to 500 µg/kg.

Data on contaminant concentration in tree-core samples and gw samples were reported in two different types of units, i.e., mass/mass (typically µg/kg) and mass/volume (typically µg/L), respectively. No conversion was performed from the mass/mass unit to the mass/volume unit for tree-cores. This was considered acceptable since the focus was on the correlation between the

concentration in different matrices along with the detectability potential. The unfeasibility of the conversion is mostly due to the lack of information on sampled tree-core dry weights and volumes.

TABLE 2.1. References used for statistical analysis of the database: geographical location, number of tree-core samples, and correspondent detected compounds (Above Detection Limit: A.D.L.). Total number of data and Non-Detection% in the last columns.

Reference	Location	n° of tree-core samples	Contaminants A.D.L.	n° of data	ND %
Vroblesky et al. (1999)	Savannah River site (South Carolina, USA)	86	TCE, cDCE	179	40
Cox (2002)	Site SS-34N, McChord AFB (Washington, USA)	14	TCE	14	100
Vroblesky et al. (2004)	Carswell Golf Course (Texas, USA)	24	TCE	24	4
	Air Force Plant PJKS (Colorado, USA)	9	TCE	9	0
	Naval Weapons Station Charleston (South Carolina, USA)	10	TCE	10	0
Struckhoff & Burken (2005)	Front Street, Riverfront Superfund site (Missouri, USA)	20	PCE	20	15
Larsen et al. (2008)	North Bohemia Carcass Disposal Plant (Czech Republic)	17	PCE, TCE, cDCE	51	47
Holm & Rotard (2011)	Former military base Potsdam-Krampnitz (Germany)	23	TCE, cDCE	46	7
Wittlinglerova et al. (2013)	North Bohemia Carcass Disposal Plant (Czech Republic)	58	Sum of CEs	58	0
Duncan et al. (2017)	Nogales site (Arizona, USA)	4	PCE	4	0
	Park-Euclid (Arizona, USA)	1	PCE, TCE	2	0
	Motorola 52nd Street Superfund site (Arizona, USA)	1	TCE	2	50
8	*11*	*267*		*419*	*28*

Besides, wood-water partition coefficients of the contaminants would also be needed for a reliable conversion. Very few studies estimated the latter for a small number of tree species (e.g., poplars in Baduru et al., 2008). The lack of conversion hindered the possibility of performing multivariate statistical analyses. Due to this limitation, a meta-analysis of the influence of each factor was performed to analyze the database. It is worth noting that the results of this analysis will be subject to an intrinsic uncertainty associated with processing each factor as independent of one another. Information on the factors influencing the correlation between tree-cores and gw concentration as well as the potential for detectability in trees (i.e., the hydrogeological conditions of the underlying contaminated aquifers, tree identity and anatomy, and sampling and extraction protocols; TABLE 2.2) were retrieved from the 8 selected articles and associated to each of the 419 tree-core concentration data.

As for hydrogeological parameters, involving either the permeable porous medium (aquifer) or gw flowing inside it, we retrieved: depth to water table (DWT in m below ground level), intended as the distance between ground level and the surface at water pressure equal to atmospheric pressure (information retrieved for all the 419 tree concentration data); thickness of the saturated portion of the aquifer (b in m) intended as the distance between the water table and the low permeability bottom of the aquifer (retrieved for 235 out of 419 tree concentration); bulk saturated hydraulic conductivity of the aquifer (K in m/s; 373 out of 419 tree concentration). When K values of the aquifers were not specified (25% of the database), ranges of conductivities were inferred in agreement with the local description of the lithology (Freeze & Cherry, 1979).

With regards to tree identity and anatomy, we retained information on the genus (398 out of 419 data) and on the tree diameter at breast height (DBH in cm; 142 out of 419 data). Based on the genus, we retrieved the correspondent xylem structure, intended as the distribution of pores and vessels among growth rings. The xylem, or sapwood, is the active portion of the trunk where water transport takes place. We considered three xylem types: coniferous, diffuse-porous, and ring-porous (Panshin & de Zeeuw, 1970). Coniferous xylems are characterized by small cells used for water transport and

TABLE 2.2. Factors potentially affecting the effectiveness of phytoscreening of CEs in gw and relative descriptive statistics. Selected intervals, relative number of observations, and relative sites per interval.

Topic	Factors	Measuring unit	n° of available data (out of 419)	Min.	1st Quartile	Median	Mean	3rd quartile	Max.	Selected intervals	n° of observation per interval	n° of sites per interval
Hydrogeology	Depth to water table (DWT)	m b.g.l. (below ground level)	419	0.35	0.75	1	2.39	2.5	27	DWT<1, 1≤DWT<3, and DWT≥3	204, 138, and 77	3, 5, 9
	Average aquifer thickness (b)	m	235	0.9	3	3	3.29	4	6.6	b≤3.5, b>3.5	157 and 77	5, 4
	Aquifer hydraulic conductivity (K)	m/s	373	$4x10^{-6}$	$1x10^{-5}$	$1x10^{-5}$	$9x10^{-5}$	$1x10^{-4}$	$1x10^{-3}$	K<$1x10^{-5}$, K≥$1x10^{-5}$	189 and 184	2, 9
Tree identity and anatomy	Family	e.g., Salicaceae	398							Cupressaceae, Pinaceae, Salicaceae, Nyssaceae, Betulaceae, Altingiaceae, Fagaceae, Platanaceae, Ulmaceae, Rosaceae	112, 71, 62, 14, 68, 18, 45, 4, 3, 2	2, 6, 7, 1, 3, 1, 6, 1, 1, 1
	Xylem structure	e.g., coniferous	398							Coniferous/Diffuse-porous/Ring-porous	183,169, 46	6, 9, 6
	Tree diameter at breast height (DBH)	cm	142	11	24	25	31.96	36	102	DBH<25, 25≤DBH<40 cm, and DBH≥40 cm	51, 66, 24	3, 5, 2
Sampling and extraction methodology	Trunk drilling length (L)	cm	369	3.8	6	6.8	6.92	6.8	12.5	L≤6 and L>6 cm	123, 245	6, 5
	Sampling height (H)	cm a.g.l. (above ground level)	398	50	100	150	129.1	150	900	H<99, 99<H≤120, and H>120 cm a.g.l.	46, 123, 228	1, 3, 7
	Extraction method	e.g., methanol extraction	419							Dry/Water extraction/Methanol extraction/SPME	307, 8, 58, 46	7, 1, 3, 1

structural support. Diffuse-porous xylems additionally contain large vessels that are randomly distributed throughout the wood, while ring-porous xylems have larger diameter vessels concentrated in the earlywood. Conifers and diffuse-porous trees tend to have deep functional xylems as well as low average conductivity due to small and short conduits. In contrast, most of the conductance in ring-porous species is isolated to the outermost annual growth ring that contains functional vessels (Bush et al., 2010; Cermak et al., 1992).

When available, sampling and extraction protocols used to prepare tree-cores for analysis were retrieved: length of tree-core samples (L in cm; 369 out of 419 data), sampling height on the trunk (H in cm above ground level; 398 out of 419 data), and extraction method (419 out of 419 data) including extraction from dry vials (Cox, 2002; Larsen et al., 2008; Struckhoff et al., 2005; Vroblesky et al., 1999, 2004), vials containing organic-free water (Wittlingerova et al., 2013), or methanol solutions (Duncan et al., 2017), Solid Phase Micro-Extraction (SPME; Holm & Rotard, 2011).

2.2.2 Statistical meta-analysis

The correlation between gw and tree-core concentration was quantified by Spearman's rank coefficient ρ (Journel and Deutsch, 1997), a widely used approach for assessing the relationship between parameters when it is expected to be non-linear, as in highly skewed datasets. Indeed, both tree-core and gw concentrations represent highly skewed data sets, as regularly found in contaminated sites (Juang et al., 2001). As an example, tree-core concentrations had a distribution with positive skewness of 3.17, 8.21, and 6.85 for PCE, TCE, and cDCE, respectively. A useful property of ρ is that its value is invariant to any monotonic transformation applied to the data (e.g., logarithmic transformation). Outliers were not removed from the database due to the lack of knowledge about the uncertainty associated with the measurements. It is worth noting that ρ is insensitive to outliers, therefore representing a robust statistic tool for our database. The detectability potential of

contaminants in trees was quantified as the percentage of ND (ND%) data to the total number of observations.

Spearman's ρ and ND% were calculated separately for each compound (PCE, TCE, and cDCE) to assess the influence of contaminant-specific properties such as molecular weight (M_w), water solubility (S_w), Henry's constant (H_c), and octanol-water partition coefficient (log K_{ow}). In the case of the dataset of Wittlingerova et al. (2013) reporting only sums of CEs (PCE, TCE, cDCE, tDCE, 1,1-DCE, and VC), ρ and ND% were calculated on the sums.

Factors in TABLE 2.2 were then split into intervals and Spearman's ρ were derived for the concentration data within each interval. For continuous factors (e.g., aquifer properties or tree diameter), we determined discrete intervals based on medians and percentiles associated with each factor to have a similar number of observations within each interval. Only concentration data above detection limits were considered. In the case of discrete factors (e.g., tree species, extraction method), only values associated with a minimum of 10 observations were considered in the statistical analysis, except for one single case where only 8 observations were associated with extraction with methanol (Duncan et al., 2017). The ND% was determined within each of the aforementioned intervals to assess the influence of the different factors on detectability. To avoid biases associated with trees that could be growing above more dilute contamination areas, the ND% was calculated only when the concentration in gw was above 11 µg/L. This threshold was determined as the 5^{th} percentile of gw concentration data. The final number of ND data was 104 out of 118 ND tree-core data. It is noteworthy that in some cases, such as when processing hydrogeological parameters like b and K, results may be uncertain since some parameters do not vary spatially across a specific site.

Results were interpreted in terms of high or low correlations (determining optimal factors conditions to characterize the contamination) and high or low detectability potential (determining optimal factors conditions to screen gw contamination).

2.3. RESULTS AND DISCUSSION

2.3.1 Contaminant properties

The correlation between the concentration in tree-cores and gw was statistically meaningful (*p*-value ≤ 0.05) for all four series (PCE, TCE, cDCE, and the sum of CEs).

The ρ values indicate a low variability among CEs in terms of correlation between tree-core and gw concentration (FIGURE 2.1), with slightly lower values for higher chlorinated compounds PCE and TCE (ρ of 0.37 and 0.34, respectively) compared to the lower chlorinated cDCE (ρ of 0.41). On the other hand, ND% widely differed between higher chlorinated compounds PCE and TCE (12 and 23%, respectively) and cDCE (47%) with the first two performing better in terms of detectability potential. It is noteworthy that the highest correlation coefficient (0.63) and lowest ND% value (0%) were found for the sum of CEs (reported by Wittlingerova et al., 2013). This could be explained by contaminant transformation processes taking place either in the rhizosphere or in the xylem (Newman and Reynolds, 2004) that would negatively affect the correlation of single compounds. However, this result is associated with only one site.

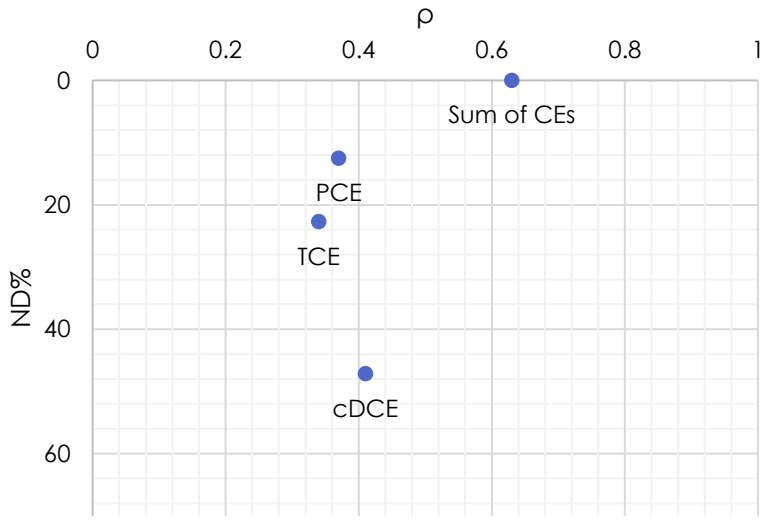

FIGURE 2.1. Spearman's ρ (x-axis) and ND% (y-axis, values in inverse order) of compounds series. Blank symbols refer to as *p*-values>0.05. Solid symbols refer to as *p*-values≤0.05

TABLE 2.3. Physico-chemical properties of the chlorinated ethenes: molecular weight (M_W), water solubility (S_w), Henry's constant (H_c), octanol-water partition coefficient (log K_{ow}). Derived from Mackay et al. (2006)

COMPOUND	M_w [g/mol]	S_w at 25°C [mg/L]	H_c [at 17.5°C] [adim.]	log K_{ow} [adim.]
PCE	165.8	206	0.492	3.40
TCE	131.3	1118	0.265	2.61
cDCE	96.9	3500	0.111	1.86
VC	62.4	2700	0.811	1.46

The physicochemical properties of CEs (TABLE 2.3) likely influence the behavior of each compound in trees. Larsen et al. (2008) observed a better correlation for cDCE compared to TCE and PCE which was attributed to the higher volatility (higher H_c) of the latter possibly causing a higher loss through the bark (Vroblesky et al., 1999). According to Limmer & Burken (2015), contaminant concentrations decreased with increasing volatility, due either to volatilization from the roots, bark, or subsurface. The results of our study are consistent with these findings, with PCE and TCE showing a slightly lower ρ compared to cDCE. In addition, the correlation potential of PCE and TCE may be hindered by their lower tendency to plant uptake compared to cDCE, driven by their higher M_w and K_{ow}, and lower S_w. Uptake from tree roots was indeed reported to be favored for compounds with low M_w due to their higher tendency to diffuse (Baduru et al., 2008), whereas higher S_w would possibly favor contaminant dissolution in water and consequent tree uptake. Besides, high sorption compounds (log K_{ow}>3) were reported to tend to be absorbed primarily by root surfaces, resulting in less translocation to the xylem (Schnoor et al., 1995). Similarly, a study by Dettenmaier et al. (2009) indicated that high-hydrophilic compounds are most likely absorbed by roots and transferred to the xylem. We may also assume that once in the xylem, higher log K_{ow} compounds likely tend to be absorbed by xylem tissues, resulting in a prolonged accumulation in the tree and thus a higher detectability potential. This could explain the higher detectability potential of PCE and TCE (lower ND%) compared to cDCE. Moreover, their higher H_c can aid the analytical detection when using headspace methods.

Concurrently, the lower log K_{ow} and M_w of cDCE may hinder accumulation and favor contaminant loss through the bark despite its low H_c (Baduru et al., 2008), resulting in an overall lower detectability potential. The extremely rare detection of VC confirms the role of H_c, $M_{w,}$ and log K_{ow} in contaminant detectability in trees.

2.3.2 Hydrogeology and aquifer parameters

Three intervals were considered for DWT: DWT < 1, 1 ≤ DWT < 3, and DWT ≥ 3 m b.g.l.

Concentration data show a statistically significant correlation value (*p*-value ≤ 0.05; FIGURE 2.2) in the three cases. A slightly decreasing correlation with increasing DWT was observed (ρ=0.63, 0.54, and 0.52 for DWT < 1, 1 ≤ DWT < 3, and DWT ≥ 3 m b.g.l., respectively). On the other hand, the shallow interval showed the higher ND% (35%) whereas the inferior intervals had significantly lower ND% (16% and 17% for the medium and deep interval, respectively). Duncan & Brusseau (2018) assessed for the first time how DWT could affect the correlation between VOCs concentration in tree tissues and gw (based on 100 measurements). They observed a higher correlation in samples from sites with a DWT<4 m, concluding that a low thickness of the unsaturated zone significantly affects phytoscreening efficiency. Despite the overall consistency of our results with the cited literature (decreasing ρ with increasing DWT), ρ shows small differences among DWT intervals, suggesting a low influence of this factor on the degree of correlation. The difference with Duncan & Brusseau (2018) may lie in the use of different correlation coefficients and interval divisions. In our analysis ρ was chosen due to the non-linear distribution of the concentration dataset while Duncan & Brusseau (2018) assessed the correlation through Pearson's coefficient (r^2) thus assuming linearity of the dataset. Besides, at sites with a more substantial vadose zone, mineralization of CEs can occur before translocation of the contaminant in the tree due to more hypoxic conditions (Bradley & Chapelle, 2011), leading to lower correlation potential for deeper aquifers. Similar findings have been reported by Wilson et al. (2013) for BTEX translocation in trees. At the same time, when DWT is lower, volatilization loss of CEs is promoted at the interface between the saturated and the vadose zone,

being the thickness and water content of the latter more subject to atmospheric variations (Pankow & Cherry, 1996). As tree roots are usually located at this interface, the enhanced volatilization of CEs could decrease their detectability potential (higher ND% for the shallow interval).

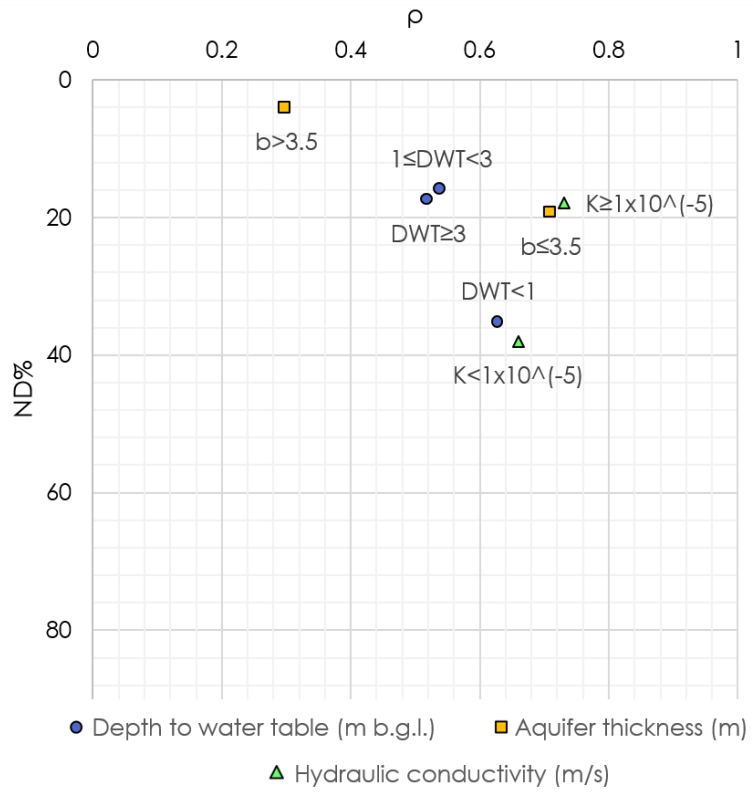

FIGURE 2.2. Spearman's ρ (x-axis) and ND% (y-axis, values in inverse order) of each interval considered for the hydrogeological parameters. Blank symbols refer to as *p*-values>0.05. Solid symbols refer to as *p*-values≤0.05

Aquifer thicknesses were clustered into two intervals: b ≤ 3.5 and b > 3.5 m. Data associated with lower b show a very high positive correlation (ρ = 0.71), whereas those associated with higher b have a significantly weaker correlation (ρ = 0.30). This may be because CEs, in the majority of contaminant events, enter the subsoil as dense non-aqueous phase liquids (DNAPLs), which tend to sink towards deeper sections of the aquifer, thus influencing the shape of dissolved contaminant plumes (e.g., Parker et al., 2003). In particular, the sinking of CEs could result in an increased distance of the dissolved contaminant plume from the root zone in thicker aquifers. Notably, aquifer thickness appears to have the highest influence on correlation compared to other factors. On the other hand, a

lower ND% is associated with the thicker aquifer interval compared to the thinner interval (4% and 19% for b > 3.5 m and b ≤ 3.5 m, respectively). This result has poor validations: we can speculate that thin aquifers have a lower geometrical probability of being intercepted by tree roots than thick ones.

Two intervals of K were considered: $K < 1x10^{-5}$ and $K \geq 1x10^{-5}$ m/s. Concentrations referred to higher K values show a slightly higher correlation ($\rho = 0.73$) compared to those referred to lower conductivities ($\rho = 0.66$). These results suggest that K poorly affects the correlation between tree-core and gw concentration. On the other hand, the lower K interval includes 38% of ND whereas the higher K interval includes 18%. More permeable aquifers are therefore more suited in terms of detectability potential. A relatively higher permeability can indeed enhance the mobility of contaminants in the subsoil, likely favoring plant uptake, similarly to what happens when extracting gw from wells or soil gas from soil gas probes.

2.3.3 Tree identity and anatomy

The 22 tree genera of our database were clustered by families and xylem structures.

Results show a significant positive correlation with most families (FIGURE 2.3), with ρ being highest for coniferous, i.e., Pinaceae ($\rho = 0.86$) and Cupressaceae ($\rho = 0.66$). These conifers also have moderately low ND% (24% and 30%, for Pinaceae and Cupressaceae, respectively). Consistently with our observations, Trapp et al. (2007) stated that conifers are best suited for phytoscreening because they have a broad xylem zone, and transpire throughout the whole year, resulting in a continuous uptake of gw. Ring-porous Fagaceae (primarily *Quercus)* presented a slightly positive correlation ($\rho = 0.39$) and a high ND% (57%). The ring-porous structure likely promotes volatilization loss through the bark, possibly affecting the observed low correlation and detectability potential. Indeed, over 90% of water is transported in the outermost growth ring in ring-porous trees whereas in diffuse-porous and coniferous trees water flow is more equally distributed among rings (Ellmore

and Ewers, 1986). Diffuse-porous Nyssaceae and Betulaceae show a slightly lower ρ compared to conifers (0.74 and 0.65, respectively), and a low ND% (29 and 25%, respectively) although results for Nyssaceae must be taken with caution because they refer to one single study site (Savannah River Site, USA; Vroblesky et al., 1999) where the aquifer was shallow (DWT<1 m b.g.l.). On the other hand, diffuse-porous Salicaceae and Altingiaceae do not show a significant correlation (p-value > 0.05) and highly fluctuating ND% (very low for Salicaceae – 3% and very high for Altingiaceae – 64%). The high variability among diffuse-porous families in terms of ρ and ND% could be associated with different arrangements and sizes of the vessels regulating the conductivity of the xylem, which in turn can also vary with age. For example, Salicaceae (*Salix* and *Populus*), widely used in phytoscreening and phytoremediation due to their fast growth, high uptake rates, and widespread occurrence in temperate climates, showed the highest detectability potential although no correlation between tree-core and gw concentration. Besides, Negri et al. (2003) stated that Salicaceae are genetically predisposed to develop roots extending to the water table at depths greater than 12 m b.g.l., thereby widening their detectability potential to deep aquifers. Altingiaceae (*Liquidambar*; present only in the study of Vroblesky et al., 1999) also showed no correlation whilst a low detectability potential. This family was studied by Strycharz and Newman (2009) in a greenhouse experiment where also Platanaceae and Salicaceae were involved. Results showed that among the 3 families, Altingiaceae was the less recommended for phytoremediation activities. Other diffuse-porous, like Betulaceae (*Alnus* and *Betula*), showed instead a correlation and detectability potential comparable to conifers. Lewis et al. (2015) calculated that *Betula pendula* can accumulate similar amounts of TCE as *Populus* trees due to its lack of heartwood (nonfunctioning xylem) and homogeneous xylem flow (Westhoff et al., 2008), making this species a suitable candidate for phytoremediation and phytoscreening activities. Eventually, the low number of Platanaceae (diffuse-porous), Ulmaceae (ring-porous), and Rosaceae (diffuse-porous) in the database (TABLE 2.2) hindered an analysis on these families. Even so, Limmer & Burken (2015) showed that the genus *Platanus* (Platanaceae) had a high detectability potential, especially for PCE gw contamination, if compared to

non-*Platanus* trees. Their result was although associated with *Platanus* trees growing in areas with shallow gw. Conversely, our data on Platanaceae showed that 3 out of 4 times this family did not detect contaminants even with shallow gw (DWT<1 m b.g.l.; Savannah River Site, USA; Vroblesky et al., 1999) albeit in that particular site aquifer K was low ($5.3x10^{-6}$ m/s). Yung et al. (2017) pointed out that besides *Populus* and *Salix* (Salicaceae, diffuse-porous) and *Betula* (Betulaceae, diffuse-porous), *Quercus and Ulmus* (Fagaceae and Ulmaceae, both ring-porous) are also efficient biomonitors of PCE and TCE contamination. Notwithstanding the contrast with our results on Fagaceae, the 2 Ulmaceae trees in our database (Carswell Golf Course, USA; Vroblesky et al., 2004) showed TCE concentrations above detection limits, with DWT at 1 to 5 m b.g.l., aquifer K of $7x10^{-5}$ m/s, and b of 0.9 m. This may suggest that even among ring-porous trees a great variability in concentration results is expected.

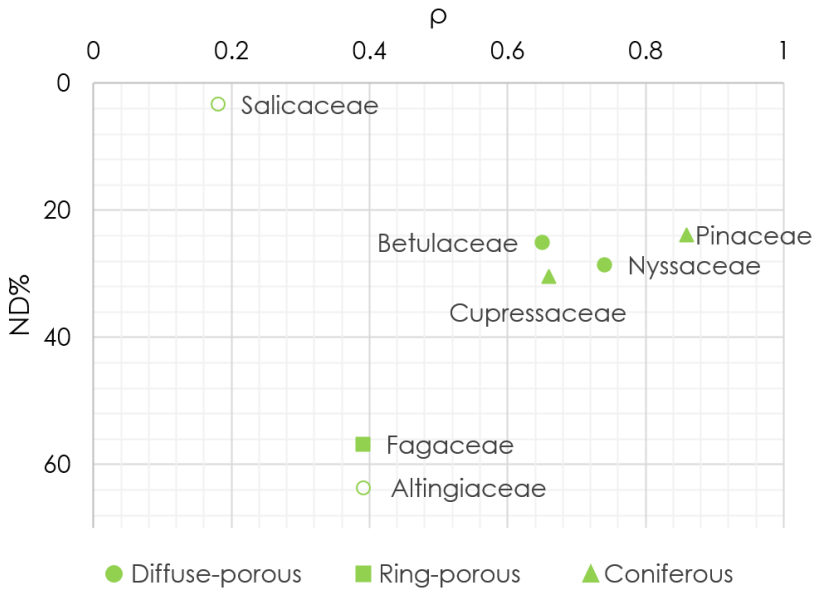

FIGURE 2.3. Spearman's ρ (x-axis) and ND% (y-axis, values in inverse order) of each family and correspondent xylem structure. Blank symbols refer to as *p*-values>0.05. Solid symbols refer to as *p*-values≤0.05

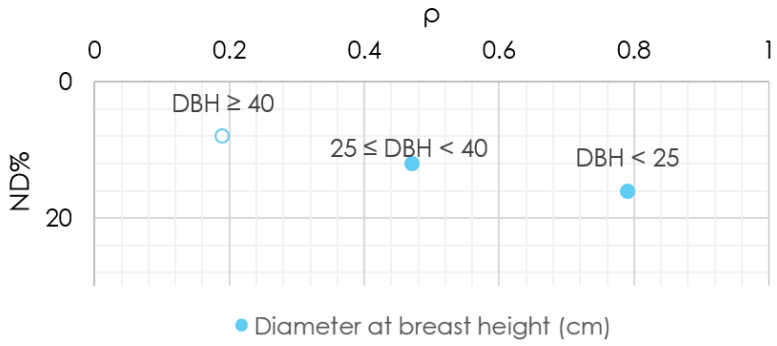

FIGURE 2.4. Spearman's ρ (x-axis) and ND% (y-axis, values in inverse order) of each interval considered for tree diameters. Blank symbols refer to as *p*-values>0.05. Solid symbols refer to as *p*-values≤0.05

Tree size (measured as DBH) in our database ranges between 18 and 102 cm and values were split into 3 intervals: DBH < 25, 25 ≤ DBH<40, and DBH ≥ 40 cm (FIGURE 2.4). Since data were filled only for 34% of the database (TABLE 2.2), results must be considered with caution. The lower interval shows a high positive correlation (ρ = 0.79). The correlation decreases significantly in the medium interval (ρ = 0.47). The higher interval shows no significant correlation (*p*-value > 0.05). ND% is instead comparable among DBH intervals (10%, 8%, and 8%, respectively for DBH < 25, 25 ≤ DBH < 40, and DBH ≥ 40 cm). Several studies suggest that tree size has little effect on tree-core concentration (Limmer & Burken, 2015; Wahyudi et al., 2012) while other studies demonstrated that diffusional loss in small trees (DBH of 2 cm) occurs at a rate 10 times higher than in trees with DBH 15 cm due to their greater surface area to volume ratio that more quickly depletes the compound reservoir in the trunk (Schumacher et al., 2004; Struckhoff, 2003). This could explain the slightly higher ND% of smaller trees. In contrast, our results show that smaller trees have greater efficiency in terms of quantitative analysis of gw contamination (high ρ). In smaller trees, we could indeed expect less variability in concentration around and across the trunk due to a less compartmentalized flow in the xylem. Also, in smaller trees it is highly probable to sample a consistent thickness of the total xylem, resulting in a concentration that averages the radial variability. More variability is instead

observed in larger trees where sampling direction has a strong influence on the concentration, thus influencing the correlation.

2.3.4 Sampling and analysis protocols

In our database tree-core L ranges from 3.8 to 12.5 cm and was clustered into two intervals: $L \leq 6$ and $L > 6$ cm (FIGURE 2.5). Shorter cores do not show a significant correlation between tree-core and gw concentration (p-value > 0.05) whereas longer cores have a high positive correlation ($\rho = 0.71$). This result agrees with Ma & Burken (2003) and the USGS user guide published by Vroblesky (2008), which suggest a better correlation when the core samples are longer than ~ 7-8 cm. Shorter cores may be also acceptable for ring-porous trees, in which water transport takes place mostly in the outermost ring (Ellmore and Ewers, 1986). The detectability potential is lower for the higher L interval (ND of 11% and 30% for $L \leq 6$ and $L > 6$ cm, respectively), likely indicating that drilling longer tree-cores could promote diffusional loss out of the sample since sampling requires relatively longer periods (tree-cores are usually cut in small pieces before being put in the vials).

Sampling H from the base of the trunk ranges between 50 and 900 cm a.g.l. and was clustered into three intervals: $H < 99$, $99 < H \leq 120$, and $H > 120$ cm a.g.l. The medium interval shows a very high correlation between tree-core and gw concentration ($\rho = 0.84$), which decreases for higher H ($\rho = 0.42$). The lower interval shows no significant correlation (p-value > 0.05) although the data pertain to only one survey by Holm & Rotard (2011). The reason for the high ρ value at medium H is still unknown. We can speculate that this is related to the attainment of an equilibrium of the contaminant inside the wood-air-water partitioning system. On the other hand, a low ND% was registered for the lower H interval (7%) whereas the higher intervals are associated with higher ND% (24% and 33% for the medium and higher H interval, respectively). This result is consistent with the experiments of Ma & Burken (2003) where a higher TCE loss was observed higher up the trunk. Thus, a lower rate of diffusional loss from the bark may be expected for the lower H intervals. On the other hand, Ottosen

et al. (2018) sampled tree-cores just above the ground surface without distinguishing a clear advantage from this sampling strategy.

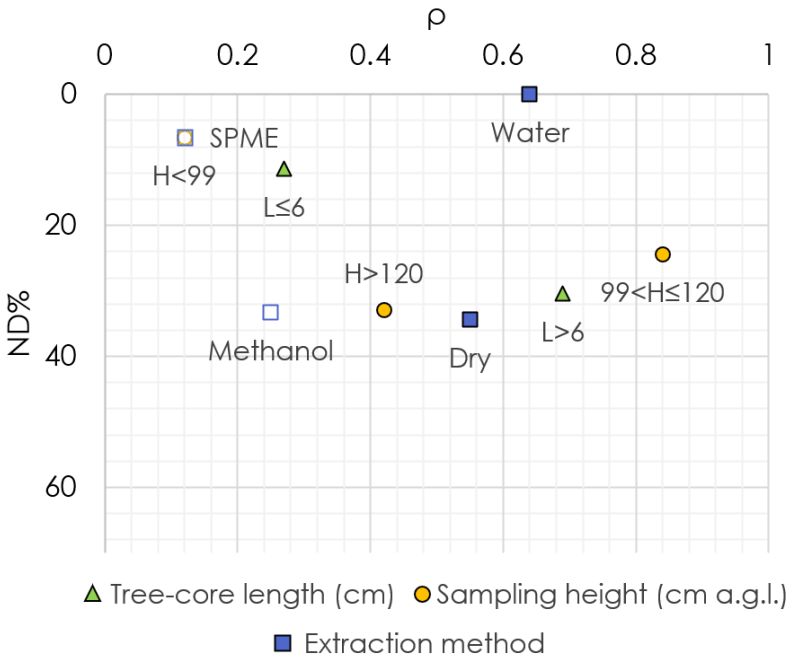

FIGURE 2.5. Spearman's ρ (x-axis) and ND% (y-axis, values in inverse order) of each interval considered for sampling and analysis protocols. Blank symbols refer to as *p*-values>0.05. Solid symbols refer to as *p*-values≤0.05

Our database includes 4 extraction methods used for analysis (dry sample, organic-free water, methanol solution, and SPME). The dry and the water extracted samples showed moderately high correlation ($\rho = 0.55$ and $\rho = 0.64$ for dry and water extraction, respectively). However, data from water extracted samples pertain to only one survey where concentration data relate to the sum of CEs (Wittlingerova et al., 2013). The high ρ could be associated either with the extraction method or with the fact that the sum of CEs was considered (see SECTION 2.3.1). Methanol extracted samples, related to the study cases of Duncan et al. (2017), were collected with unfavorable conditions in arid-hot environments (Nogales site, Park-Euclid, and Motorola 52nd superfund site in Arizona, USA). The small number of tree-cores (8) sampled with this method may explain the observed non-significant correlation value (*p*-value > 0.05). Tree-core concentrations associated with arid environments are possibly more a function of vadose zone vapor phase concentration than gw concentration since roots

would unlikely reach DWT of 26 m b.g.l. as in the case of the Park-Euclid site. The fact that 5 out of 8 tree-core concentrations of were higher than 300 µg/kg despite being associated with low gw concentrations of PCE (2 µg/L, i.e., lower than the gw concentration threshold defined for ND% calculation; See SECTION 2.2.2) further supports the hypothesis that trees were absorbing contaminants from a matrix other than gw. This may have hindered correlation with gw in the case of methanol extraction. The analysis following SPME, associated with only one site (Potsdam-Krampnitz military base, Germany; Holm & Rotard, 2011), also showed no significant correlation (p-value > 0.05). Even so, the ND% was very low for SPME (7%) as well as water extracted samples (0%). However, since these methods were used in single study cases, these results may be related to other site-specific conditions or sampling protocols. In terms of ND%, the dry and methanol extraction produced comparable results (34%, and 33% for dry and methanol extraction, respectively).

2.4. SUMMARY AND CONCLUSIONS

The effectiveness of phytoscreening has been assessed via a meta-analysis of literature data to determine the potential of trees to a) monitor groundwater plumes of CEs, expressed as the degree of correlation between tree-core and gw concentration, and b) detect the occurrence of gw contamination events by CEs in poorly investigated areas, expressed as the rate of tree-cores that showed concentrations above the detection limit in significantly contaminated areas. Several factors likely influencing correlation and detectability were considered. These factors included physicochemical properties of CEs, hydrogeological conditions of the underlying contaminated aquifers, trees identity and anatomy, and sampling and extraction protocols.

The correlation (quantitative monitoring potential) is higher when the hydrogeological dynamics favor direct uptake of contaminated water and the concentration is homogeneously distributed in the tree and the tree-core sample. Direct tree uptake is favored for the lighter and more soluble cDCE and in the case of shallow (DWT<3 m b.g.l.), thin (b<3.5 m), and permeable aquifers ($K \geq 1x10^{-5}$ m/s).

The homogeneity of concentration in the xylem is higher for Pinaceae and Cupressaceae (conifers), due to their non-porous xylem, and for smaller diameter trees (DBH<25 cm) whereas homogeneity of concentration in the tree-core is enhanced when sampling longer tree-cores (L>6 cm) and at a height on the trunk between $99 < H \leq 120$ cm a.g.l.

The detectability (qualitative screening potential) is higher when factor conditions favor accumulation in the xylem and hinder volatilization loss through the bark. In these terms, PCE and TCE are more suited compared to cDCE due to their higher sorption and weight. Low volatilization loss was also inferred in the case of large-diameter trees (DBH≥40 cm), at a low height on the trunk (H<99 cm a.g.l.), and for shorter cores due to reduced time of sampling (L≤6 cm). In the case of Salicaceae, high uptake rates may compensate for volatilization losses, thus increasing detectability. Finally, the process of contaminant extraction appears to be maximized when using organic-free water extraction and SPME.

Despite the clarifications provided by our meta-analysis, several factors influencing phytoscreening effectiveness remain unexplored at a global scale as in the case of 1) climatic and meteorological conditions affecting uptake and loss from the tree; 2) porosity and volumetric water content of the unsaturated zone influencing uptake and volatilization loss at the ground surface; 3) organic content in saturated and unsaturated layers influencing sorption of CEs to the solid matrix; 4) phytodegradation processes that may hinder correlation with CEs concentration in gw; 5) radial distance to boreholes likely affecting correlation between tree-core and gw concentration. It is therefore necessary to conduct additional research in these areas to improve the applicability of the technique.

ACKNOWLEDGMENTS

We would like to thank the Reviewers and Editor for taking the time and effort necessary to review the manuscript. We sincerely appreciate all valuable comments and suggestions, which helped us to

improve the quality of the manuscript. This research did not receive any specific grant from funding agencies in the public, commercial, or not-for-profit sectors.

REFERENCES

Algreen, M., Trapp, S., Rein, A., 2014. Phytoscreening and phytoextraction of heavy metals at Danish polluted sites using willow and poplar trees. Environ. Sci. Pollut. Res. 21, 8992–9001. https://doi.org/10.1007/s11356-013-2085-z

Algreen, M., Trapp, S., Jensen, P.R., Broholm, M.M., 2015. Tree Coring as a Complement to Soil Gas Screening to Locate PCE and TCE Source Zones and Hot Spots. Groundw. Monit. Remediat. 35, 57–66. https://doi.org/10.1111/gwmr.12133

Baduru, K.K., Trapp, S., Burken, J.G., 2008. Direct measurement of VOC diffusivities in tree tissues: Impacts on tree-based phytoremediation and plant contamination. Environ. Sci. Technol. 42 (4), 1268–1275. https://doi.org/10.1021/es071552l

Balouet, J.C., Oudijk, G., Smith, K.T., Petrisor, I., Grudd, H., Stocklassa, B., 2007. Applied dendroecology and environmental forensics. Characterizing and age dating environmental releases: Fundamentals and case studies. Environ. Forensics 8, 1–17. https://doi.org/10.1080/15275920601180487

Bradley, P.M., Chapelle, F.H., 2011. Microbial mineralization of dichloroethene and vinyl chloride under hypoxic conditions. Gr. Water Monit. Remediat. 31, 39–49. https://doi. org/10.1111/J.1745-6592.2011.01339.X.

Burken, J.G., Vroblesky, D.A., Balouet, J.C., 2011. Phytoforensics, Dendrochemistry, and Phytoscreening: New Green Tools for Delineating Contaminants from Past and Present. Environ. Sci. Technol 45, 44. https://doi.org/10.1021/es2005286

Bush, S.E., Hultine, K.R., Sperry, J.S., Ehleringer, J.R., 2010. Calibration of thermal dissipation sap flow probes for ring-and diffuse-porous trees. Tree Physiol. 30 (12), 1545–1554.

https://doi.org/10.1093/treephys/tpq096.

Cantonati, M., Stevens, L.E., Segadelli, S., Springer, A.E., Goldscheider, N., Celico, F., Filippini, M., Ogata, K., Gargini, A., 2020. Ecohydrogeology: The interdisciplinary convergence needed to improve the study and stewardship of springs and other groundwater-dependent habitats, biota, and ecosystems. Ecol. Indic. 110. https://doi.org/10.1016/j.ecolind.2019.105803

Cermak, J., Cienciala, E., Kucera, J., Hallgren, J.-E., 1992. Radial velocity profiles of water flow in trunks of Norway spruce and oak and the response of spruce to severing. Tree Physiol. 10 (4), 367–380. https://doi.org/10.1093/treephys/10.4.367.

Cox, S.E., 2002. Preliminary assessment of using tree-tissue analysis and passive diffusive samplers to evaluate trichloroethene contamination of groundwater at site SS-34N, McChord Air Force Base, Washington, 2001. Masters ThesesWater-Resources Investigations Report 02-4274. U.S. Geological Survey, Tacoma, Washington.

Dettenmaier, E.M., Doucette, W.J., Bugbee, B., 2009. Chemical hydrophobicity and uptake by plant roots. Environ. Sci. Technol. 43 (2), 324–329. https://doi.org/10.1021/es801751x.

Duncan, C.M., Brusseau, M.L., 2018. An assessment of correlations between chlorinated VOC concentrations in tree tissue and groundwater for phytoscreening applications. Sci. Total Environ. 616–617, 875–880. https://doi.org/10.1016/j.scitotenv.2017.10.235

Duncan, C.M., Mainhagu, J., Virgone, K., Ramírez, D.M., Brusseau, M.L., 2017. Application of phytoscreening to three hazardous waste sites in Arizona. Sci. Total Environ. 609, 951–955. https://doi.org/10.1016/j.scitotenv.2017.07.236

Ellmore, G.S., Ewers, F.W., 1986. Fluid flow in the outermost xylem increment of a ring-porous tree, Ulmus americana. Am. J. Bot. 73, 1771–1774. https://doi.org/10.1002/j.1537-2197.1986.tb09709.x

Freeze, R.A., Cherry, J.A., 1979. Groundwater. Prentice-Hall, Englewood Cliffs, N.J.

Gobelius, L., Lewis, J., Ahrens, L., 2017. Plant uptake of per- and Polyfluoroalkyl substances at a contaminated fire training facility to evaluate the phytoremediation potential of various

plant species. Environ. Sci. Technol. 51, 12602–12610. https://doi.org/10.1021/acs.est.7b02926.

Gopalakrishnan, G., Negri, M.C., Minsker, B.S., Werth, C.J., 2007. Monitoring Subsurface Contamination Using Tree Branches. Ground Water Monit. Remediat. 27, 65–74. https://doi.org/10.1111/j.1745-6592.2006.00124.x

Holm, O., Rotard, W., 2011. Effect of Radial Directional Dependences and Rainwater Influence on CVOC Concentrations in Tree Core and Birch Sap Samples Taken for Phytoscreening Using HS-SPME-GC/MS. Environ. Sci. Technol. 45, 9604–9610. https://doi.org/10.1021/es202014h

Journel, A.G., Deutsch, C.V., 1997. Rank order geostatistics: a proposal for a unique coding and common processing of diverse data. Geostatistics Wollongong '96. Kluwer Academic Publishers, Dordrecht, Netherlands, pp. 174–187.

Juang, K., Lee, D., Ellsworth, T.R., 2001. Using rank-order geostatistics for spatial interpolation of highly skewed data in a heavy-metal contaminated site. J. Environ. Qual. 30, 894–903. https://doi.org/10.2134/jeq2001.303894x.

Larsen, Morten, Burken, J., Machackova, J., Karlson, U.G., Trapp, S., 2008. Using tree core samples to monitor natural attenuation and plume distribution after a PCE spill. Environ. Sci. Technol. 42, 1711–1717. https://doi.org/10.1021/es0717055

Lewis, J., Qvarfort, U., Sjostrom, J., 2015. Betula pendula: a promising candidate for phytoremediation of TCE in northern climates. Int. J. Phytoremediation 17 (1), 9–15. https://doi.org/10.1080/15226514.2013.828012.

Limmer, M., Burken, J., 2015. Phytoscreening with SPME: Variability Analysis Article in. Int. J. Phytoremediation. https://doi.org/10.1080/15226514.2015.1045127

Limmer, M.A., West, D.M., Mu, R., Shi, H., Whitlock, K., Burken, J.G., 2014. Phytoscreening for perchlorate: rapid analysis of tree sap. Environ. Sci. Water Res. Technol. 1, 138. https://doi.org/10.1039/c4ew00103f.

Ma, X., Burken, J.G., 2003. TCE diffusion to the atmosphere in phytoremediation applications.

Environ. Sci. Technol. 37, 2534–2539. https://doi.org/10.1021/es026055d

Mackay, D., Shiu, W.Y., Ma, K.C., Lee, S.C., 2006. Handbook of physical-chemical properties and environmental fate for organic chemicals. Taylor & Francis Group, LLC, p. 4216.

Negri, M.C., Gatliff, E.G., Quinn, J.J., Hinchman, R.R., 2003. Root development and rooting at depths. In: McCutheon, S.C., Schnoor, J.L. (Eds.), Phytoremediation-Transformation and Control of Contaminants. John Wiley and Sons, Inc., Hoboken, New Jersey, pp. 232–233.

Newman, L.A., Reynolds, C.M., 2004. Phytodegradation of organic compounds. Curr. Opin. Biotechnol. 15, 225–230. https://doi.org/10.1016/j.copbio.2004.04.006

Ottosen, C.B., Rønde, V., Trapp, S., Bjerg, P.L., Broholm, M.M., 2018. Phytoscreening for Vinyl Chloride in Groundwater Discharging to a Stream. Groundw. Monit. Remediat. 38, 66–74. https://doi.org/10.1111/gwmr.12253

Pankow, J.F., Cherry, J.A., 1996. Dense chlorinated solvents and other DNAPLs in groundwater. Oregon, Waterloo Press, Portland, p. 522.

Panshin, A.J., Zeeuw, C.de, Brown, H.P., 1949. Textbook of wood technology. Structure, identification, uses, and properties of the commercial woods of the United States. Vol. 1. McGraw-Hill Book Co., p. 695.

Parker, B.L., Cherry, J.A., Chapman, S.W., Guilbeault, M.A., 2003. Review and analysis of chlorinated solvent dense nonaqueous phase liquid distributions in five sandy aquifers. Vadose Zone J. 2, 116–137. https://doi.org/10.2113/2.2.116.

Schnoor, J.L., Licht, L.A., McCutcheon, S.C., Wolfe, N.L., Carreir, L.H., 1995. Phytoremediation of organic and nutrient contaminants. Environ. Sci. Technol. 29, 318A–323A. https://doi.org/10.1021/es00007a747.

Schumacher, J.G., Struckhoff, G.C., Burken, J.G., 2004. Assessment of subsurface chlorinated solvent contamination using tree cores at the front street site and a former dry cleaning facility

at the Riverfront Superfund site, New Haven, Missouri, 1999-2003, U.S. Geological Survey Scientific Investigations Report 2004-5049. https://doi.org/https://doi.org/10.3133/sir20045049

Sorek, A., Atzmon, N., Dahan, O., Gerstl, Z., Kushisin, L., Laor, Y., Mingelgrin, U., Nasser, A., Ronen, D., Tsechansky, L., Weisbrod, N., Graber, E.R., 2008. "Phytoscreening": The use of trees for discovering subsurface contamination by VOCs. Environ. Sci. Technol. 42, 536–542. https://doi.org/10.1021/es072014b

Struckhoff, G., 2003. Uptake of vapor phase PCE by plants: impacts to phytoremediation. Masters theses.

Struckhoff, G.C., Burken, J.G., Schumacher, J.G., 2005. Vapor-phase exchange of perchloroethene between soil and plants. Environ. Sci. Technol. 39, 1563–1568. https://doi.org/10.1021/es049411w

Strycharz, S., Newman, L., 2009. Use of native plants for remediation of trichloroethylene: I. deciduous trees. Int. J. Phytoremediation 11, 150–170. https://doi.org/10.1080/15226510802378442

Trapp, S., 2007. Fruit tree model for uptake of organic compounds from soil and air. SAR QSAR Environ. Res. 18, 367–387. https://doi.org/10.1080/10629360701303693

Trapp, S., Larsen, M., Legind, C.N., Burken, J., Macháčková, J., 2007. A Guide to Vegetation Sampling for Screening of Subsurface Pollution, in: BIOTOOL Project GOCE 003998.

Vroblesky, D.A., 2008. User's Guide to the Collection and Analysis of Tree Cores to Assess the Distribution of Subsurface Volatile Organic Compounds, Scientific Investigations Report 2008–5088. U.S. Geological Survey. https://doi.org/https://doi.org/10.3133/sir20085088

Vroblesky, D.A., Clinton, B.D., Vose, J.M., Casey, C.C., Harvey, G.J., Bradley, P.M., 2004. Ground water chlorinated ethenes in tree trunks: Case studies, influence of recharge, and potential degradation mechanism. Gr. Water Monit. Remediat. 24, 124–138. https://doi.org/10.1111/j.1745-6592.2004.tb01299.x

Vroblesky, D.A., Nietch, C.T., Morris, J.T., 1999. Chlorinated Ethenes from Groundwater in Tree

Trunks. Environ. Sci. Technol. 33, 510–515. https://doi.org/10.1021/es980848b

Wahyudi, A., Bogaert, P., Trapp, S., MacHáčková, J., 2012. Pollutant plume delineation from tree core sampling using standardized ranks. Environ. Pollut. 162, 120–128. https://doi.org/10.1016/j.envpol.2011.11.010

Westhoff, M., Schneider, H., Zimmermann, D., Mimietz, S., Stinzing, A., Wegner, L.H., Kaiser, W., Krohne, G., Shirley, St, Jakob, P., Bamberg, E., Bentrup, F.W., Zimmermann, U., 2008. The mechanisms of refilling of xylem conduits and bleeding of tall birch during spring. Plant Biol. 10, 604–623. https://doi.org/10.1111/j.1438-8677.2008.00062.x.

Wilcox, J.D., Johnson, K.M., 2016. Trichloroethylene (TCE) in tree cores to complement a subsurface investigation on residential property near a former electroplating facility. Environ. Monit. Assess. 188. https://doi.org/10.1007/s10661-016-5603-x.

Wilson, J., Bartz, R., Limmer, M., Burken, J., 2013. Plants as Bio-Indicators of Subsurface Conditions: Impact of Groundwater Level on BTEX Concentrations in Trees. Int. J. Phytoremediation 15, 257–267. https://doi.org/10.1080/15226514.2012.694499

Wilson, J.L., Samaranayake, V.A., Limmer, M.A., Schumacher, J.G., Burken, J.G., 2017. Contaminant Gradients in Trees: Directional Tree Coring Reveals Boundaries of Soil and Soil-Gas Contamination with Potential Applications in Vapor Intrusion Assessment. Environ. Sci. Technol. 51, 14055–14064. https://doi.org/10.1021/acs.est.7b03466

Wittlingerova, Z., Machackova, J., Petruzelkova, A., Trapp, S., Vlk, K., Zima, J., 2013. One-year measurements of chloroethenes in tree cores and groundwater at the SAP Mimoň Site, Northern Bohemia. Environ. Sci. Pollut. Res. 20, 834–847. https://doi.org/10.1007/s11356-012-1238-9

Yung, L., Lagron, J., Cazaux, D., Limmer, M., Chalot, M., 2017. Phytoscreening as an efficient tool to delineate chlorinated solvent sources at a chlor-alkali facility. Chemosphere 174, 82–89. https://doi.org/10.1016/j.chemosphere.2017.01.112.

3
Fieldwork results

3.1. INTRODUCTION

Phytoscreening has been used in recent years on several occasions to aid in subsurface contaminant plume delineation, particularly in sites contaminated by volatile organic compounds (VOCs) such as chlorinated ethenes (CEs; Burken et al., 2011; Duncan et al., 2017; Larsen et al., 2008; Sorek et al., 2008; Vroblesky et al., 1999; Wahyudi et al., 2012). Although this technique performs plant-based indirect measurement of groundwater (gw) contaminant concentration, the results can lead to fast, cost-effective, and systematic site assessments (e.g., Sorek et al., 2008). Phytoscreening is based on tree uptake of gw, resulting in tree-core VOCs concentrations that are correlated with gw VOCs concentrations. Many previous works have reported that several factors are responsible for the scarce performance of phytoscreening in terms of quantitative analysis. Seasonal changes (Limmer and Burken, 2014), different tree sizes (Baduru et al., 2008), and tree genus (Vroblesky et al., 2004), are some of the variables that were reported as affecting groundwater to tree concentration correlation by modifying *in planta* accumulation and distribution as well as volatilization loss through the trunk.

Measuring trace levels of VOCs in trees require sensitive analytical methods. Various *in vitro* and *in planta* methods have been utilized, such as heated headspace (e.g., Larsen et al., 2008), *in planta* passive sampling (e.g., Shetty et al., 2014), and headspace solid-phase microextraction (e.g., Holm and Rotard, 2011). To increase confidence in and understanding of phytoscreening, improvements are needed in both standardization of the sampling method and understanding of the impact of seasonality, site setting parameters, and sampling methodology on the relationship between plants and subsurface contaminant concentration.

In the presented Chapter, we tested the traditional analysis of tree-cores via Gas Chromatography-Mass spectrometry, and we coupled two new *in planta* sampling approaches: the photoionization detector (PID) and the colorimetric vials. The contaminated sites, located in the Emilia-Romagna territory in Italy, have in common underground contamination by CEs and have been chosen based on their uniqueness in terms of hydrogeological setting and the plant species present. Another crucial element for the site selection was the good degree of characterization of the field sites: a reliable network of piezometers was essential for the direct comparison of gw and tree-core concentrations. From a geomorphological point of view, the study areas occupy territories ranging from the alluvial plains of Po e Reno River (areas of Bologna, Ferrara, and Parma) to the alluvial fans of the Faenza area, up to the less intravallive recent fluvial terraces in the surrounding of Bologna. The lithologies range from well-sorted gravels through silty or gravelly sands to mainly clayey and silty deposits with variable content of organic matter. The aquifers are usually shallow and not confined but, in some instances, they are confined to semi-confined conditions if covered by fine-grained layers. Gw contamination is mainly characterized by the presence of CEs with gw concentrations ranging from a few μg/L to tens of mg/L. In some sites chlorinated ethanes, BTEX (benzene, toluene, ethylbenzene, xylene), and styrene are associated too to CEs.

In the investigated test sites, we characterized the extent of variability in tree-core concentrations caused by site conditions such as depth to water table (DWT), aquifer thickness (b), and aquifer hydraulic conductivity (K) as well as meteorological conditions such as precipitation rate and average air temperature in the weeks before sampling. Field data were also used to examine the effect of tree diameter, tree genus, and contaminant properties on VOCs concentrations and verify the precision and accuracy of the results.

3.2. MATERIALS AND METHODS

3.2.1. Field sites

The level of accuracy of the geological frameworks is variable depending on the degree of characterization performed on the various sites and limited to what is considered essential in the discussion phase. Investigated sites are located as in FIGURE 3.1 and the number of phytoscreening surveys (tree-core sampling and analysis) carried out per site is indicated in TABLE 3.1.

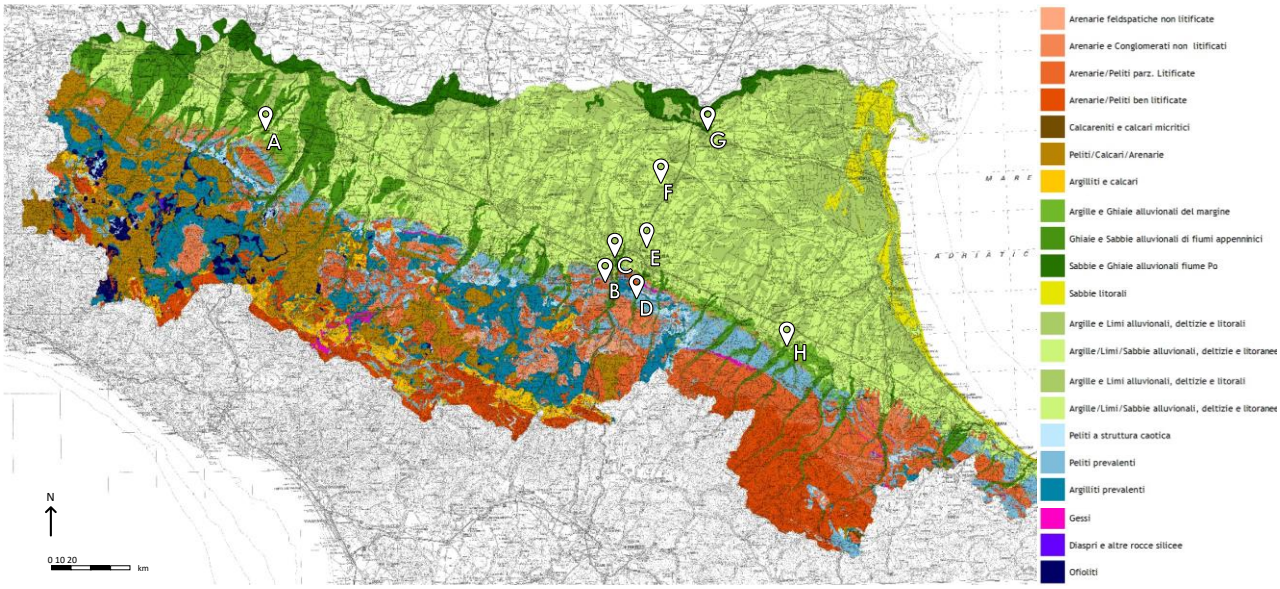

FIGURE 3.1. Lithological map of Emilia-Romagna with location of study sites (https://ambiente.regione.emilia-romagna.it)

TABLE 3.1 Location and number of surveys carried out at each site, related to the number of sampled trees.

Site	Location	n° of surveys	n° of sampled trees
A	Fidenza (PR)	2	6, 5
B	Casalecchio di Reno (BO)	2	7, 7
C	Bologna (BO)	2	4, 6
D	Pianoro (BO)	3	9, 9, 9
E	Granarolo dell'Emilia (BO)	4	7, 8, 10, 10
F	Galliera (BO)	2	6, 5
G	Ferrara (FE)	5	10, 3, 3, 3
H	Faenza (RA)	2	5, 9

3.2.1.1 A site

The A site is located in the northern sector of the town of Fidenza (Parma, Italy) at an average elevation of 72 m a.s.l. The area is characterized by the outcrop of distal alluvial cone deposits, locally terraced, consisting of prevalent sandy gravels and gravels, with local intercalations of sands and sandy silts and clayey layers (FIGURE 3.2).

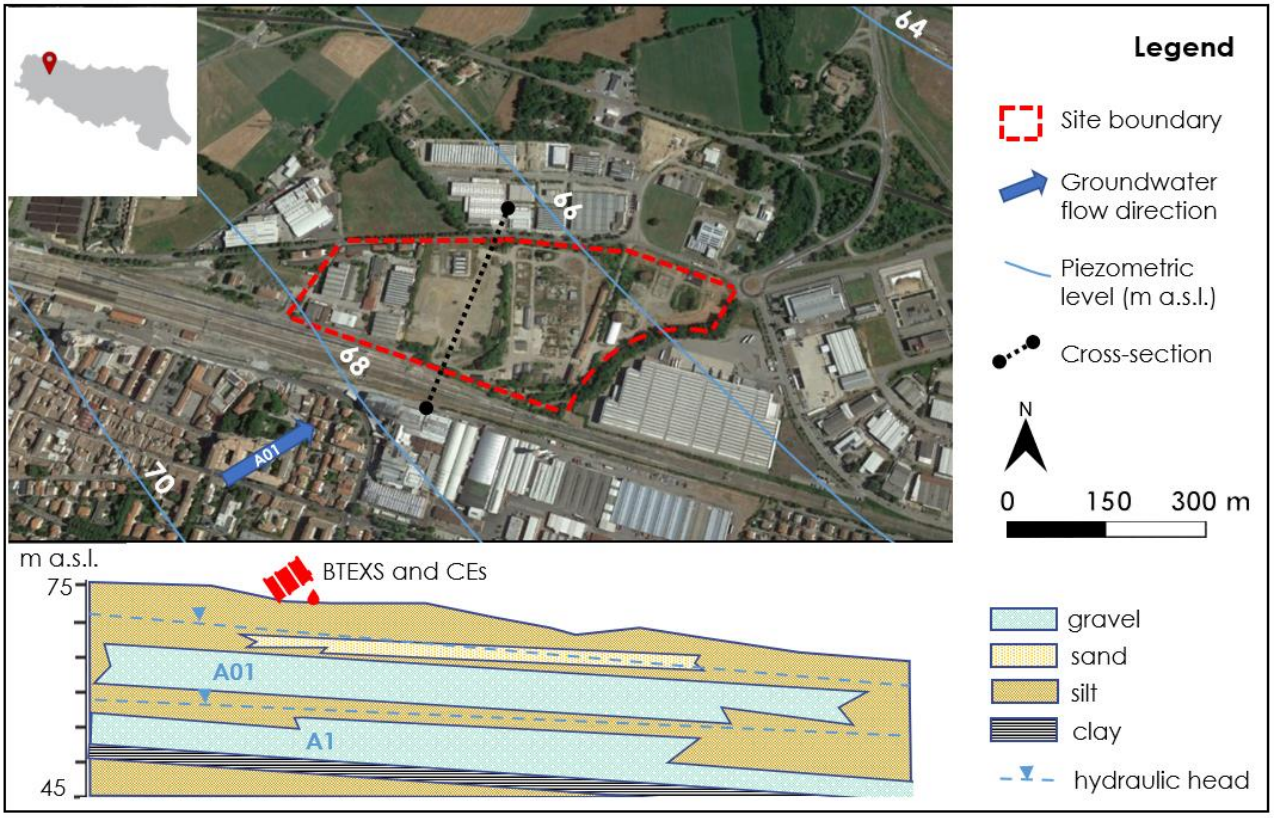

FIGURE 3.2. Map of the A site showing piezometric levels related to the phreatic aquifer (A01) and summary hydrogeological stratigraphic section

Two locally interconnected aquifer units composed of gravels in a silty-clayey matrix were identified. The deepest aquifer (A1), confined and locally semi-confined, occurs between 19 and 26 m below ground level (b.g.l.) and is deeply affected by the contamination produced by a former carbo-chemical plant present on the territory since the beginning of the 20th century. At the bottom of A1, a clayey or silty clayey layer between 2 and 4 m thick acts as an aquiclude. At the top, a non-continuous 2 m thick layer of clays and clayey silts separates the deep aquifer from the shallow aquifer. The latter (A01) is hosted by a gravelly layer with thickness varying between 3 and 7 m and partly covered by

silts intermingled with sands and silty gravels. Groundwater flow direction in aquifer A1 shows an SW-NE direction and an estimated gw flow velocity of 5.3 x 10^{-4} m/s (estimated with a constant rate pumping test), while aquifer A01 shows a WSW-ENE direction and a gw flow velocity of 1.6 x 10^{-4} m/s. The hydraulic head is at about 15 m b.g.l. in aquifer A1 while the DWT is around 3 to 5 m b.g.l. in A01. The contamination, detected in the 90s, is attributed to the production cycle of the carbo-chemical plant. The contamination is mainly composed of BTEXS (particularly benzene, and toluene in amounts reaching thousands of µg/L). In lower quantities and in the westernmost part of the industrial site, CEs were also detected (tens of µg/L of PCE and TCE). A Pump & Treat barrier as an emergency measure was activated in the early 2000s in the A1 aquifer.

The sampling location was chosen to investigate the eventual migration of the contamination in A01 right outside the northern boundary of the contaminated site.

3.2.1.2 B site

The B site is located in the town of Casalecchio di Reno, near Bologna, on an alluvial cone of debris deposited above alluvial terraced gravels (FIGURE 3.3) at an average elevation of 86 m a.s.l. A gravelly-sandy aquifer is bounded at the bottom at around 12 m b.g.l. by an approximately 4 m clayey layer that serves as an aquiclude. The aquifer is unconfined to semi-confined and is approximately 4 m thick with a saturated K of around 10^{-4} – 10^{-3} m/s (estimated from Freeze & Cherry, 1979). The macroclastites are intermingled with silty and silty-sandy layers that become finer as approaching the more distal portion of the cone debris to the east of the contaminated site. At the top of the aquifer, a heterogeneous cover of alternating silts, clays, and sandy gravels occurs.

The water table is located at a depth of about 9 m b.g.l. and the prevailing groundwater direction is W-E. Gw is contaminated by CEs related to an electrical equipment factory that ceased operations in 2010. The contamination, mainly composed of PCE (up to some thousands of µg/L) and in lesser quantity, TCE (some tens of µg/L), is attributable to the improper disposal of industrial waste produced by the company.

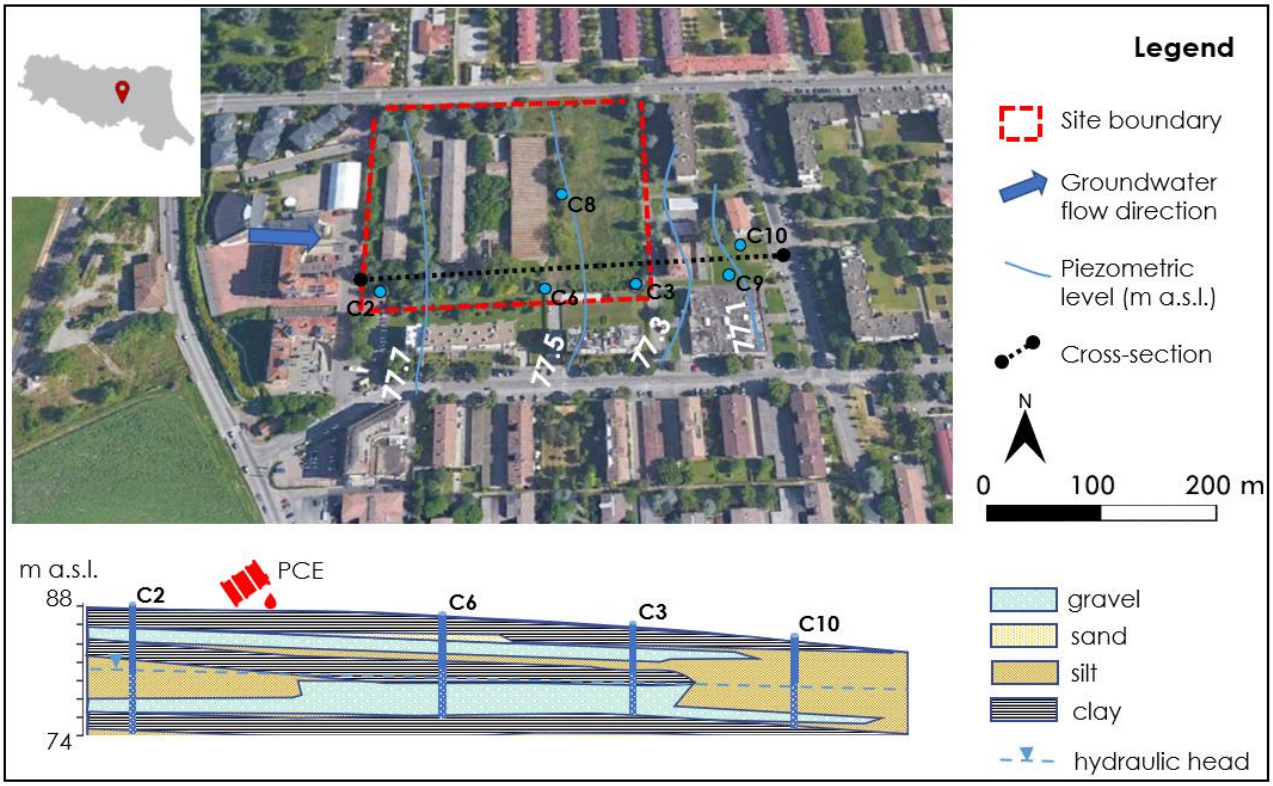

FIGURE 3.3. Map of the B site showing piezometric levels related to the phreatic aquifer and summary hydrogeological stratigraphic section with piezometers (in blue) indicating filters interval

3.2.1.3 C site

The C site is included within the city of Bologna residential area at an average elevation of 47 m a.s.l. The area is located on the alluvial cone of the Reno River and presents a wide lithological heterogeneity (FIGURE 3.4). The stratigraphic succession of the first 30 m b.g.l. shows a confined to semi-confined aquifer, at a depth of 22 to 26 m b.g.l. and composed mainly of gravels in a sandy or sandy silt matrix with an estimated K of $4x10^{-4}$ m/s (measured with a dissipation test). At the bottom, a layer of plastic clays forms the base of the aquifer. At the top, a discontinuous thick layer of clays and silts occurs with a maximum thickness of 3-4 m. More superficially, a sandy and gravelly layer of about 10 m lies below a layer of silts and clays that marks the top of the stratigraphic log. The DWT is around 23-24 m b.g.l. and the prevailing gw flow direction is SSE-NNW. The contamination is mainly composed of PCE. PID analyses related to MIP (Membrane Interface Probe) surveys also showed a shallower contamination (between 3 and 8 m b.g.l.) possibly related to a gaseous-phase or

capillary or retention water contamination trapped in more granular lenses occurring in the upper part of the mainly silty vadose zone.

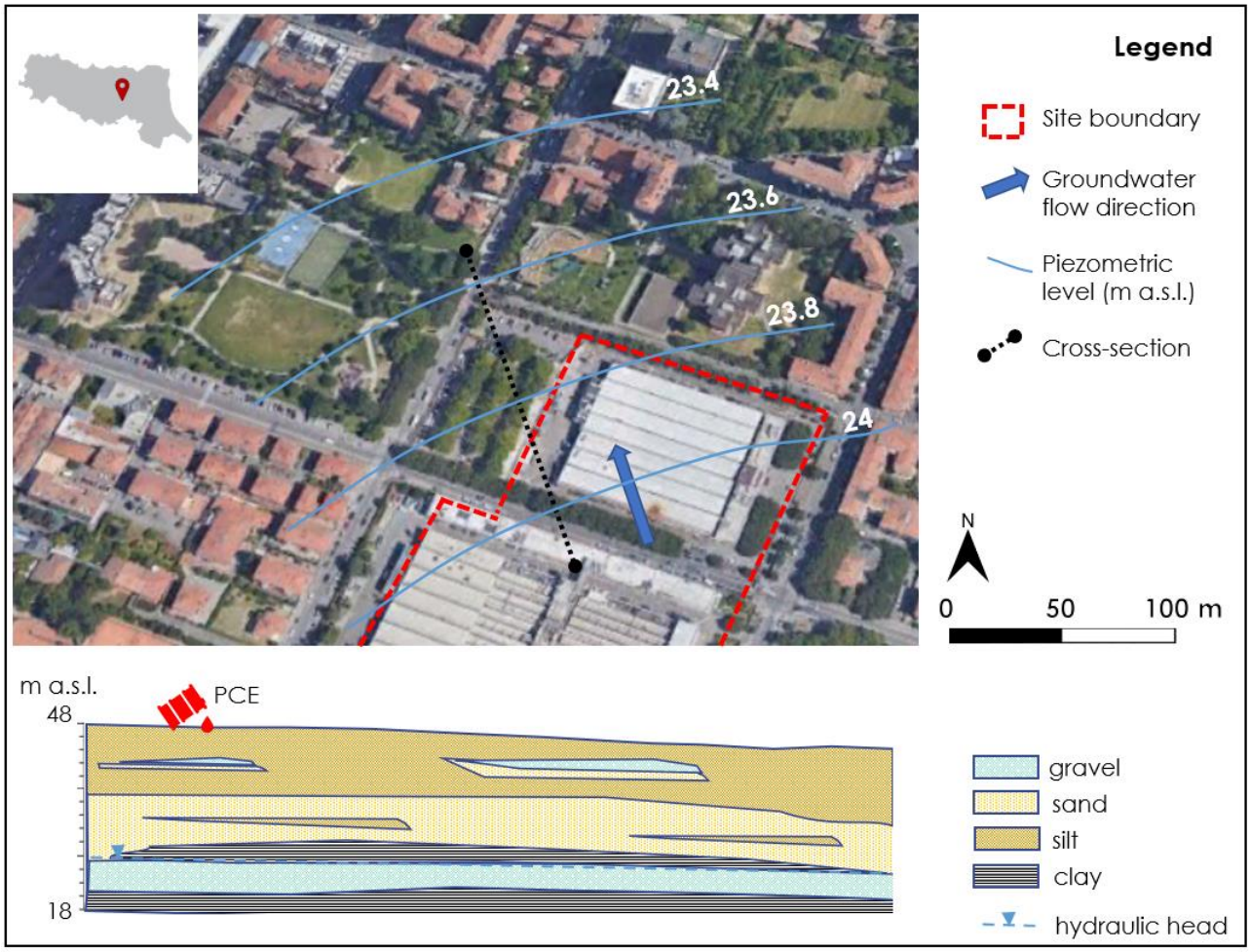

FIGURE 3.4. Map of the C site showing piezometric levels and summary hydrogeological stratigraphic section of the first 30 m b.g.l.

3.2.1.4 D site

The D site is located on the alluvial terraces of the Savena River at an average elevation of 126 m a.s.l., in the hills located south of Bologna. Down to about 7 m b.g.l., the sediments are mainly silty and gravelly-sandy and lie above a clayey bedrock (FIGURE 3.5). The gravelly-sandy units, acting as the local unconfined aquifer with an estimated K of 10^{-3} m/s (from Freeze & Cherry, 1979), attain a maximum thickness of 4 m. At the bottom, there is a continuous clayey layer at depths between about 3 and 5 m b.g.l., while at the top a layer with alternating silts and sands occurs.

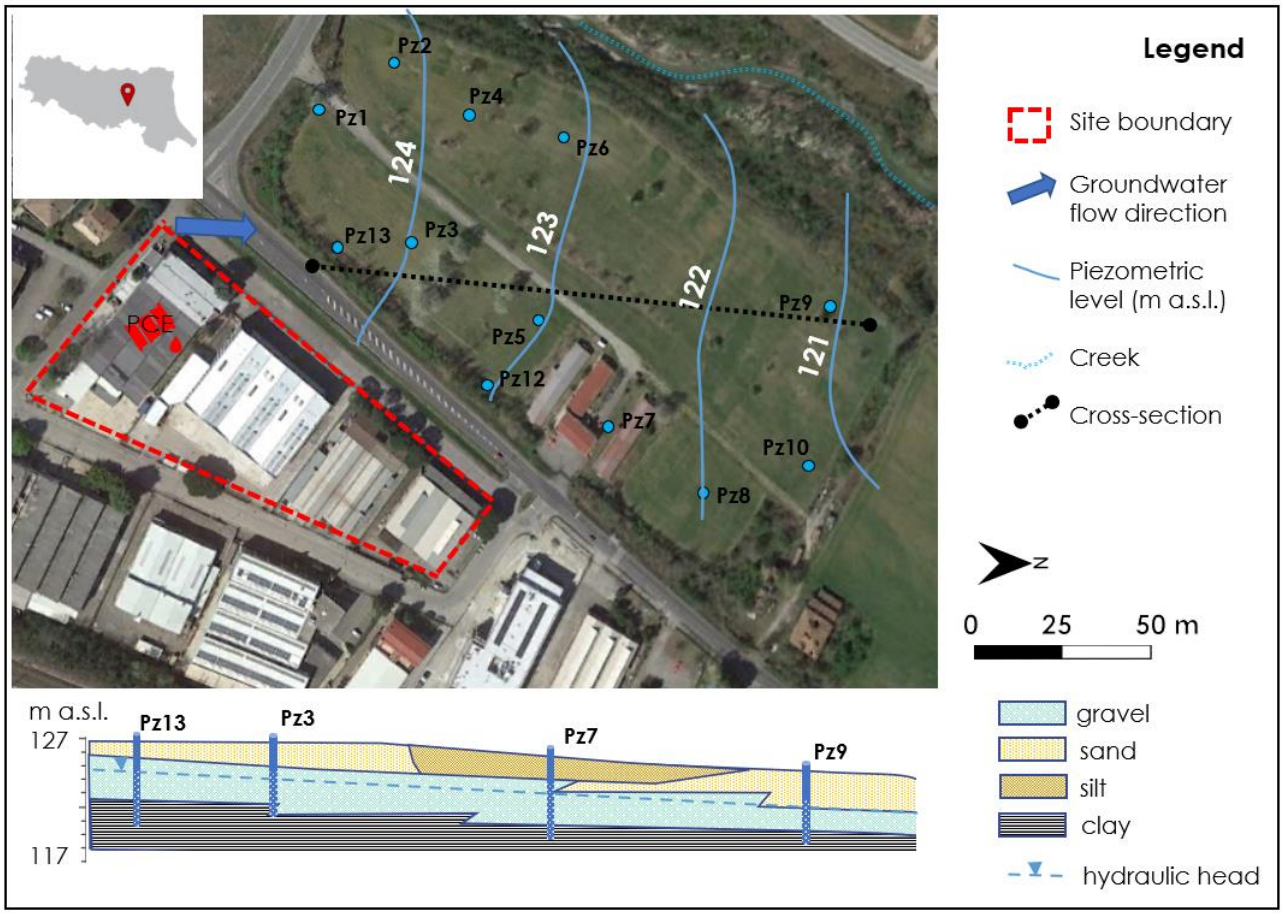

FIGURE 3.5. Map of the D site showing piezometric levels and summary hydrogeological stratigraphic section of the first 20 m b.g.l. with piezometers (in blue) indicating filters interval

The water table is around 3 m b.g.l. with SSE-NNW gw flow direction. The contamination found in gw, downstream of the site, is mainly composed of PCE and, in lower quantities, TCE, in total concentrations of a few hundred µg/L. At the source, PCE occurs in the pure phase. Immediately downgradient of the site, a Pump & Treat emergency hydraulic barrier was activated in 2012.

3.2.1.5 E site

The E site at Quarto Inferiore (Bologna) is located on alluvial plain sediments, predominantly related to a distal alluvial cone (FIGURE 3.6) at an average elevation of 33 m a.s.l. Although the aquifer is mainly sandy in a silty-clay matrix, it shows lithologic heterogeneity both vertically and laterally, with several clay and silty clay lenses occurring downstream of the site.

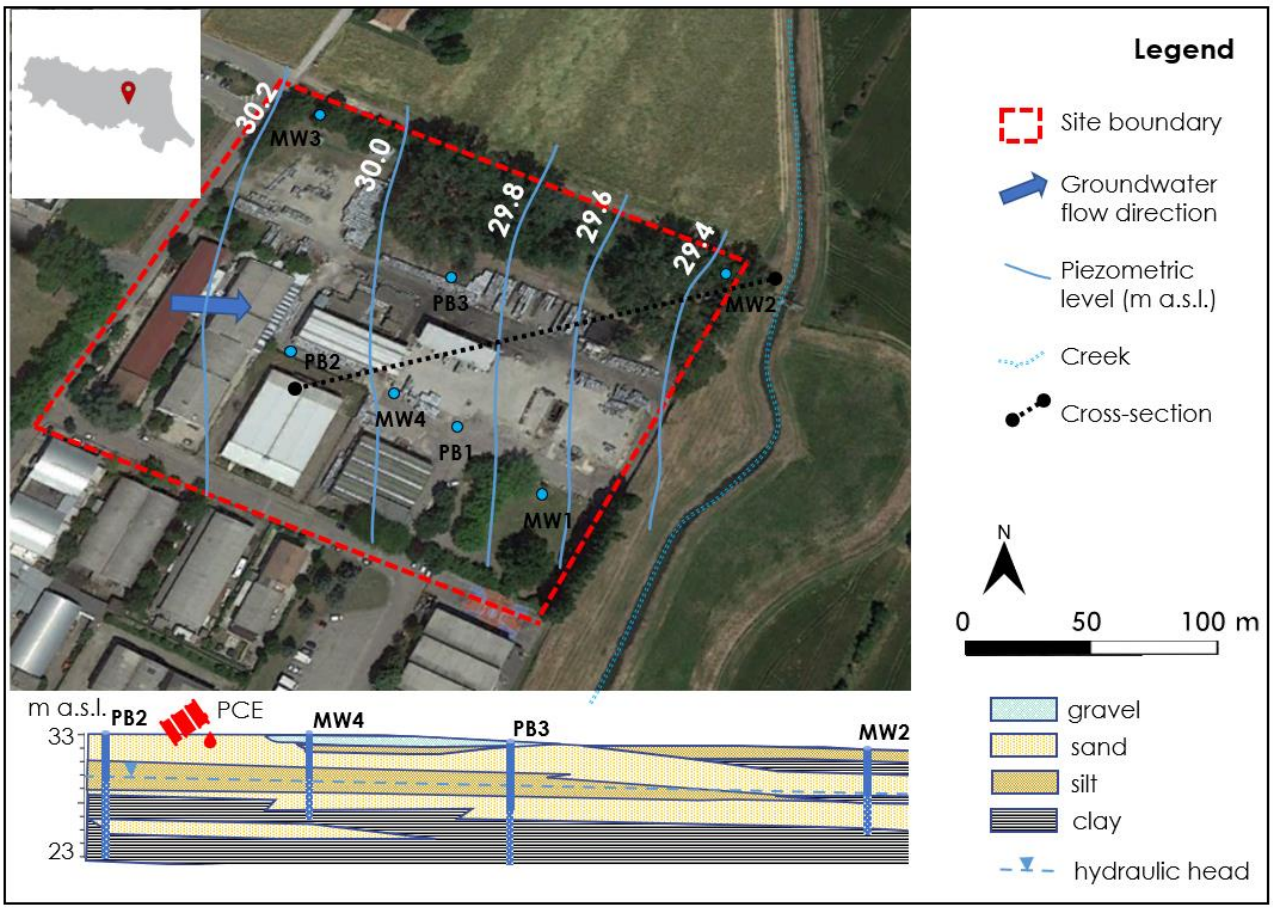

FIGURE 3.6. Map of the E site showing static piezometric levels and summary hydrogeological stratigraphic section of the first 10 m b.g.l. with piezometers (in blue) indicating filters interval

At the bottom of the aquifer, a fine-grained layer acts as an aquiclude which top was identified at around 10 m b.g.l. Varying between 3 and 5 m b.g.l., the hydraulic head slopes in a W-E direction towards a reclamation ditch used for agricultural purposes (Zanetta ditch) which, however, was found to be free of contamination. The aquifer is hydraulically unconfined with an average K of 10^{-5} m/s (estimated from several step drawdown tests), except for the eastern downstream portion of the site where a local confining layer of fine sediments exists. The saturated thickness varies between 2 and 6 m and hosts a contamination with the occurrence of all CEs, from PCE to VC, although with a greater presence of the primary compounds, PCE and TCE. A Pump & Treat system (PB1, PB2, and PB3) locally deflects the gw table and an *in situ* soil and gw remediation has been activated since 2019.

3.2.1.6 F site

The F site is represented by a former chemical plant and is located at the northern edge of a paleochannel of the Reno River, at an average elevation of 15 m a.s.l. The outcropping geology in the area is made up of crevasses splay deposits, mainly composed of alternating sandy silts and clayey silts in varying proportions, to which clay and peaty deposits can be intermingled (FIGURE 3.7).

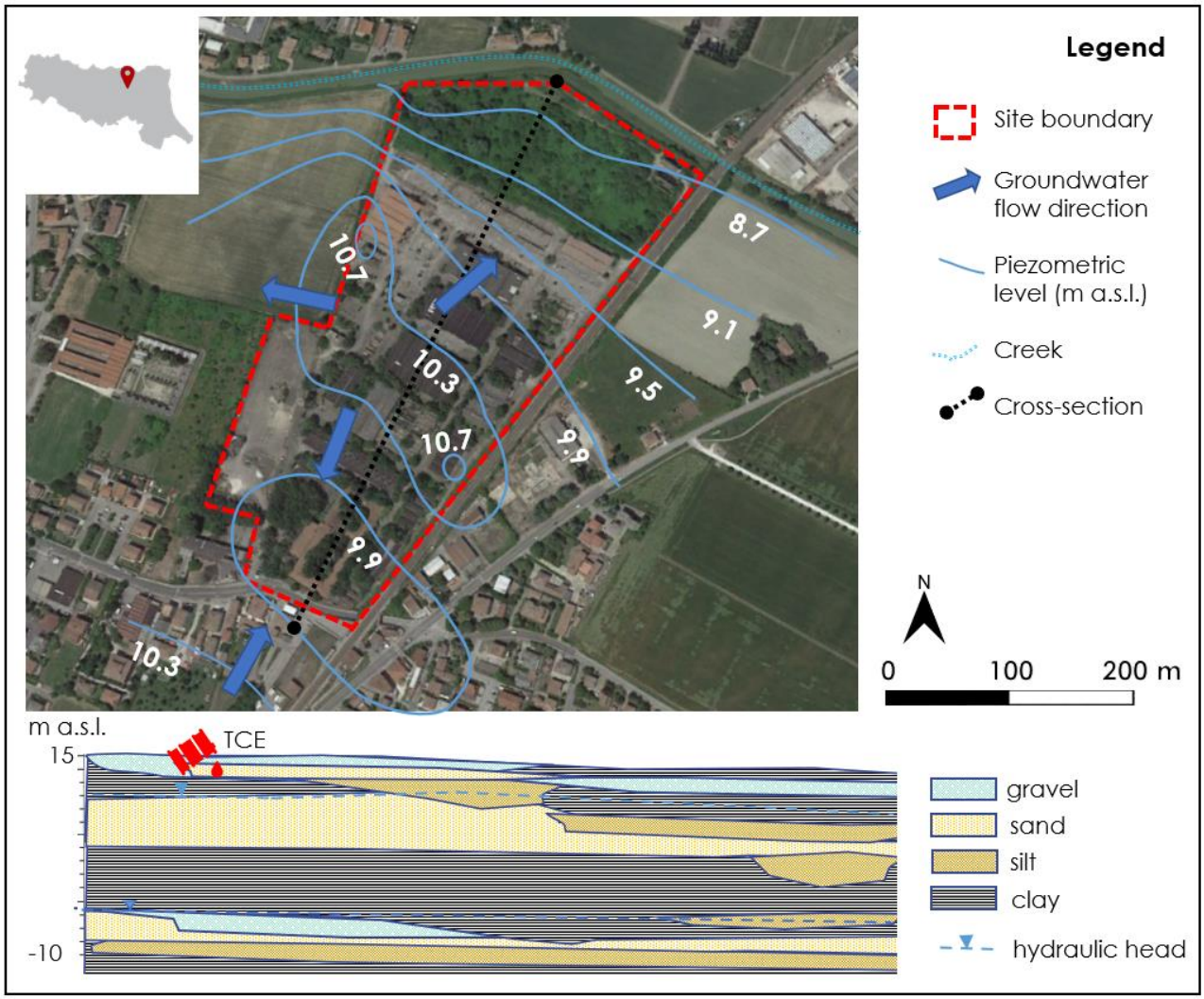

FIGURE 3.7. Map of the F site showing static piezometric levels of the phreatic aquifer and summary hydrogeological stratigraphic section of the first 25 m b.g.l.

Three relatively permeable units (estimated K of 10^{-5} – 10^{-4} m/s; Freeze & Cherry, 1979), up to 5 m thick, were recognized in the first 20 to 25 m b.g.l.; these units consist of alternating silty sands and sandy silts. The two shallowest units are separated by a level of discontinuous fine-grained layer. In some areas, the first two units coalesce to form a single permeable unit more than 10 m thick. At the

bottom, a layer of clay and silty clay rich in organic matter is occurring with a thickness of up to 10 m. This causes the deeper permeable unit to be separated from the two overlying ones. The two shallower permeable units thus constitute an unconfined aquifer locally compartmentalized into two portions (upper and lower), while the lower permeable units constitute a confined or semi-confined aquifer with little or no connection to direct recharge. On the northern boundary of the site, there is a reclamation ditch (Riolo ditch), hydraulically interconnected with the unconfined aquifer. Hydraulic head, although it has generally S-N direction, shows a piezometric mound in the central part of the site, at about 5-6 m b.g.l., probably related to the topographic high occurring in this area. From this high, gw flows in all directions down to piezometric lows at about 10 m b.g.l.

The contamination appears to be restricted to the plant area and consists largely of CEs (predominantly TCE) up to several hundred µg/L. The deeper confined aquifer does not appear to be contaminated as well as the upper unit of the unconfined aquifer. Contamination is primarily present in the lower unit of the unconfined aquifer (6 to 10 m b.g.l.).

3.2.1.7 G site

The G site, on the outskirts of Ferrara and at an average elevation of 5 m a.s.l., is located in a sector of the Po plain that represents a classic example of a complex alluvial system, resulting in a group of stacked aquifers. The two main aquifers present, at the site, in the first 40-60 m b.g.l. are known as A0 and A1 (FIGURE 3.8). In particular, in the first 30 m b.g.l., two layers of fluvial sands, medium-fine to medium-coarse, alternate with fine-grained overbank sediments. The deepest unit (A1), composed of medium-coarse sands and included between 15 and 25 m b.g.l., rests on a layer of 8 to 10 m of clay and silt. At the top of A1 clays and silts occur with thicknesses varying between 5 and 10 m. The 10 m thick unconfined to locally semi-confined aquifer (A0) is constituted by medium-fine sands. In the study area, hydraulic conductivity is in the range of 10^{-4} - 10^{-6} m/s in the A0 aquifer and 10^{-5} - 10^{-4} m/s in the upper A1 aquifer (Molinari et al., 2007; Nijenhuis et al., 2013).

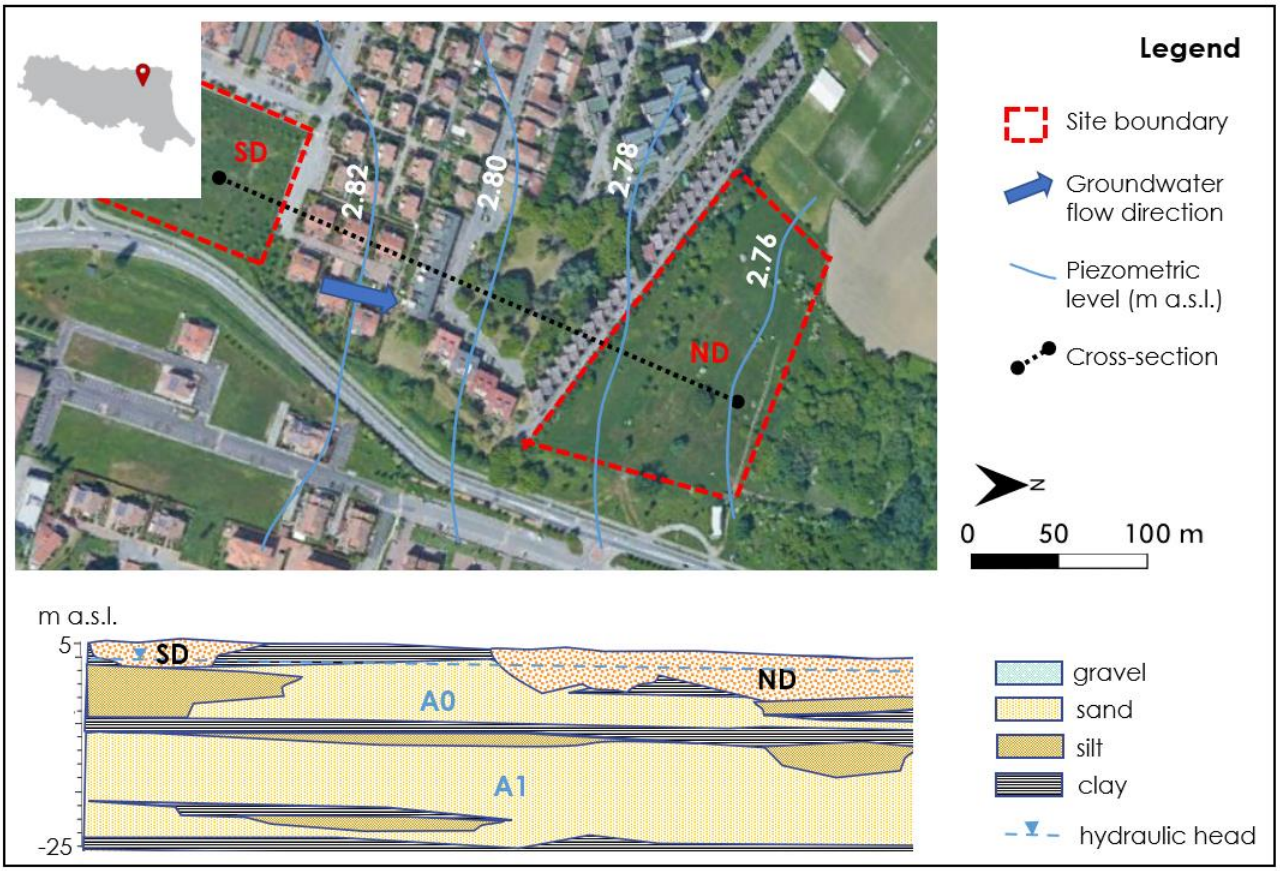

FIGURE 3.8. Map of the G site showing static piezometric levels of the phreatic aquifer and summary hydrogeological stratigraphic section of the first 30 m b.g.l.

Above A0 are located, interspersed with a layer of clays and peats, two dismissed clay quarries filled with mixed wastes, called the northern dump (ND) and the southern dump (SD), sources of the contamination in the study, which in the 60s have been subject to improper disposal of industrial waste. The DWT referred to A0 is between 2 and 4 m b.g.l. and the flow direction is from S-SW to N-NE. Contamination in A0 attains tens of mg/L of VC (Filippini et al., 2016, 2019; Nijenhuis et al., 2013).

3.2.1.8 H site

The H site falls within the alluvial cone of the Lamone river in Faenza (Italy) at an average elevation of 39 m a.s.l., thus the stratigraphic sequence is largely heterogeneous both vertically and laterally. FIGURE 3.9 shows an excerpt of the section in correspondence to the contamination source. A shallow low permeability aquifer unit (S1), with a prevalence of fine sands and silts and which goes down to

a depth of about 15 m b.g.l., presents an average hydraulic head (water table) at 8-9 m b.g.l. A second layer (GS1), which is highly permeable (K = $1.5x10^{-4}$ m/s from pumping tests measurements) and semi-confined, is composed mainly of gravels and occurs between 15 and 30 m b.g.l. GS1 hydraulic head is between 12 and 14 m b.g.l. Gw in GS1 is the main vector of the contamination outside the site with the occurrence of the whole spectrum of CEs with total concentrations attaining hundreds of mg/L. The source of the contamination is a former metal working industry plant.

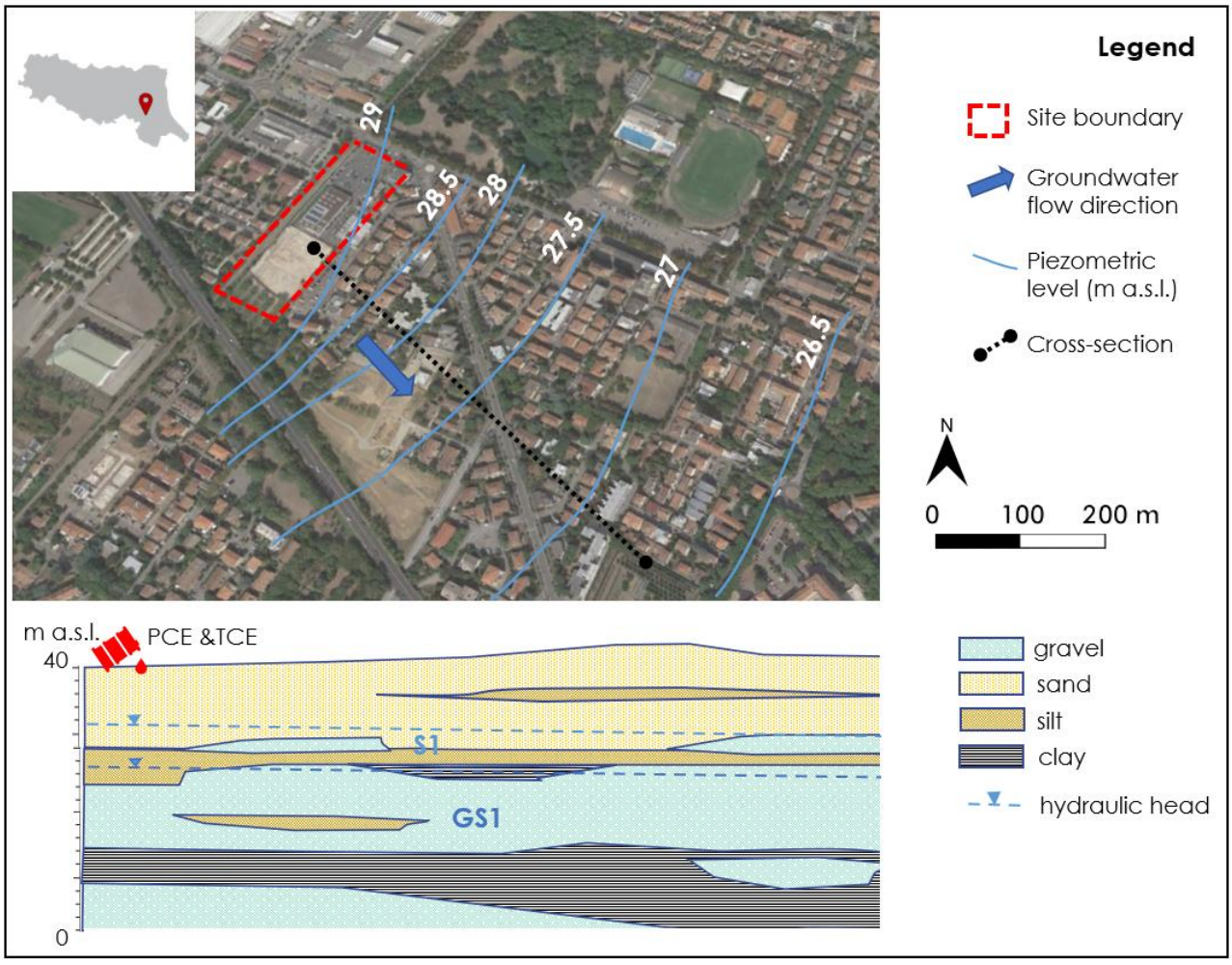

FIGURE 3.9. Map of the H site showing static piezometric levels of the phreatic aquifer (S1) and summary hydrogeological stratigraphic section of the first 40 m b.g.l.

3.2.2 Sample collection and analysis

3.2.2.1 Tree-core sampling and analysis

Tree-core samples were collected from each tree at 100 cm a.g.l. (above ground level) in the trunk, except for 2 sites (A and F sites) in which we also sampled at 50 cm a.g.l. as previously done by Ottosen et al. (2018) to assess phytovolatilization losses along the trunk. Drilling direction was chosen based on the direction of the contaminant plume as suggested by Holm and Rotard (2011). Tree-core samples of around 10 cm in length were collected using an increment borer of 40 cm in length and 4.3 mm in diameter.

The samples were collected in duplicates approximately 10 cm laterally from each other on each tree and placed in 40-mL glass vials containing 10 mL of methanol (>99.9% pure) and 5 mL of ultrapure water (Milli-Q). The vials were capped with PFTE/Silicone septa, placed in a cooler, and transported to the laboratory. The extraction method was modified from EPA method 8260C (2006). The quality assurance and quality control measures include the collection of field blanks, trip blanks, and background samples.

It is to be noted that, for laboratory analysis, a selection had to be performed among the species to be sampled. Specifically, we selected species that do not produce plant resins containing volatile terpenes. Monoterpenes such as pinene from conifers could indeed provoke damage to the analytical instrumentation. Upon receipt in the laboratory, methanol-filled vials were stored in a refrigerator at 4° C while water-filled vials were analyzed with a Purge & Trap method followed by headspace gas chromatography/mass spectrometry (GC/MS). When the measured concentration of an analyte exceeded the point of calibration (0.200 mg/kg), the extract in methanol was analyzed. The extraction in methanol is completed in an ultrasonic bath for 10 min. After dilution of 200 µl of extract in 40 ml of ultrapure water, the analysis is carried out by GC/MS. Laboratory QA/QC included sample blanks and internal standards with acceptable recoveries. This method applies to tree-core samples for concentrations of PCE, TCE, cDCE, and VC above 0.0005 mg/kg.

3.2.2.2 In planta sampling and analysis

In planta sampling was used in most surveys to estimate the gaseous-phase concentration of the VOCs present in the hole produced by the extraction of the tree-core. To do that, we used both compound-specific colorimetric vials (or detector tubes) and a PID.

Colorimetric vials (GASTEC, AMS®), graduated glass tubes filled with an oxidant reagent substance, were inserted in each tree-hole to detect the presence of PCE, TCE, and VC. The method was introduced by ARTA Abruzzo (Agenzia Regionale Per La Tutela Dell'Ambiente; Luchetti and Diligenti, 2018). To avoid atmospheric influence, vials were clothed with Teflon tape. A GASTEC manual pump was used to create an inflow into the tube of the air present in the tree holes and pores. For each compound-specific detector tube, a number of pump strokes and a volume per stroke is indicated by the manufacturer based on the measuring range of the tube. For example for VC, two consecutive 50 mL pump strokes of 15 s duration were performed, with a resting interval of 45 s between the two. The measure is then noted manually by visualizing the graduated scale on the tube. After collection, each compound-specific measurement needs a correction for temperature (with specific correction factors given by the manufacturer) and for atmospheric pressure following the formula:

$$\frac{Tube\ reading\ (ppm)\ \times 1013\ (hPa)}{Atmospheric\ Pressure\ (hPa)}$$

Detection ranges vary among compounds: 0.2 – 3 ppm, 0.5 - 4.0 ppm, and 0.2 - 3 ppm for PCE, TCE, and VC, respectively. Moreover, colorimetric vials can show, during the detection phase, interference with other CEs. Particularly, since the substances that result from the chemical reaction occurring in the tube are identical to the target gases, a higher value than the actual concentration will be indicated.

Concurrently to detector tubes, a PID was inserted in the tree hole left by the coring tool, and measurements of VOCs sum concentration were detected. The instrument is equipped with a MiniRAE Lite monitor (Model PGM-7300), manufactured by RAE System (Honeywell Analytics®).

This model is equipped with a 10.6 eV lamp, a humidity compensator, and a suction pump. It detects VOCs in the range of 0-5000 ppm and the lamp is suitable for CEs with maximum detection values between 2000 and 5000 ppm. The lamp is also suitable for several other VOCs, such as BTEXS.

3.2.3 Statistical analysis

Following Leoncini et al. (2022) meta-analysis of literature data, Spearman's rank correlation coefficients (ρ; Journel and Deutsch, 1997) and Non-Detection rates (ND%) were determined on our data for each variable affecting the phytoscreening technique. ρ was calculated for assessing the correlation between gw and tree-core concentrations (quantitative phytoscreening) while ND% indicates the feasibility of a certain condition for the detection of CEs in trees (qualitative phytoscreening). The 22 surveys completed on the 8 sites led to a raw database of 112 samples, which correspond to 448 tree-core concentration data (as data were available for PCE, TCE, cDCE and VC). Data were then filtered for the tree-cores concentration that were also associable with gw concentration data. The final database included 198 tree-core concentration to use for ρ and ND% analysis with several outliers.

The data were not normally distributed and contained several outliers. Still, elimination of the outliers seemed unfeasible since the reasons for their occurrence lie in the many possible different factors affecting the technique, which is also the focus of this work. FIGURE 3.10 illustrates the difference between treating the data with the traditional Pearson's correlation coefficient (r^2) and with ranks as done with ρ. Spearman's ρ is indeed insensitive to outliers because it performs calculations on the ranks, so the difference between actual values does not have significance.

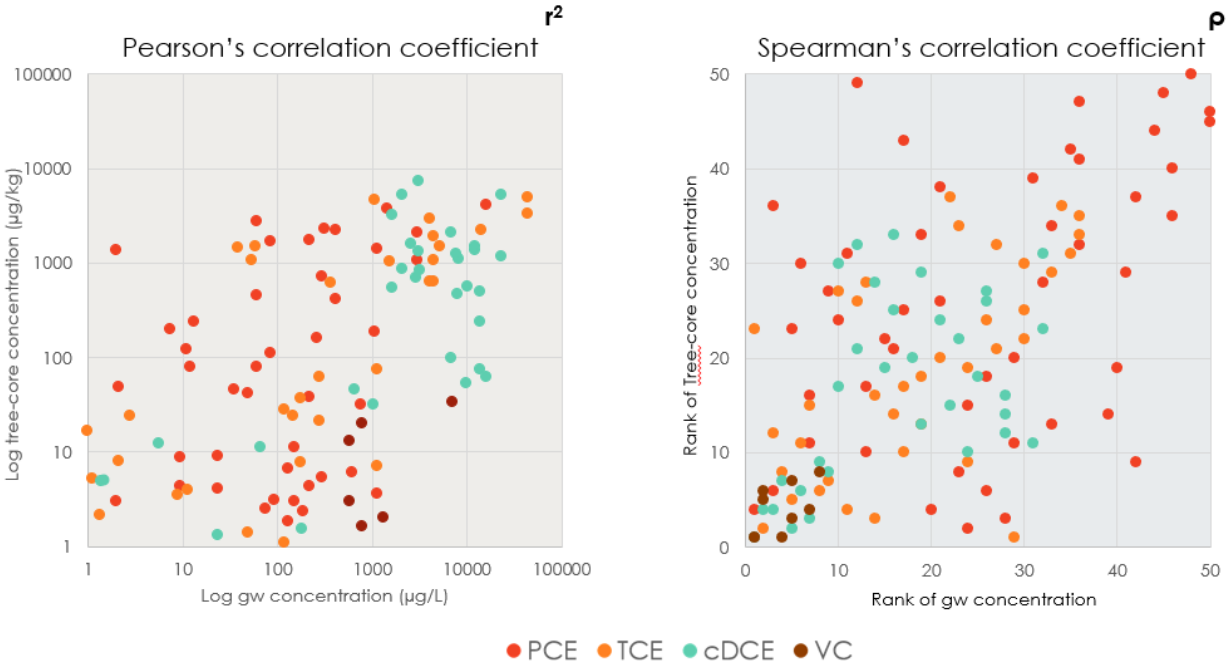

FIGURE 3.10. Comparison between Pearson's correlation (on the left) and Spearman's correlation (on the right) data treatment.

ρ and ND% were calculated separately for each compound (PCE, TCE, cDCE, and VC) to assess the influence of contaminant-specific properties such as molecular weight (M_w), water solubility (S_w), Henry's constant (H_c), and octanol-water partition coefficient (log K_{ow}). ρ and ND% were then calculated on the sum of the cited CEs. Factors in TABLE 3.2 were then split into intervals and ρ and ND% were derived for the concentration data within each interval. Only values associated with a minimum of 10 observations were considered in the statistical analysis.

TABLE 3.2. Factors potentially affecting the effectiveness of phytoscreening of CEs in selected intervals and number of observations.

Topic	Factors	Measuring unit	n° of available data (out of 198)	Selected intervals
Hydrogeology	Depth to water table (DWT)	m b.g.l. (below ground level)	110	DWT < 3, DWT ≥ 3
	Average aquifer thickness (b)	m	198	b ≤ 3, b > 3.5
	Aquifer hydraulic conductivity (K)	m/s	198	$K \leq 1x10^{-5}$, $K > 1x10^{-5}$
Tree identity and anatomy	Genus	e.g., *Populus*	198	*Aesculus, Celtis, Fraxinus, Platanus Populus, Quercus, Tilia*
	Xylem structure	e.g., coniferous	198	Diffuse-porous/Ring-porous
	Tree diameter at breast height (DBH)	cm	198	DBH < 50, DBH ≥ 50

As for hydrogeological parameters we considered: depth to water table (DWT in m b.g.l.), intended as the distance between ground level and the surface at water pressure equal to atmospheric pressure; thickness of the saturated portion of the aquifer (b in m) intended as the distance between the water table and the low permeability bottom of the aquifer; bulk saturated hydraulic conductivity of the aquifer (K in m/s). When K values of the aquifers were not specified in the sites' technical reports, ranges of conductivities were inferred in agreement with the local description of the lithology (Freeze & Cherry, 1979).

With regards to tree identity and anatomy, we retained information on the genus and the tree diameter at breast height (DBH in cm). Based on the genus and since only two genera exceeded the limit of 10 observations, we retrieved the correspondent xylem structure, intended as the distribution of pores and vessels among growth rings. The xylem, or sapwood, is the active portion of the trunk where water transport takes place. Since no conifer was sampled during our surveys due to the possible damages to the GC/MS, we considered only diffuse-porous and ring-porous xylem types (Panshin & de Zeeuw, 1970). Diffuse-porous xylems are characterized by small cells and randomly distributed large vessels, while ring-porous xylems have larger diameter vessels concentrated in the earlywood. Diffuse-porous trees tend to have deep functional xylems as well as low average conductivity due to small and short conduits. In contrast, most of the conductance in ring-porous species is isolated to the outermost annual growth ring that contains functional vessels (Bush et al., 2010; Cermak et al., 1992). For continuous factors (e.g., aquifer properties or tree diameter), we determined discrete intervals based on medians and percentiles associated with each factor to have a similar number of observations within each interval. To avoid biases associated with trees that could be growing above more dilute contamination areas, the ND% was calculated only when the concentration in gw was above 0.3 µg/L. This threshold was determined as the 5th percentile of gw concentration data. The final number of ND data was 63 out of 198 tree-core data. It is noteworthy that in some cases, such as when processing hydrogeological parameters like b and K, results may be uncertain since some parameters do not vary spatially across a specific site. Results were interpreted in terms of high or low correlations

(determining optimal factors conditions to characterize the contamination) and high or low detectability potential (determining optimal factors conditions to screen gw contamination).

3.3 RESULTS AND DISCUSSION

3.3.1 Study results

Below the results of the surveys are presented and followed by preliminary interpretations. For the results of chemical analyses, see the tables attached to this document (see Supplementary Materials). Afterward, the meta-analysis of the results of the global database of our study sites is presented.

3.3.1.1 A site

A preliminary survey was conducted at the site on June 29, 2020. The survey involved six trees: two lindens (A_PB1 and A_SP22; *Tilia sp.*), two maples (A_PB11 and A1_SP22; *Acer campestris* and *Acer saccharinum*), one oak (A2_SP22; *Quercus sp.*), and one alder (A_SI08; *Alnus sp.*). FIGURE 3.11 shows the results of the survey in terms of concentrations of CEs, BTEXS (BTEX + Styrene), and naphthalene (a polycyclic aromatic hydrocarbon; PAH) in the tree-cores (µg/kg). In 3 of the 6 trees sampled, BTEXS contamination (particularly styrene and benzene) was found in the order of tens of µg/kg. In similar concentrations, one of the sampled linden trees (A_SP22) showed the presence of naphthalene. In the westernmost area, another linden (A_PB1) showed a minimal presence of PCE and TCE (~2 µg/kg) and 1,1,2,2-TCA (Tetrachloroethane; 5 µg/kg), as well as styrene (~23 µg/kg). Colorimetric vials for benzene, PCE, and TCE were used on all trees sampled in the first survey without detecting any contamination.

These preliminary results were obtained in summer drought conditions and with temperatures peaking at 35° C, thus it was decided to undertake a further survey, which was carried out on 15 April 2021. The results are shown in FIGURE 3.12.

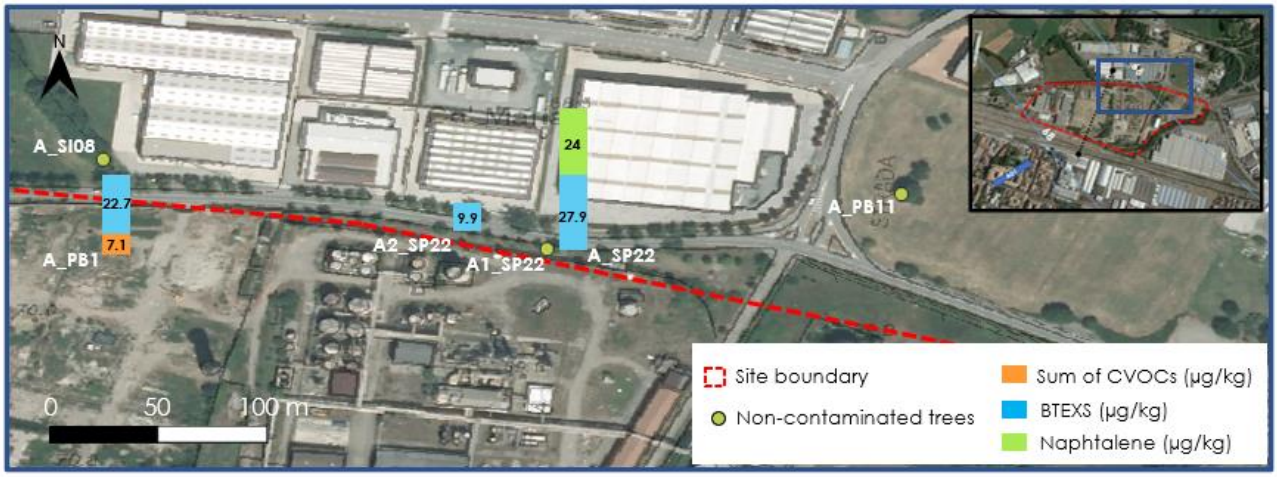

FIGURE 3.11. Site map and results of the first survey on the A site.

FIGURE 3.12. Site map and results of the second survey on the A site.

PCE (~1 µg/kg) and 1,1,2,2-TCA (14.4 µg/kg) and styrene (3 µg/kg) were again detected in the linden located at the western boundary of the company (A_PB1). Benzene (5.2 µg/kg) was again detected in the oak located in the central zone of the investigated area. A large size poplar tree (A_PB11b; *Populus nigra*), which was not investigated in the preliminary survey, showed a styrene concentration of 6 µg/kg. Alongside the traditional sampling at 100 cm a.g.l., it was also decided to drill at a lower elevation of the trunk (50 cm a.g.l.). The results are shown in FIGURE 3.13 and demonstrate a generally higher concentration of the compounds when sampling at 50 cm a.g.l. Colorimetric vials, once again, did not indicate the presence of contamination in the gaseous phase. The PID also showed no significant results, with the only exception for the poplar (A_PB11b) in which a concentration of VOCs of 0.1 ppm was registered.

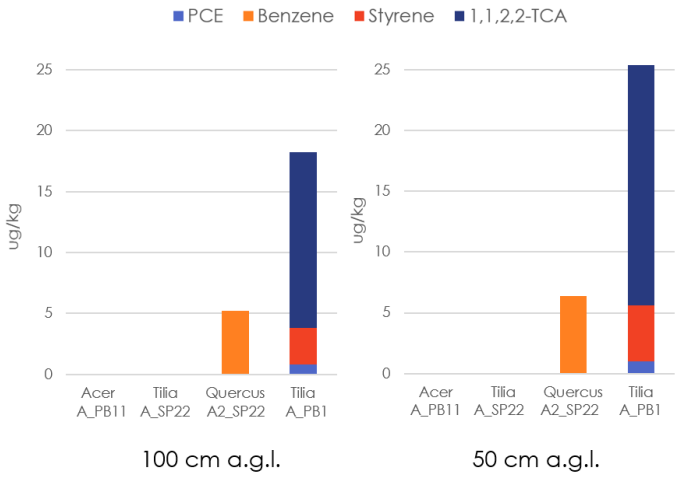

FIGURE 3.13. Comparison of tree-core concentrations detected at 100 and 50 cm a.g.l.

Although styrene was present in many samples, thus being traceable to a ubiquitous presence in the aquifer, it is worth noting that this hydrocarbon is also naturally produced by some species of trees. This may therefore lead to some misinterpretations when dealing with phytoscreening for styrene contaminations. Moreover, an overall higher concentration of the investigated compounds was found when sampling tree-cores at 50 cm a.g.l., confirming the occurrence of an increase in volatilization loss as the compounds travel up in the trunk as also found in Leoncini et al. (2022). We have also to take into account that the general decrease in concentrations in trees in the second survey (with the exclusion of the linden tree in the western portion of the study area) could be due to the important difference in cumulative precipitation between the summer period of the first survey and the spring period of the second survey (FIGURE 3.14). Precipitation, in the form of recharge, can dilute concentrations in the aquifer, impairing the effectiveness of the technique.

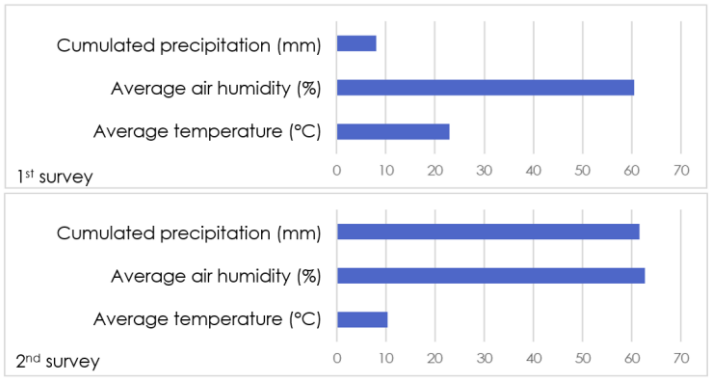

FIGURE 3.14. Meteorological conditions in the two weeks before each survey (Salso Maggiore meteo station; source: Dext3r - ARPAE)

3.3.1.2 B site

The 2 surveys on the B site (upper part of FIGURE 3.15) were carried out 2 months apart (September 3 and November 4, 2020). On October 14, 2020 (lower part of FIGURE 3.15) gw sampling was also performed. In one linden tree (*Tilia sp.*; A_C2) the PCE and TCE are in the order of thousands of µg/kg, while in the nearby piezometer C2 only a PCE gw concentration of 2 µg/L was detected (see FIGURE 3.16 for tree and piezometer locations). On the contrary, the results on a poplar (*Populus alba*; A_C6) located downstream to A_C2, were comparable to gw concentrations. Especially in the second survey, the sum of CEs concentration detected in A_C6 was ~120 µg/kg, while the concentration detected in gw (piezometer C6) was ~70 µg/L. Slightly to the east, an oak (A_C3; *Quercus sp.*) shows results (average of ~20 µg/kg) not in agreement, in terms of the relative magnitude of concentration, with gw concentrations (piezometer C3; ~200 µg/L) in both surveys. In a linden located west of the site (A_C10), PCE concentrations in gw (~200 µg/L) are comparable to the average PCE concentration detected in the two phytoscreening surveys (343 and 38 µg/kg in the first and second survey, respectively).

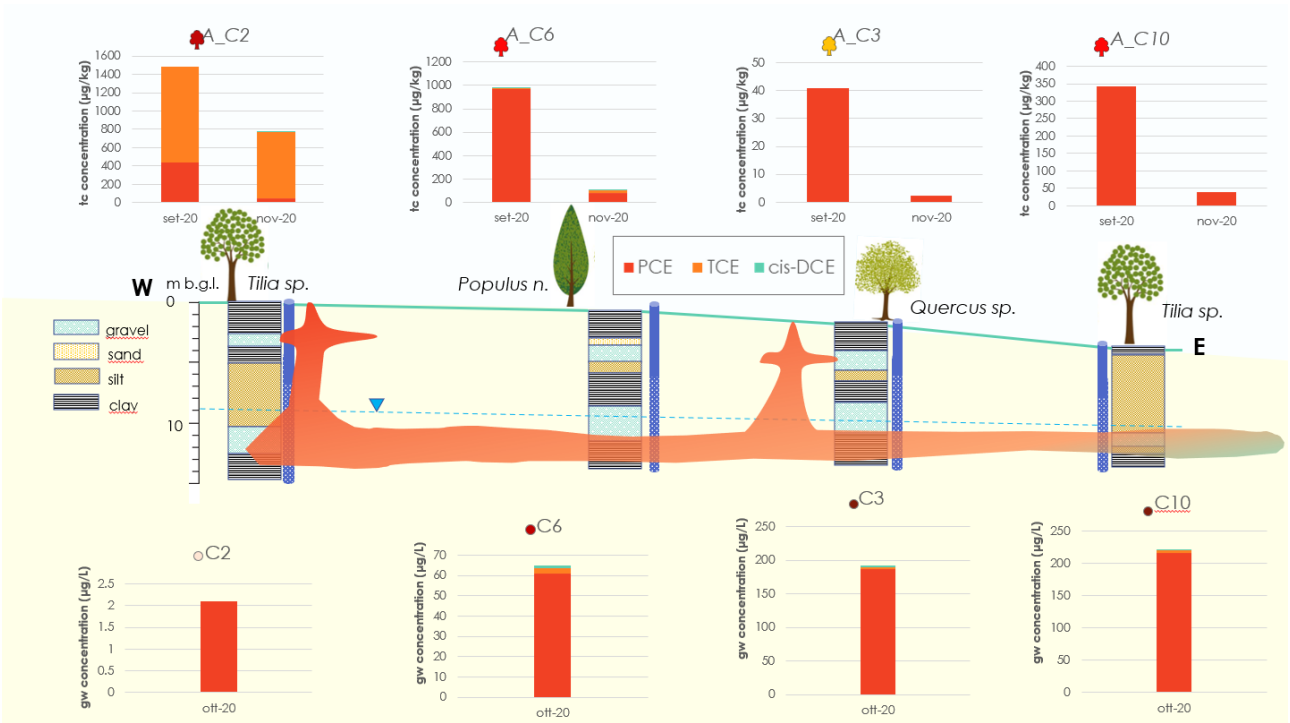

FIGURE 3.15. Hydrogeological section of B site showing tree-core concentrations in the 2 surveys (upper part) and gw concentrations (lower part). See FIGURE 3.16 for the map reference section.

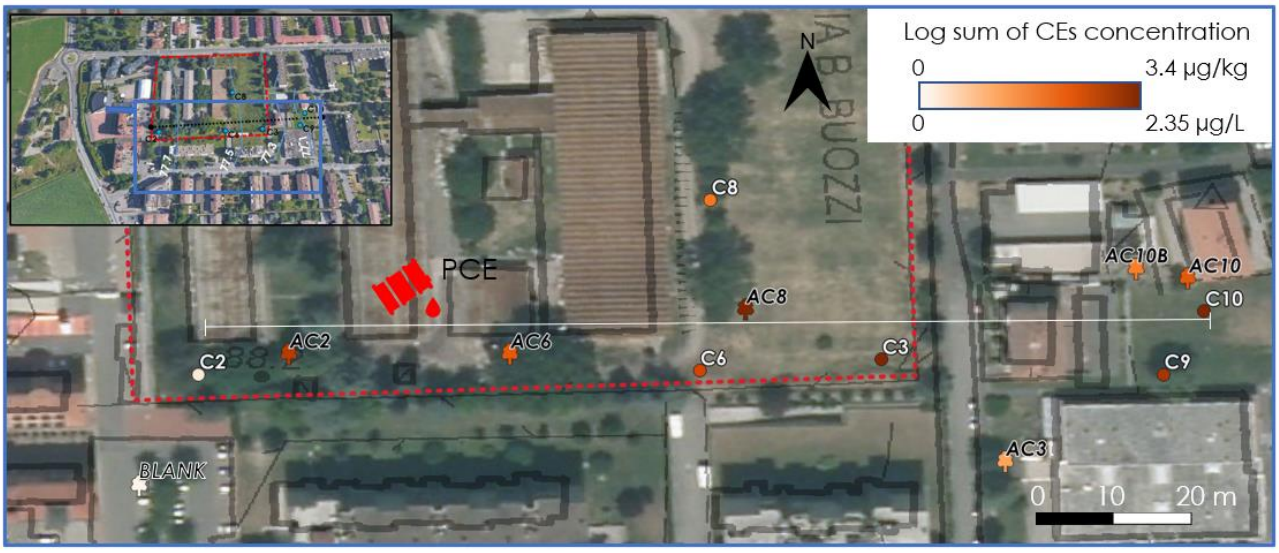

FIGURE 3.16. Site map with indication of the section of FIGURE 3.15 (in white), piezometers (indicated with circles), and trees. Concentrations in tree-cores and gw are indicated in log terms. A possible location of the source zone is indicated in red

In both surveys, it was also possible to test the quality of the results obtained using the PID along with the PCE and TCE colorimetric vials.

FIGURE 3.17 shows a comparison between tree-core and PID concentrations. It is to note that, although in absolute terms the concentrations are higher in the tree-core analysis, the concentrations measured with the PID are comparable in log value terms. On the other hand, there are also critical issues related to PID measurements. The instrument indeed detected a relevant concentration of VOCs in the tree-core of an elm tree (indicated as BLANK in FIGURE 3.16 and 3.18A), which was sampled as a blank, being located upstream of the probable contaminant plume. In the same tree, both the tree-core and the colorimetric vials analysis did not show any contamination by CEs (FIGURE 3.18A). Other doubts on the PID effectiveness arise from the analysis of the linden located downstream of the site (A_C10). In the first survey, the linden shows a relevant CEs tree-core concentration (~340 µg/kg), while both the PID and the colorimetric vials did not detect the presence of VOCs in the gaseous-phase. These drawbacks seem exceptions since PID analyses were able to detect concentrations as low as 0.1 ppm when the concentrations in the tree-core were around 0.1 µg/kg, as confirmed also by results on the D site (SECTION 3.3.1.4).

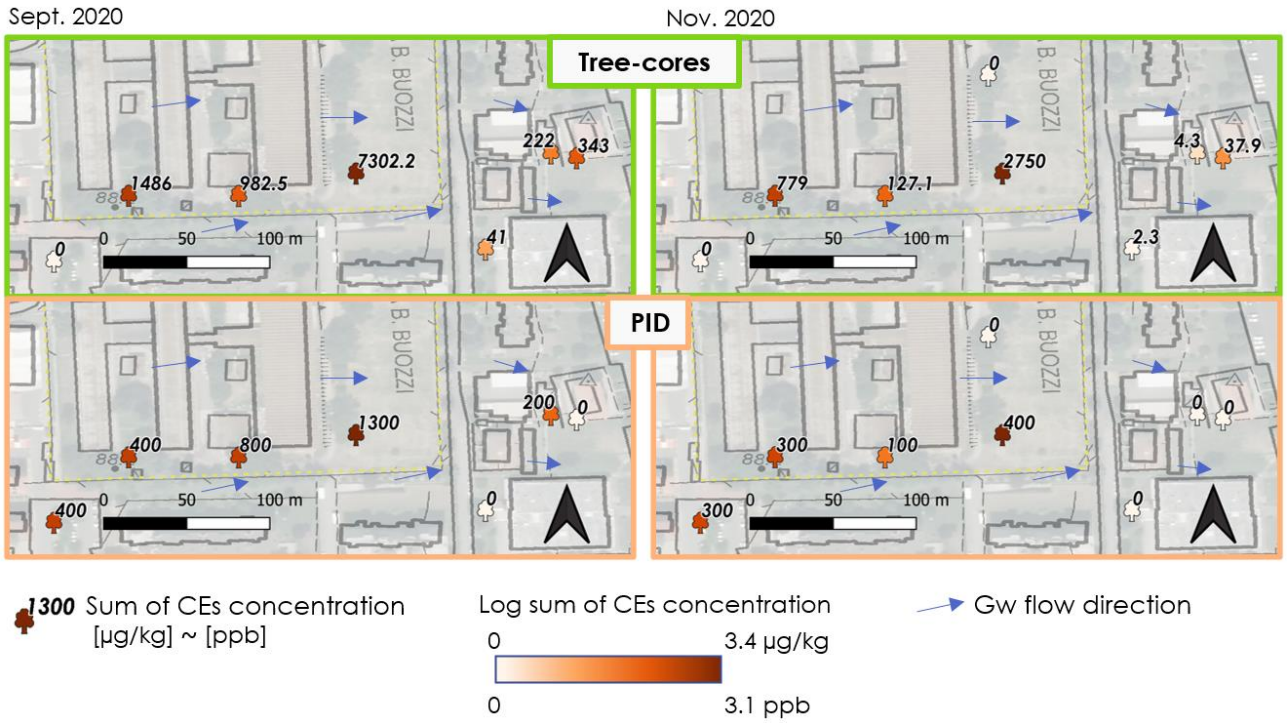

FIGURE 3.17. Comparison between tree-core and PID concentrations in the first survey (on the left) and in the second survey (on the right). Concentrations are given in log terms of the sum of CEs.

The same rule did not apply to colorimetric vials, for which the lower available measurement was 0.2 ppm with respect to a tree-core concentration of almost 1000 µg/kg. As a final consideration, the correlation between tree-cores and PID concentration and tree-cores and colorimetric vials concentration differs widely. The PID shows correlation values that are comparable among the two surveys (r^2 = 0.77 and 0.71 for the first and second survey, respectively), while the vials reveal a very high correlation in the first survey (r^2 = 0.96) and a very low one in the second (r^2 = 0.26; FIGURE 3.18B). An important concentration of TCE was detected in the western upgradient linden (A_C2) although this compound did not occur in gw. This evidence might indicate vadose zone contamination, which is absorbed by the tree together with capillary water. A thin gravel layer is indeed present at around 2 to 3 m b.g.l. This could act as a storage for this shallow contamination, which is not detectable by gw analysis since piezometers are filtered deeper into the aquifer (7 to 15 m b.g.l.).

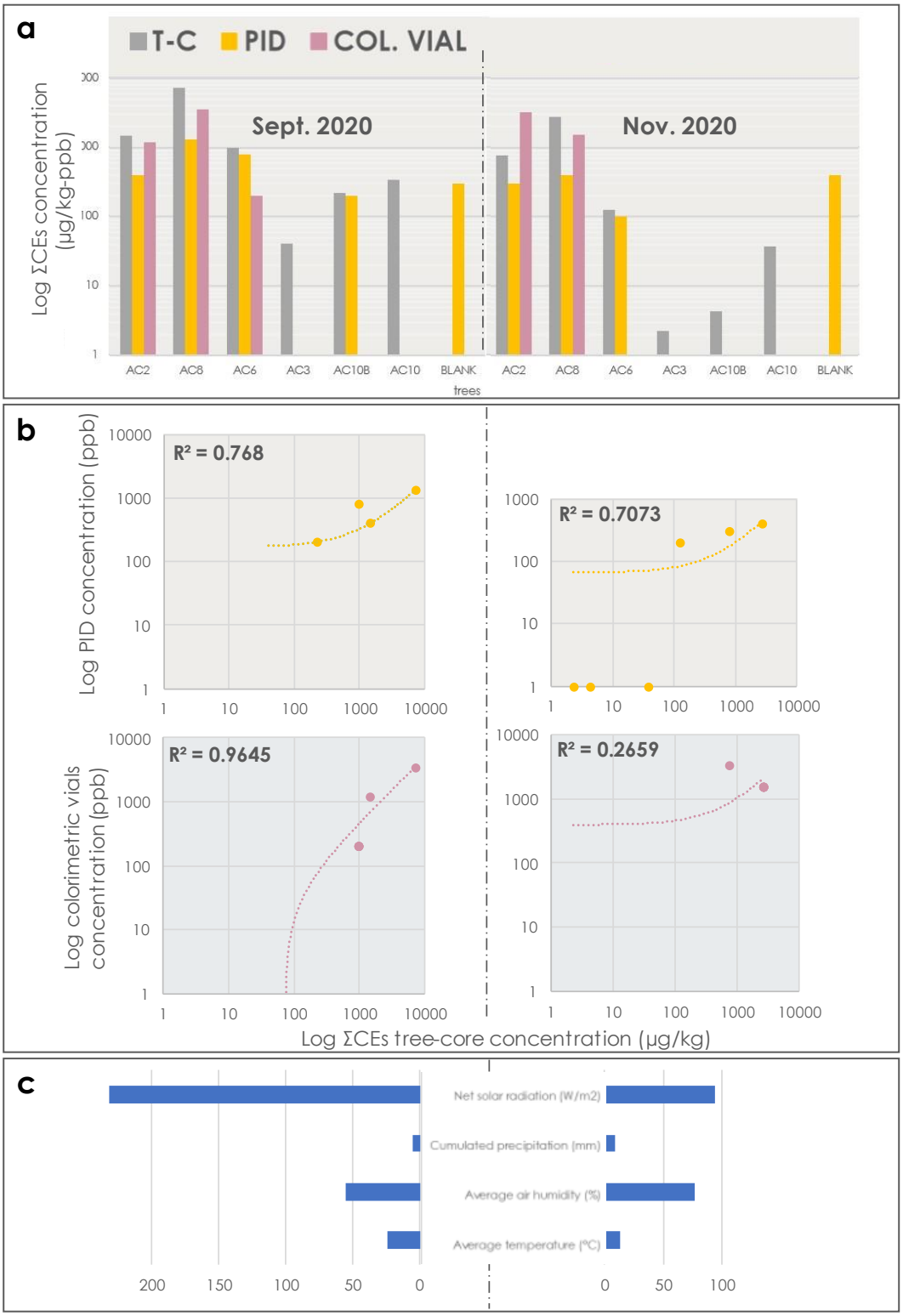

FIGURE 3.18. a) Comparison between tree-cores (T-C; green), PID (orange), and colorimetric vials (pink) concentrations in the two surveys; b) Correlation between PID and tree-core concentrations (orange) and colorimetric vials and tree-core concentrations (pink) in the two surveys; and c) Meteorological conditions in the two weeks before each survey (Sasso Marconi - Casalecchio Canale meteo station; source: Dext3r - ARPAE)

The high concentration detected in the poplar (A_C6; ~1000 µg/kg of the sum of CEs) in the first and second surveys could be attributed to both the vicinity to the source zone and the ability of this genus to uptake and store large amounts of water and contaminants compared to other genera, a quality for which poplars are often used in phytoremediation activities (e.g.; Hirsh et al., 2004).

The incompatibility in concentrations among gw and the investigated oak (A_C3) could be related to the specific xylem structure of this genus. Oaks are indeed ring-porous trees that, unlike conifers and diffuse-porous trees, have an annular porosity among tree rings. Because of this plant physiology property, the flow of absorbed gw is concentrated in the outermost rings of the trunk (Ellmore and Ewers, 1986), thus promoting compounds phytovolatilization out of the tree.

Finally, we could speculate that the finer sediments occurring below the eastern linden (A_C10; see FIGURE 3.15) are responsible for a delay in the uptake of the contaminants by the plant which is not visible in trees located in areas above macroclastites. This delay could explain why the concentration in gw corresponds to the mean concentration in tree-cores in the two surveys. More investigations are needed to corroborate this hypothesis.

Generally, a great difference in concentrations in trees was observed between the two surveys. In the second survey, CEs concentrations are reduced by up to an order of magnitude compared to the first survey in the light of similar precipitation rates (5.2 and 8.6 mm, in the first and second survey, respectively; FIGURE 3.18C). Most probably, the higher average temperatures (24° and 13.5° C, in the first and second survey, respectively) and higher net solar radiation (232 and 94 W/m^2, in the first and second survey, respectively) observed in the two weeks before sampling in the second survey are responsible for an increased tree transpiration process. This increase causes a higher gw uptake by the tree, resulting in a higher contaminant availability in the tree tissue. Eventually, the effectiveness of tree-core analysis has been demonstrated for deep contaminated aquifers (DWT ~ 9 m b.g.l.).

Notwithstanding the difference in concentration in absolute terms between tree-cores and PID measurements, the observed correlation is good. PID concentrations are however given in terms of

the sum of all VOCs and among these compounds, there is also styrene. Its presence is probably attributable to the same origin of the blank samples extracted from the eastern elm (BLANK). Indeed, concentrations in the tree-cores and colorimetric vials measurements showed the absence of CEs in this tree (BLANK in FIGURE 3.18A), demonstrating indirectly the likely presence of styrene or other VOCs.

The comparison between PID and colorimetric vials results shows that the PID analysis has a lower limit of detection (100 µg/kg) than the colorimetric vials (1 mg/kg) with respect to tree-core analysis concentration range. PID analyses showed a detection limit comparable to its instrumental detection limit (100 ppb), demonstrating its high practical utility in phytoscreening surveys.

One of the causes for the absence of a PID detection noted in the eastern linden tree (A_C10; tree-core analysis showing a total of CEs concentration up to 340 µg/kg) could be related to the less permeable lithology of the vadose zone in this area (see stratigraphy of piezometer C10 in FIGURE 3.15) that could hinder volatilization processes from the unconfined aquifer thus limiting the migration of CEs gaseous-phase and preventing its uptake by the tree and the consequent detection with the PID.

The correlation between PID and tree-core concentration did not differ between the two surveys whereas the correlation between colorimetric vials and tree-core concentrations differed widely between the two surveys. We can speculate that colorimetric vials measurements are subject to atmospheric water vapor content and temperature variations, whilst results obtained by the PID are less dependent on seasonal variations. Relative air humidity and temperature were indeed respectively higher and lower in the second survey (FIGURE 3.18C) when the colorimetric vials mostly failed in the detection of CEs.

3.3.1.3 C site

Two surveys were completed on the C site on September 9 and December 1, 2020 (FIGURE 3.19 and 3.20). In the preliminary survey, two poplars (A_PZPARCO and A_MM1; *Populus nigra* and

Populus alba) of large trunk diameter (~60 cm), located in poorly investigated areas that were presumed to be free of contamination, showed PCE concentrations around 1 µg/kg. In contrast, a linden (A_PZPIAVE12; *Tilia sp.*) and a horse chestnut (A_MM2; Aesculus hippocastanum), located above the supposed plume area, did not detect any contamination. In the second survey, the same poplars did not show any contamination.

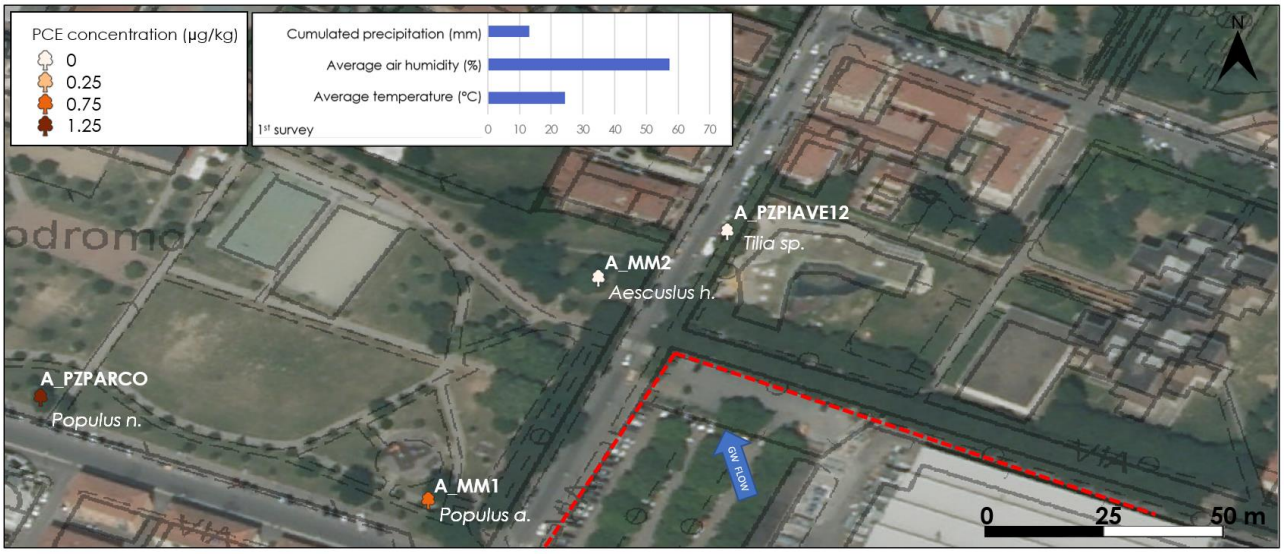

FIGURE 3.19. Site map and results of the first survey with the indication of meteorological conditions in the two weeks before the survey (Bologna idrografico -Torre Asinelli meteo station; source: Dext3r - ARPAE)

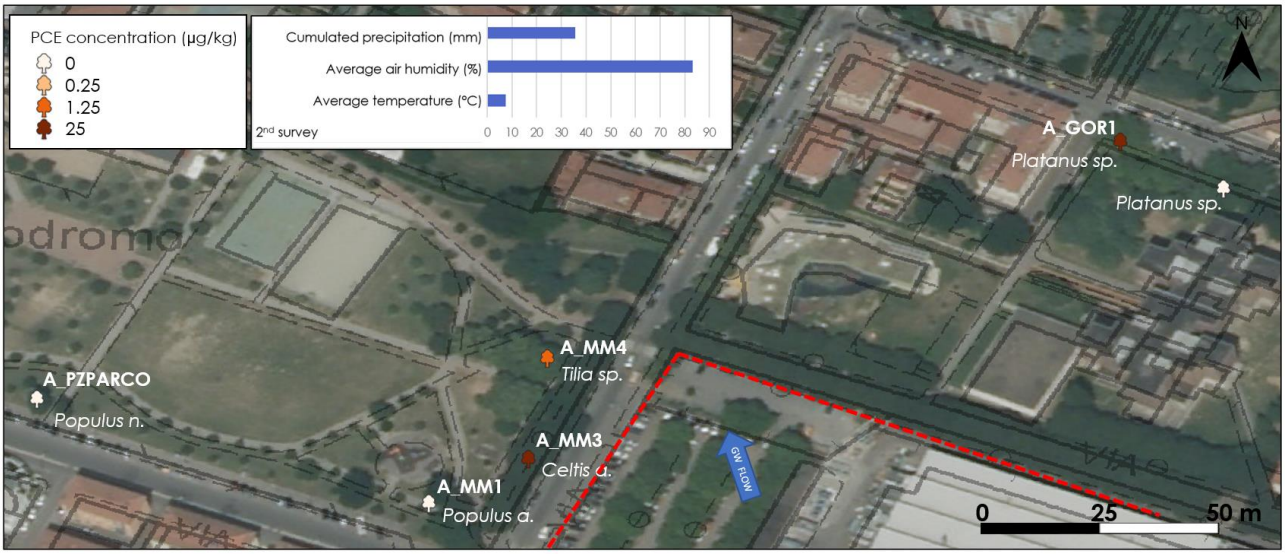

FIGURE 3.20. Site map and results of the second survey with the indication of meteorological conditions in the two weeks before the survey (Bologna idrografico -Torre Asinelli meteo station; source: Dext3r - ARPAE)

However, a linden (A_MM4; *Tilia sp.*) and a hackberry (A_MM3; *Celtis australis*) of large diameter (> 60 cm), located at less than 20 m from the previously investigated linden and chestnut, showed PCE concentration of 0.5 and 25.6 µg/kg, respectively. Further downgradient to the gw flow, two planetrees (A_GOR1 and A_GOR2; *Platanus sp.*), which were close to each other (~10 m) and with similar diameters (~50 cm), showed different responses: only one of them showed contamination by PCE of 1.4 µg/kg.

On this site, the PID showed results that are rarely comparable to tree-core analyses. In the second survey, as an example, whilst the instrument did not detect VOCs contaminations in the most contaminated tree (hackberry; A_MM3), it did detect contamination in the two poplars (A_PZPARCO and A_MM1; 0.4 and 0.1 ppm for the black and white poplar, respectively) which showed a PCE tree-core contamination only in the first survey.

Although these were only exploratory findings, we can speculate that the concentrations detected in the trees of this site are the result of the uptake, in the vadose zone, of either gaseous-phase contamination or contaminants in the capillary or retention water where the dissolved phase is partitioned from the gaseous phase. Other than the PID measurements, this assumption is based on the occurrence of a very deep contaminated aquifer (DWT ~ 23 m b.g.l.) and shallow contamination in the vadose zone. Site investigations could furtherly explain the reason for the non-detection of CEs in several sampled trees (neither by tree-core analysis nor by the PID). It is indeed evident from MIP profiles that in certain areas the contamination is located slightly deeper than in other areas. This could be due, for example, to the local higher thickness of the fine-grained layer above the main aquifer thus preventing gaseous-phase contaminants to travel further up and being absorbed by roots. Another reason for the different detection rates in the two surveys might be associated with seasonal variability, with the second survey having higher precipitation rates and lower temperatures than the first one (cumulative precipitation of 13 and 37 mm and an average temperature of 25 and 8° C, in the first and second survey, respectively). In this specific site, these different conditions could have either hindered accumulation in the tree, with higher temperature causing volatilization loss out of

the trunk, or promoting a more effective uptake with precipitation diluting gaseous-phase contaminants in the vadose zone. Despite these uncertainties, the coupling of tree-core and PID analyses returns a quite comprehensive contamination profile, even in the case of deep confined aquifers and the occurrence of contaminants in the vadose zone.

3.3.1.4 D site

On the D site, 10 trees were sampled on January 10, June 30, and November 11, 2020. Gw sampling (conducted in February and November 2020) and relative tree-coring data show a good correspondence between both detected compounds and concentration values (FIGURE 3.21). In all the surveys a delineation of the contaminant plume was possible through tree-core data (e.g., FIGURE 3.22). In addition, in two poplars (A_PZ9 and A_PZ10; *Populus nigra* and *Populus sp.*), located downgradient, relevant contamination was detected (sum of CEs concentration ~ 90 and 1000 µg/kg in A_PZ9 and A_PZ10, respectively) although low concentrations were detected in gw (sum of CEs concentration ~ 10 and 200 µg/L in PZ9 and PZ10, respectively).

Among all the sampled species, one of the ash trees (A_PZ12; *Fraxinus Excelsior*) showed concentrations that were incomparable to nearby trees and boreholes. For example, in the third survey, the ash tree showed a PCE concentration of 2.5 µg/kg, while the nearer borehole showed 74.3 µg/L. The nearest poplar (A_PZ3; *Populus alba*) and another nearby ash tree (A_PZ13) showed PCE concentrations of 2260 and 187 µg/kg, respectively.

Overall, a very high correlation between tree-core and gw concentration was achieved for PCE (r^2 = 0.94), being also the prevalent compound in gw. The lighter TCE and cDCE were more rarely detected in trees, whilst VC, scarcely occurring in gw (< 5 µg/L), was not detected in trees.

The correlation between colorimetric vials and tree-core concentration was fairly good for PCE (r^2 = 0.53), whilst poorer for TCE (r^2 = 0.37). The correlation between PID and tree-core concentration for total CEs was good (r^2 = 0.67).

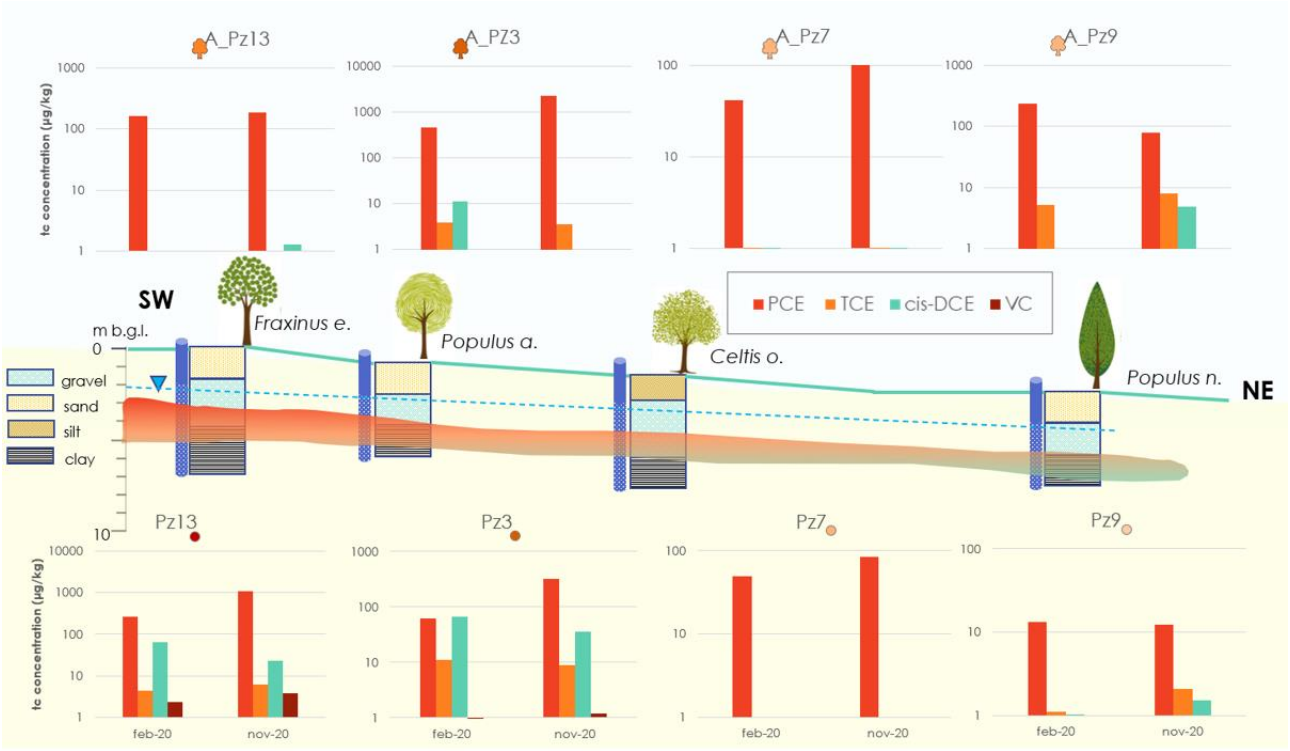

FIGURE 3.21. Hydrogeological section of D site showing first and third survey tree-core concentrations (upper part) and respective gw concentration (lower part). See FIGURE 3.22 for the map reference section

FIGURE 3.22. Site map with indication of the section of FIGURE 3.21 (in white), piezometers (indicated with circles), and trees. Concentrations in tree-cores and gw are indicated in log terms and correspond to the third survey

The survey of this site showed that phytoscreening can improve a contamination delineation in poorly investigated areas, especially when the DWT is shallow (~3 m b.g.l.) and the aquifer is permeable (K ~ 1 x 10^{-3} and b = 2 m). The results indeed suggest a more advanced downgradient migration of the contamination than expected, and further investigations are needed on the fate of CEs downstream of the investigated area. With regards to the ash tree (A_PZ12) which presented lower concentrations than expected, a possible explanation is that this specific tree has a smaller diameter (20 cm) than the other nearby trees (54 and 27 cm for the poplar and the other ash tree, respectively) and thus a shorter tree-core was sampled. Moreover, the data and the higher correlation of the most prevalent PCE suggests that there is a certain threshold of gw concentration below which the trees seem to not be able to detect the contamination. Among CEs, PCE is the compound with the highest tendency to be adsorbed to organic matter ($\log K_{ow}$ = 3.4), thus possibly being more subject to phytoaccumulation in the tree tissue. Moreover, the high correlation found in this site with both colorimetric vials and PID measurements could be associated with PCE relatively higher volatility (H_c = 0.492), promoting its occurrence in the gaseous-phase inside the tree.

3.3.1.5 E site

Phytoscreening surveys were carried out on the E site on November 30, 2018, March 26 and October 10, 2019, and March 6, 2020. FIGURE 3.23 shows the CEs gw isoconcentration map of the E site on the second survey compared to tree-core concentrations in log terms. Very similar results were obtained in the four surveys in terms of correspondence between tree-core and gw concentration (FIGURE 3.24). PCE correlation between tree-cores and gw denoted higher values with respect to TCE and cDCE, such as shown in site D (SECTION 3.3.1.4). VC was detected rarely in concentrations corresponding to the GC/MS detection limit (~ 0.0005 mg/kg). Colorimetric vials measurements also detected VC in trees, in concentrations up to 2 ppm.

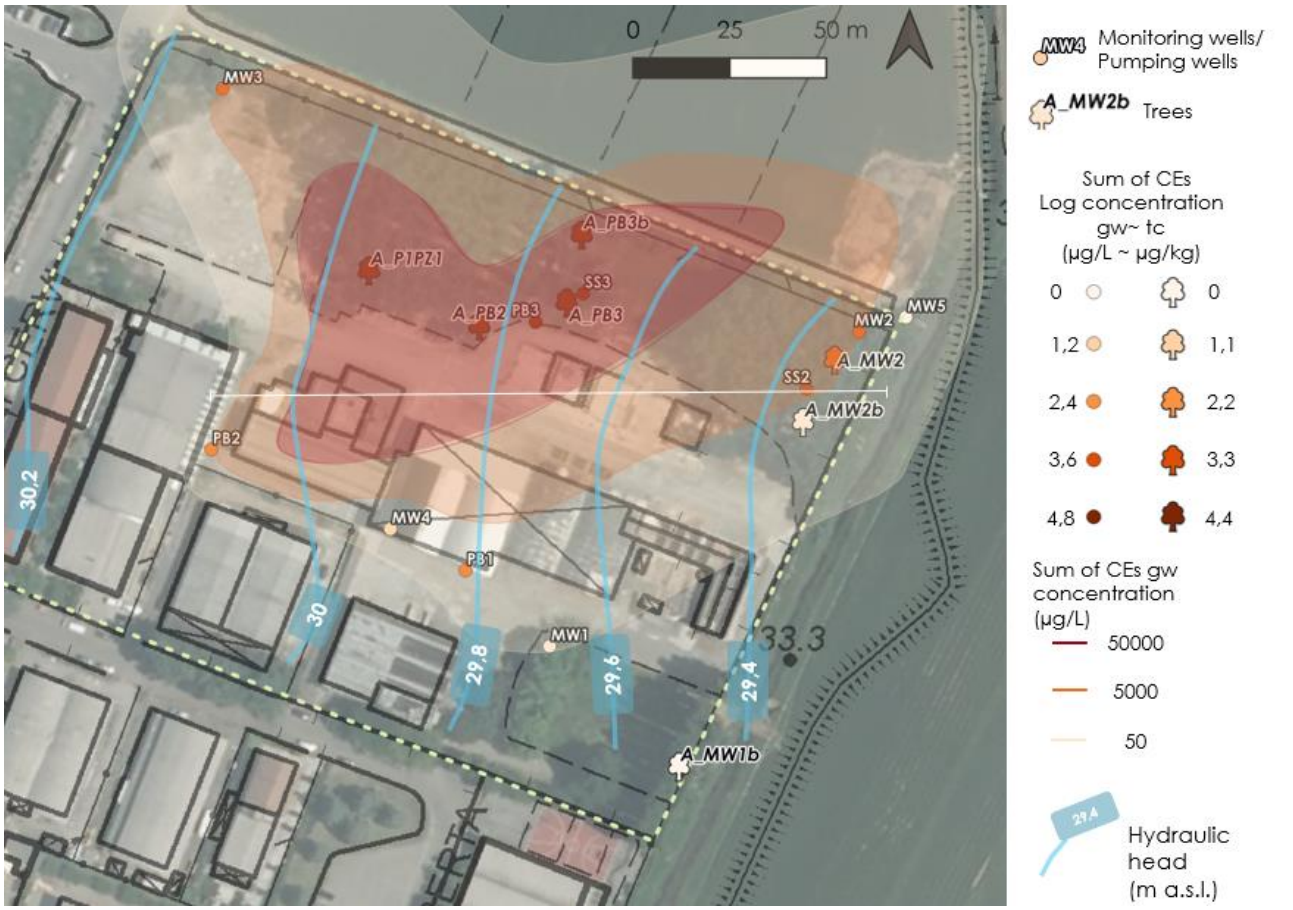

FIGURE 3.23. Site gw isoconcentration contour map with indication of the section of FIGURE 3.24 (in white) and relative gw and tree-core concentration expressed in log terms.

The comparison of the gw contamination (related to the blue piezometers in the section in FIGURE 3.24) and the contamination in trees (related to the poplars illustrated on the section) shows an accumulation of the higher CEs in trees, namely PCE and TCE, whilst the lighter cDCE and VC are more poorly represented. Also, similar temporal variation in concentrations in gw and tree-cores can be seen, especially when considering the total CEs rather than single compounds. One exception is given by the poplar located downstream of the contaminant plume (A_MW2). Gw monitoring indeed showed an increase in cDCE and VC, due to active bioremediation activities, while the tree shows a decrease in concentrations of all the compounds.

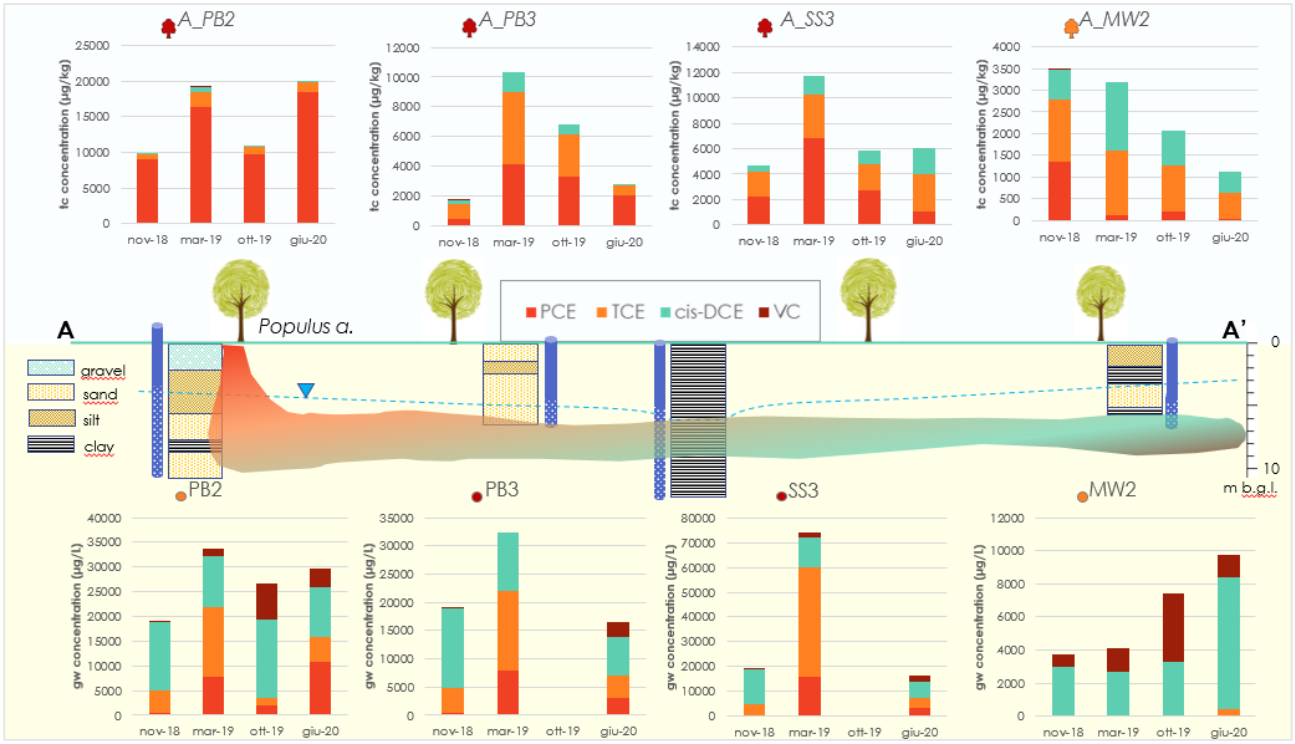

Figure 3.24. Hydrogeological section of E site showing tree-core concentration in the 2 surveys (upper part) and respective gw concentration (lower part). See FIGURE 3.23 for the map reference section

The E site was an excellent test field for phytoscreening given the presence of an extensive poplar grove (*Populus Alba* and *Populus Nigra*) just above the contaminated area. The delineation of the contamination assessed by the trees almost perfectly fits the gw concentration map. This is possible thanks to the great absorbing capacities of poplars and the presence of a shallow (DWT ~ 3 m b.g.l.) and relatively thin aquifer (b ~ 3 m). The results also show that trees are accumulating higher chlorinated compounds. Other than the poplars themselves, a possible explanation is related to the higher sorption of PCE and TCE with respect to cDCE, while the absence of VC in trees is possibly explained by its very high volatility.

Even though colorimetric vials revealed contamination by VC, the compound barely showed its occurrence in the tree-cores. Moreover, VC colorimetric vials can show, during the detection phase, interference with other CEs, in particular with TCE and cDCE. This may further contradict the hypothesis of its presence in trees. The overall good temporal consistency of CEs concentration in

trees with respect to gw demonstrates that the use of trees in hydrogeology may also have effectiveness in monitoring contamination status over time. The different results associated with the downstream poplar tree (A_MW2) could indeed be associated with the presence of a confining layer in that aquifer section, which could have delayed the tree uptake of the lighter compounds.

3.3.1.6 F site

Two surveys were carried out on the F site on September 9, 2020, and May 5, 2021, for a total of 10 investigated poplars (*Populus alba*). FIGURE 3.25 shows the location of the investigated trees and related piezometers along with the sum of CEs detected in tree-cores and gw. Several times, tree-core analyses detected contaminants that were not or were detected in small amounts in nearby piezometers (FIGURE 3.26), such as PCE, trichloromethane (CF), and tetrachloroethane (1,1,1-TCA). Besides sampling at 100 cm a.g.l., a second core extraction was performed at 50 cm a.g.l. The results are shown in FIGURE 3.27. Such as in the A site, an overall increase in concentrations is reported for samples extracted at 50 cm a.g.l. In some cases, sampling at a lower height allowed the detection of contaminants that were not detected higher up the trunk, such as in A_PZ3 and A_PM4 where PCE and CF were detected only at 50 cm a.g.l.

The analyses performed with the PID at 100 cm a.g.l. showed a concentration of 2.5 ppm only in one poplar (A_PM1), where the total of CEs was 1.6 µg/kg and CF was also detected (5.9 µg/kg) in tree-cores. In the same poplar (A_PM1) the PID analysis at 50 cm a.g.l. showed a concentration of 2.9 ppm. The PID analysis also showed a concentration of 0.3 ppm in another poplar (A_PZ3), only at 50 cm a.g.l. In this case, the sum of CEs was 3.6 µg/kg. On the contrary, colorimetric vials measurements did not show any contamination in the gaseous-phase in any of the sampled trees.

FIGURE 3.25. Site map with indication of gw and tree-core concentrations of the sum of CEs in the second survey.

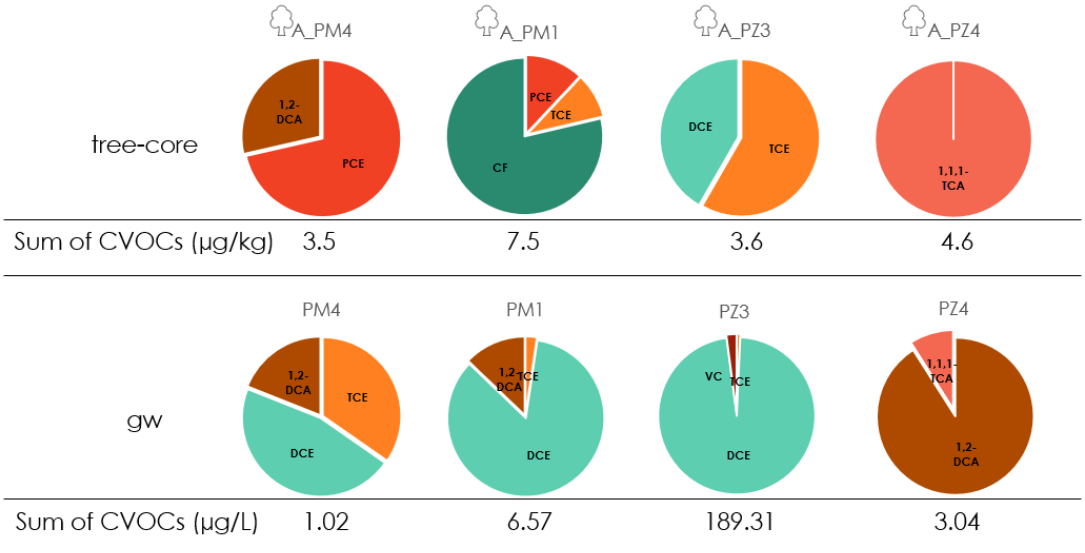

FIGURE 3.26. Comparison between tree-core and gw concentrations of chlorinated VOCs (CVOCs) at the F site in the second survey.

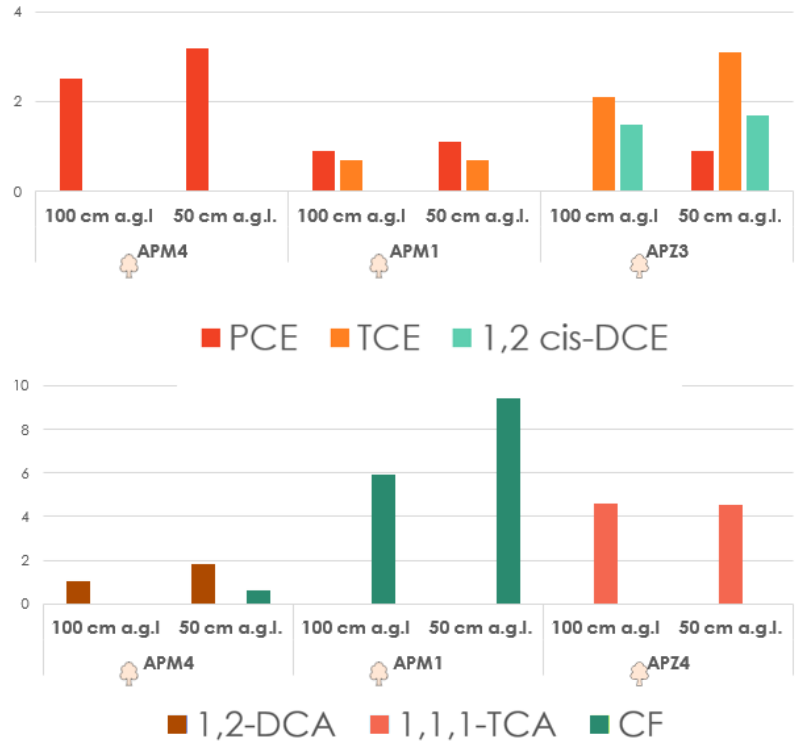

FIGURE 3.27. Comparison of tree-core concentrations detected at 100 and 50 cm a.g.l.

The results of the surveys carried out at the F site reflect the underground complexity of the contaminated site. The trees indeed seem to uptake contaminants that were not detected in gw analyses. A feasible explanation could be based upon the fact that piezometers at the site are usually screened at an interval between 6 and 10 m b.g.l., thus in the lower portion of the unconfined aquifer. Tree roots usually penetrate down to the capillary fringe or water table without going further inside the saturated zone. In this way, tree uptake of gw and correspondent tree-core analysis at this site could be associated with the higher portion of the unconfined aquifer rather than the lower one, showing concentrations that are widely different from gw samples.

Eventually, the results of the extraction at 50 cm a.g.l. corroborate the hypothesis that phytovolatilization processes could happen along the tree trunk, discriminating between detection and non-detection in the tree-core analysis, as well as the PID measurement. Colorimetric vials were not effective in this case, presenting a higher detection limit than the PID.

3.3.1.7 G site

On July 16, 2018, a first survey was carried out aiming at identifying the CEs plume flowing out of the Southern Dump (SD) of the G site in Ferrara. The focus of this survey was the detection of VC in trees, which is here strongly occurring both in A0 and in the deeper A1 aquifers. However, the survey did not detect the presence of CEs in the 10 sampled trees (FIGURE 3.28). Following these results, the samplings were transferred to the Northern Dump (ND) of the site, where the shallow aquifer is also heavily contaminated by VC. Here, a multilevel monitoring system (MLS), drilled for another research (Filippini et al., 2020), is screened in 8 intervals of A0, 1 m long each. The MLS, named MS2, is adjacent to a branched black poplar (A_MS2; *Populus Nigra*; FIGURES 3.28 and 3.29) with two large-diameter branches (A1_MS2 and A2_MS2; 60 and 46 cm, respectively).

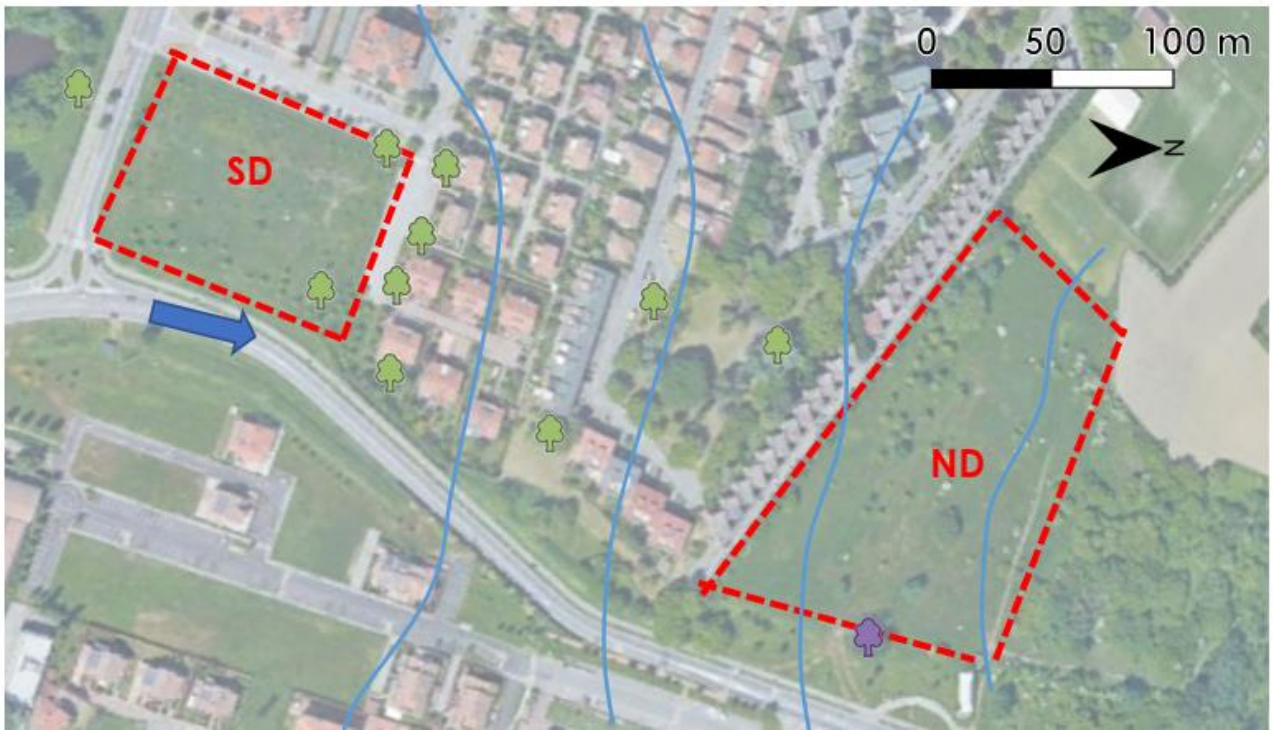

FIGURE 3.28. Site map showing the investigated trees in the first survey (green) and poplar A_MS2 (purple)

In order to investigate and monitor the presence of VC in this poplar, 4 surveys were carried out on May 22 and October 11, 2019, and on June 24 and September 24, 2020.

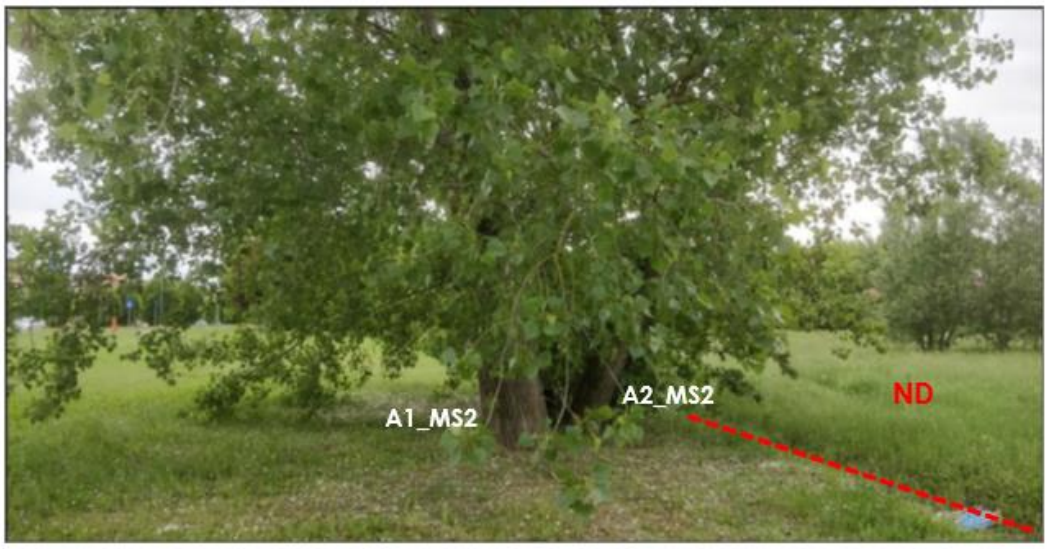

FIGURE 3.29. Picture of the branched black poplar A_MS2 on the edge of the ND

In these surveys, besides tree-core samples from the two branches, gw samples were retrieved from the different screened intervals of the MLS. Except for the last sampling, in all the surveys VC was detected in the poplar with concentration in a range from 1.6 to 33 µg/kg. Concentration in gw in the upper interval of the MLS (2 to 3 m b.g.l.) ranged from 119 and 7181 µg/L, with a substantial decrease from the first to the last survey. The upper interval (MS2_-3) was the one denoting a higher correlation between the concentration in gw and the tree-cores in both the poplar branches (r^2 ranging from 0.87 to 0.99 among the surveys). The correlation decreased slightly for the second screened interval from the top (3 to 4 m b.g.l.; r^2 ranging from 0.5 to 0.84), while it dropped down in the deeper intervals (e.g., MS2_-5; $r^2 \leq 0.1$ in all the surveys; FIGURE 3.30). Even so, a good correspondence between concentrations can be observed between the trees and the first and third interval from the top of the MLS (FIGURE 3.30; MS2_-3 and MS2_-5). Besides, a substantial difference in the pattern of values of concentration can be observed between the two tree branches (FIGURE 3.31; A1_MS2 and A2_MS2).

After Ottosen et al. (2018), this is the second study that clearly identifies VC in trees. In our study, VC in tree cores was no more detectable after gw concentrations dropped under 300 µg/L, indicating a possible uptake threshold for this compound.

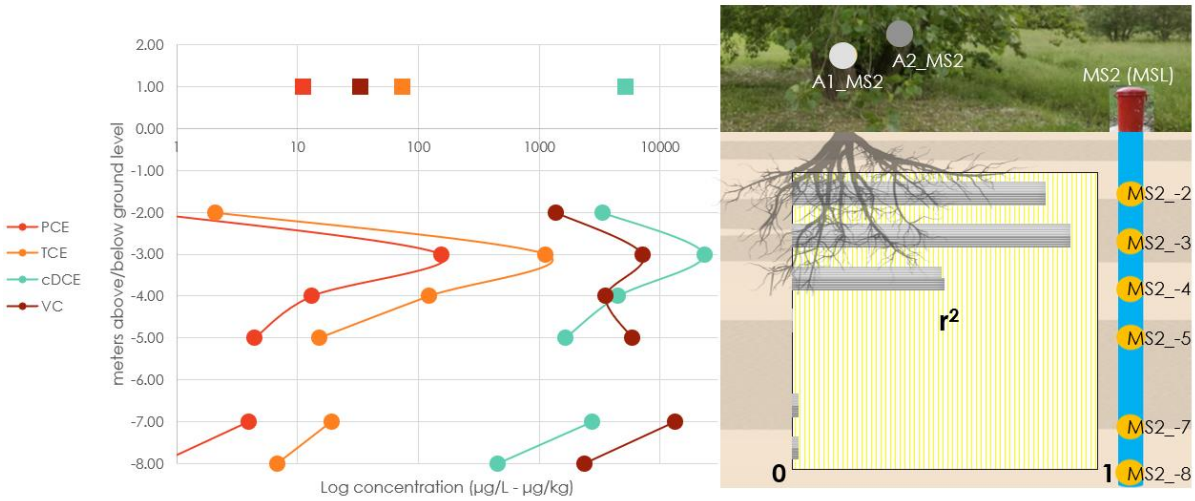

FIGURE 3.30. Concentration in the tree-cores and in gw (on the left) and correlation between tree-core and gw concentrations in the different intervals of the MLS in the first survey on the ND of G site (on the right).

FIGURE 3.31. Comparison between tree-core concentration in the two branches (upper part; A1_MS2 and A2_MS2) and gw concentration in the first and third screened intervals from the top (MS2_-3 and MS2_-5)

With regards to *in planta* gaseous-phase concentration's detection, VC was detected in both branches by colorimetric vials. In one of the surveys (June 2020) colorimetric vials concentrations in the two branches were proportional to tree-core concentrations (> 3 and 0.5 ppm, and 19.7 and 1.6 µg/kg in the vials and tree-cores, respectively). In the last survey (September 2020) colorimetric vials detected VC in concentrations of 2.5 and 1.4 ppm in the two branches, although tree-core reported VC lower than the detection limit.

As for the results of the first survey on the SD, we argue that the non-detection of CEs in trees in SD is due to the youth of the majority of sampled trees (average diameter of 20 cm), whose roots were probably not developed enough to attain the contamination. Moreover, sampling meteorological conditions (air temperature of 31°C) were not ideal to look for such a volatile compound as VC (H_c = 0.811). A further influence may be searched in the length of the sampled tree-cores, which in this survey averaged 5 cm.

The remaining surveys on the black poplar (A_MS2) showed, on the other hand, promising results for phytoscreening of VC. Firstly, the very high correlation between CEs concentrations observed in the tree-core and the shallowest level of the borehole demonstrates that tree roots are uptaking mainly in the first meter of the saturated zone. The difference in concentration in the two branches could be possibly explained by their different diameters and relative distance to the MLS, with A1_MS2 being slightly closer to the gw sampling point. Generally, a good correspondence between gw and tree-core concentrations was observed. In terms of temporal analysis, PCE and TCE seemed to better fit the concentration trend in gw with respect to cDCE and VC, possibly due to their higher sorption capacity which could hinder volatilization out of the trunk.

The results obtained with colorimetric vials showed the probable influence of weather conditions on the effectiveness of the detection. Moreover, the occurrence of other CEs interacting with the VC vial reagent could explain the detection in the last survey, where tree-core analyses resulted in VC below the limit of detection.

3.3.1.8 H site

On November 11, 2018, a preliminary survey was based on the collection of 5 samples in the area nearby to the hotspot of contamination. Among these trees, only 2 cigar trees (*Catalpa speciosa*; FIGURE 3.32), located immediately above the source of contamination, detected the occurrence of PCE, TCE, and cDCE in concentration in the order of hundreds, thousands, and tens of µg/kg, respectively.

FIGURE 3.32. Site isoconcentration contour map referring to gw and sampled trees in the second survey on H Site. Colored trees detected a contamination, white trees were free of contamination

Concentrations in gw respected the same order of magnitude. In the second survey, which occurred on October 14, 2019, 9 trees were sampled along the average direction of migration of the plume. Again, the detection was only successful in the two cigar trees, showing concentrations increased by one order with respect to the previous survey. The results suggest that the hydrogeological conditions of the H site are unsuitable for the use of phytoscreening. DWT is quite high (8-10 m b.g.l.) and the

contamination probably percolates deep down to the lower semi-confined aquifer (GS1) very proximally to the source.

3.3.2 General experimental dataset

3.3.2.1 Contaminant properties

The correlation between the concentration in tree-cores and gw was statistically meaningful (p-value ≤ 0.05) for PCE, TCE, cDCE, and the sum of CEs whilst it was not for VC (FIGURE 3.33).

The ρ values are the same for PCE and cDCE (ρ = 0.48) while a higher value is observed for TCE (ρ = 0.61). On the other hand, ND% slightly increased between the higher TCE and lower chlorinated cDCE (24 and 36%, respectively), while PCE had a significantly higher detectability (4%). VC on the other hand showed a very low detectability (76 % of ND data). Finally, a high correlation (ρ = 0.69) and low ND% (5%) were found for the sum of CEs.

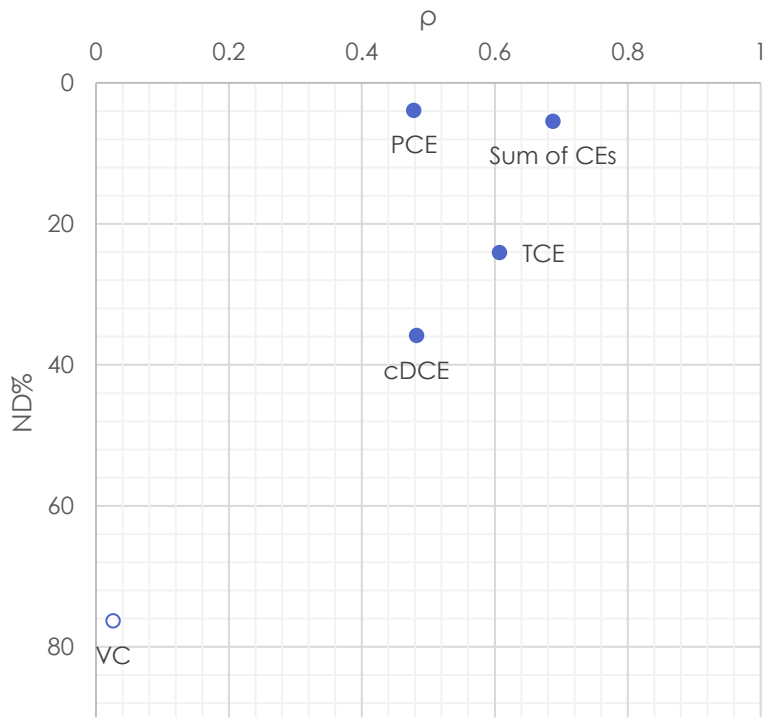

FIGURE 3.33. Spearman's ρ (x-axis) and ND% (y-axis, values in inverse order) for CEs. Blank symbols refer to as p-values > 0.05. Solid symbols refer to as p-values ≤ 0.05.

TABLE 3.3. Physico-chemical properties of the chlorinated ethenes: molecular weight (M_W), water solubility (S_w), Henry's constant (H_c), octanol-water partition coefficient (log K_{ow}). Derived from Mackay et al. (2006)

COMPOUND	M_w [g/mol]	S_w at 25°C [mg/L]	H_c at 17.5°C [adim.]	log K_{ow} [adim.]
PCE	165.8	206	0.492	3.40
TCE	131.3	1118	0.265	2.61
cDCE	96.9	3500	0.111	1.86
VC	62.4	2700	0.811	1.46

The physicochemical properties of CEs (TABLE 3.3) likely influence the behavior of each compound in trees. Consistently with previous literature, the higher H_c compounds, such as PCE, tend to be transpired out of the trunk (Vroblesky et al., 1999), with a higher mass loss inducing a lower correlation between tree-core and gw concentration. Concurrently, the low S_w of PCE can slow the contaminant dissolution in water and consequent tree uptake, resulting in a tree-concentration that does not approximate the concentration in gw. Similarly, low logK_{ow} and M_w may hinder accumulation and favor contaminant loss through the bark despite low H_c (Baduru et al., 2008), such as in the case of cDCE, interfering with the phytoscreening correlation potential. Concerning VC, with an even lower M_w and logK_{ow}, along with a high H_c, it is subjected to the greater volatilization loss among CEs, being rarely detectable and with no correlation with gw concentrations. We consider that the high ρ observed for TCE is the result of the combination between a quite low H_c and a quite high log$K_{ow,}$ in mirror contrast to VC high H_c and low logK_{ow}. The high logK_{ow} of PCE can instead promote a prolonged accumulation in the tree, thus resulting in a higher detectability potential. Moreover, a higher H_c can aid the analytical detection when using headspace methods, decreasing the ND% for PCE and TCE with respect to cDCE and VC.

By the way, the highest ρ between tree-core and gw concentration was found when the total value of CEs was considered. This could be explained by contaminant transformation processes taking place either in the rhizosphere or in the xylem (Newman and Reynolds, 2004) that would negatively affect the correlation at the level of single compounds.

3.3.2.2 Hydrogeology and aquifer parameters

Two intervals were considered for DWT: DWT < 3 and DWT ≥ 3 m b.g.l. Concentration data show a statistically significant correlation value (*p*-value ≤ 0.05; FIGURE 3.34) for both intervals. A decreasing correlation with increasing DWT was observed (ρ = 0.72 and 0.50 for DWT < 3 and DWT ≥ 3 m b.g.l., respectively). Concurrently, the shallow interval showed a good detectability potential (25%) whereas the ND% value slightly increased for the deeper interval (33%).

Duncan & Brusseau (2018) assessed for the first time how DWT could affect the correlation between VOCs concentration in tree tissues and gw (based on 100 measurements). This is consistent with the fact that, in sites with a more substantial vadose zone, mineralization of CEs can occur before translocation of the contaminant in the tree due to more hypoxic conditions (Bradley & Chapelle, 2011), leading to lower correlation and detectability potential for deeper aquifers. Similar findings have been reported by Wilson et al. (2013) for BTEX translocation in trees, and by Duncan and Brusseau (2018). At the same time, tree roots are generally located between 1.5 and 3 m b.g.l. (Stone and Kalisz, 1991), proving the significance of our results.

Aquifer thickness was clustered into two intervals: b < 3 and b ≥ 3 m. Data associated with lower b show a slightly lower correlation than those associated with higher b (ρ = 0.55). At the same time, a lower ND% is associated with the thicker aquifer interval (30% and 37% for b < 3 and b ≥ 3 m, respectively). These results show the low influence of the vertical extent of the saturated zone on phytoscreening results. Moreover, we could argue that the lower correlation and detectability potential of thin aquifers is related to a lower chance, in terms of space range, of being intercepted by tree roots than thick ones. Two intervals of K were considered: $K \leq 1x10^{-5}$ and $K > 1x10^{-5}$ m/s. K values show comparable correlations among intervals (ρ = 0.47 and 0.45 for $K \leq 1x10^{-5}$ and $K > 1x10^{-5}$ m/s, respectively). On the other hand, the lower K interval includes 37% of ND whereas the higher K interval includes 28%. These results suggest that K poorly affects the correlation between tree-core and gw concentration although more permeable aquifers are relatively more suited in terms of

detectability potential. A higher permeability could enhance the mobility of contaminants in the subsoil, likely favoring plant uptake.

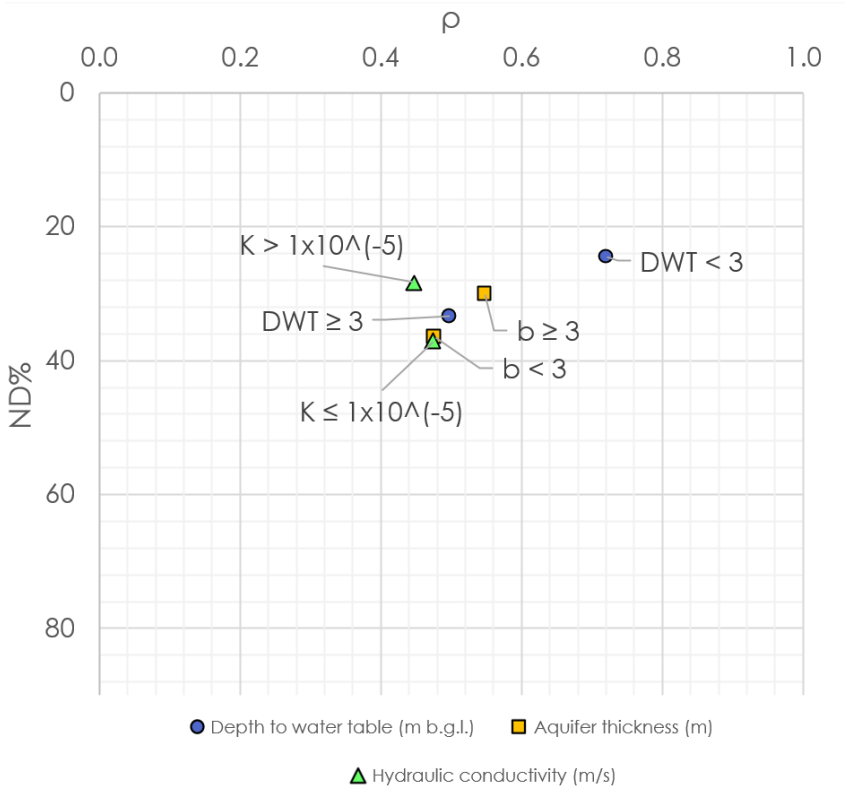

FIGURE 3.34. Spearman's ρ (x-axis) and ND% (y-axis, values in inverse order) of each interval considered for the hydrogeological parameters.

3.3.2.3 Tree identity and anatomy

Since only one genus was available for a significant correlation analysis (*Populus*, Salicaceae family), data were divided into diffuse-porous and ring-porous xylems trees. Even so, the correlation for the *Populus* genus was moderately high (ρ = 0.54) and ND% values were relatively low (27%).

FIGURE 3.35 shows the results obtained by grouping the genera according to their xylem structure. The rank correlation showed a moderately high coefficient (ρ = 0.54) for diffuse-porous while ring-porous xylems showed no significant correlation (*p*-value > 0.05). Moreover, diffuse-porous showed a much higher detectability potential (ND% = 28%) than ring-porous (65%). Most ring-porous samples (*Quercus, Celtis, and Fraxinus*) provided ND% data (56%). These results find validation in the fact that in ring-porous trees, contrarily to diffuse-porous and conifers, most of the water transport

happens in the outermost ring (Ellmore and Ewers, 1986), possibly promoting volatilization out of the trunk.

Tree size (measured as DBH) in our database ranges between 19 and 94 cm and values were split into 2 intervals: DBH<50 and DBH≥50 cm. The lower interval shows a slightly lower correlation (ρ = 0.52) than the higher one (0.62). ND% is instead clear in defining the higher interval as the one with the highest detectability (ND% values of 41% and 24% for DBH<50 and DBH≥50 cm, respectively). Several studies demonstrated that diffusional loss in small trees occurs at a higher rate than in larger diameter trees due to their greater surface area to volume ratio that more quickly depletes the compound reservoir in the trunk (Schumacher et al., 2004; Struckhoff, 2003). This can be confirmed by the results from our experimental data set that show both a higher correlation and a higher detectability potential in larger-size trunks.

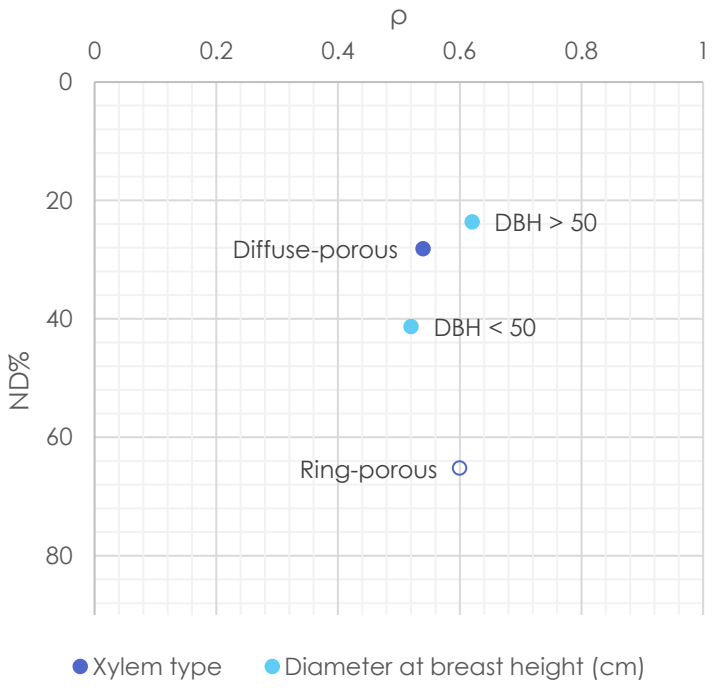

FIGURE 3.35. Spearman's ρ (x-axis) and ND% (y-axis, values in inverse order) of each xylem structure and for tree diameters. Blank symbols refer to as *p*-values>0.05. Solid symbols refer to as *p*-values≤0.05

3.4 CONCLUSIONS

The objective of this research was to evaluate the use of phytoscreening in different hydrogeological settings for sites with aquifers contaminated by CEs. Contaminant concentrations were detected in tree-core samples collected for all eight sampled sites. Moreover, the possibility of investigating the presence of benzene and naphthalene has been demonstrated at the A site. The effectiveness of tree-core analysis has been demonstrated also for relatively deep aquifers and contaminations (B site), although when the contaminated aquifer is confined the effectiveness is reduced (H site). Furthermore, soil gas diffusion in the unsaturated zone originating from a deep semi-confined aquifer was identified as responsible for tree uptake in the C site, in which meteorological conditions played a key role in the detection of CEs. Effective rainfall increases might indeed either dilute concentration in gw, hindering contaminant uptake and accumulation in the trees, or remobilize NAPL residual phase and gaseous-phase in the vadose zone, triggering uptake by trees.

In addition to standard tree-core samples, PID and colorimetric vials measurements were carried out to test the effectiveness of an even more rapid and cost-effective sampling method. Concentrations of CEs in PID and colorimetric vials were quantifiable although were generally several times lower than the corresponding tree-core sample concentrations. Moreover, it was noted how PID is more reliable for rapid in situ assessments than colorimetric vials since its measurements are more independent from meteorological variations and its measurements were accurate in identifying VOCs concentrations, if in the range of the instrumental capability of detection. The correlation between concentrations in the tree-core and the gaseous-phase is indeed comparable in different seasons and different sites (C and D sites).

Notwithstanding the overall low correlation presented by colorimetric vials measurements, their use was worth discriminating among the different CEs when the concentrations in the tree-cores were higher than 1 mg/kg. Finally, a tree-core analysis at a lower height in the trunk is preferable when dealing with low concentrations in gw, as assessed on the F site.

Generally, a certain threshold exists for the detection of the different CEs in trees. Although this threshold seems unclear and generally low for PCE, TCE, and cDCE, the specific physicochemical properties of VC characterize its detection to a high threshold in terms of gw concentrations. Our data on the G site suggests this limit is set around 300 µg/L of VC in gw. Other than that, we saw how contaminant transformation processes taking place in the tree are responsible for the lower correlation of single compounds in comparison to the correlation obtained for the sum of CEs.

Our meta-analysis confirmed what our site investigations preliminary showed us: a high correlation denotes a good quantitative monitoring potential of phytoscreening because the conditions of hydrogeological dynamics favor direct uptake of contaminated water, and the concentration is homogeneously distributed in the tree and the tree-core sample. This seems to be promoted for TCE thanks to the combination of its low volatility and high sorption in comparison to other CEs. Moreover, the correlation was higher in the case of shallow aquifers (DWT < 3 m b.g.l). The homogeneity of concentration in the xylem is higher for diffuse-porous trees (e.g., *Populus*) thanks to their more homogeneously distributed pores and vessels, as also confirmed by investigations on the E site.

The detectability, indicating the power of qualitative screening potential, is higher when factor conditions favor accumulation in the xylem and hinder volatilization loss through the bark. In these terms, PCE is more suited compared to other CEs due to its higher sorption and molecular weight. Higher uptake is also observed for shallow and permeable aquifers ($K > 1 \times 10^{-5}$ m/s). Low volatilization loss was also inferred in the case of large-diameter trees (DBH > 50 cm).

We can conclude that the integration of this technique in specific site conditions could ease the assessment of CEs contaminations before drilling the ground, or better delineate the plume for risk assessment, monitoring, and remediation. Coupling the technique with the PID could be of great use to preliminary screen potentially contaminated trees and select the ones which will undergo the follow-up step of the tree-core analysis.

REFERENCES

Baduru, K.K., Trapp, S., Burken, J.G., 2008. Direct measurement of VOC diffusivities in tree tissues: Impacts on tree-based phytoremediation and plant contamination. Environ. Sci. Technol. 42, 1268–1275. https://doi.org/10.1021/es071552l

Burken, J.G., Vroblesky, D.A., Balouet, J.C., 2011. Phytoforensics, Dendrochemistry, and Phytoscreening: New Green Tools for Delineating Contaminants from Past and Present. Environ. Sci. Technol 45, 44. https://doi.org/10.1021/es2005286

Duncan, C.M., Brusseau, M.L., 2018. An assessment of correlations between chlorinated VOC concentrations in tree tissue and groundwater for phytoscreening applications. Sci. Total Environ. 616–617, 875–880. https://doi.org/10.1016/j.scitotenv.2017.10.235

Duncan, C.M., Mainhagu, J., Virgone, K., Ramírez, D.M., Brusseau, M.L., 2017. Application of phytoscreening to three hazardous waste sites in Arizona. Sci. Total Environ. 609, 951–955. https://doi.org/10.1016/j.scitotenv.2017.07.236

Ellmore, G.S., Ewers, F.W., 1986. Fluid flow in the outermost xylem increment of a ring-porous tree, Ulmus americana. Am. J. Bot. 73, 1771–1774. https://doi.org/10.1002/j.1537-2197.1986.tb09709.x

Filippini, M., Amorosi, A., Campo, B., Herrero-Martìn, S., Nijenhuis, I., Parker, B.L., Gargini, A., 2016. Origin of VC-only plumes from naturally enhanced dechlorination in a peat-rich hydrogeologic setting. J. Contam. Hydrol. 192, 129–139. https://doi.org/10.1016/j.jconhyd.2016.07.003

Filippini, M., Parker, B.L., Dinelli, E., Wanner, P., Chapman, S.W., Gargini, A., 2019. Assessing aquitard integrity in a complex aquifer e aquitard system contaminated by chlorinated hydrocarbons. https://doi.org/10.1016/j.watres.2019.115388

Hirsh, S.R., Compton, H.R., Matey, D.H., Wrobel, J.G., Schneider, W.H., 2004. Five-Year Pilot Study: Aberdeen Proving Ground, Maryland, in: Phytoremediation. John Wiley & Sons, Inc., pp. 635–659. https://doi.org/10.1002/047127304x.ch20

Holm, O., Rotard, W., 2011. Effect of Radial Directional Dependences and Rainwater Influence on CVOC Concentrations in Tree Core and Birch Sap Samples Taken for Phytoscreening Using HS-SPME-GC/MS. Environ. Sci. Technol. 45, 9604–9610. https://doi.org/10.1021/es202014h

Journel, A.G., Deutsch, C. V., 1997. Rank Order Geostatistics: A Proposal for a Unique Coding and Common Processing of Diverse Data, in: Schofield, E.Y.B. a. N.A. (Ed.), Geostatistics Wollongong '96. Kluwer Academic Publishers, Dordrecht, Netherlands, pp. 174–187.

Larsen, Morten, Burken, J., Machackova, J., Karlson, U.G., Trapp, S., 2008. Using tree core samples to monitor natural attenuation and plume distribution after a PCE spill. Environ. Sci. Technol. 42, 1711–1717. https://doi.org/10.1021/es0717055

Larsen, M, Burken, J., Machackova, J., Karlson, U.G., Trapp, S., 2008. Using Tree Core Samples to Monitor Natural Attenuation and Plume Distribution after a PCE Spill. Environ. Sci. Technol. 42, 1711.

Leoncini, C., Filippini, M., Nascimbene, J., Gargini, A., 2022. A quantitative review and meta-analysis on phytoscreening applied to aquifers contaminated by chlorinated ethenes. https://doi.org/10.1016/j.scitotenv.2022.153005

Limmer, M.A., Burken, J.G., 2014. Plant Translocation of Organic Compounds: Molecular and Physicochemical Predictors. https://doi.org/10.1021/ez400214q

Mackay, D., Shiu, W.Y., Ma, K.C., Lee, S.C., 2006. Handbook of physical-chemical properties and environmental fate for organic chemicals. Taylor & Francis Group, LLC.

Molinari, F.C., Boldrini, G., Severi, P., Dugoni, G., Rapti Caputo, D., Martinelli, G., 2007. Risorse Idriche Sotterranee della Provincia di Ferrara (in Italian; Transl. Groundwater Resources of the Ferrara Province), Risorse idriche sotterranee della Provincia di Ferrara (in italian; transl. Groundwater Resources of the Ferrara Province). DB-MAP printer, Florence, Italy, pp. 1–62.

Nijenhuis, I., Schmidt, M., Pellegatti, E., Paramatti, E., Richnow, H.H., Gargini, A., 2013. A stable isotope approach for source apportionment of chlorinated ethene plumes at a complex multi-contamination events urban site. https://doi.org/10.1016/j.jconhyd.2013.06.004

Ottosen, C.B., Rønde, V., Trapp, S., Bjerg, P.L., Broholm, M.M., 2018. Phytoscreening for Vinyl Chloride in Groundwater Discharging to a Stream. Groundw. Monit. Remediat. 38, 66–74. https://doi.org/10.1111/gwmr.12253

Shetty, M.K., Limmer, M.A., Waltermire, K., Morrison, G.C., Burken, J.G., 2014. In planta passive sampling devices for assessing subsurface chlorinated solvents. Chemosphere 104, 149–154. https://doi.org/10.1016/j.chemosphere.2013.10.084

Sorek, A., Atzmon, N., Dahan, O., Gerstl, Z., Kushisin, L., Laor, Y., Mingelgrin, U., Nasser, A., Ronen, D., Tsechansky, L., Weisbrod, N., Graber, E.R., 2008. "Phytoscreening": The use of trees for discovering subsurface contamination by VOCs. Environ. Sci. Technol. 42, 536–542. https://doi.org/10.1021/es072014b

Stone, E.L., Kalisz, P.J., 1991. On the maximum extent of tree roots, Forest Ecology and Management. https://doi.org/10.1016/0378-1127(91)90245-Q

Vroblesky, D.A., Clinton, B.D., Vose, J.M., Casey, C.C., Harvey, G.J., Bradley, P.M., 2004. Ground water chlorinated ethenes in tree trunks: Case studies, influence of recharge, and potential degradation mechanism. Gr. Water Monit. Remediat. 24, 124–138. https://doi.org/10.1111/j.1745-6592.2004.tb01299.x

Vroblesky, D.A., Nietch, C.T., Morris, J.T., 1999. Chlorinated Ethenes from Groundwater in Tree Trunks. Environ. Sci. Technol. 33, 510–515. https://doi.org/10.1021/es980848b

Wahyudi, A., Bogaert, P., Trapp, S., MacHáčková, J., 2012. Pollutant plume delineation from tree core sampling using standardized ranks. Environ. Pollut. 162, 120–128. https://doi.org/10.1016/j.envpol.2011.11.010

SITE REFERENCES

ambiente.regione.emilia-romagna.it

dext3r (arpae.it)

4

Comparison between literature and field data

4.1 INTRODUCTION

This chapter presents the similarities and divergences that emerged from the meta-analyses of data collected from the literature and our field investigations. A focus on the optimal conditions to apply phytoscreening is given in terms of using the technique to either screen a poorly investigated area (high detectability potential expressed by ND% value) or monitor the contaminant's fate and transport (high contaminant quantification potential expressed by the degree of correlation between groundwater and tree trunk concentration). Results are given in terms of contaminants properties, hydrogeological site conditions, tree identity and anatomy, and methodological approach. The aim is to give a comprehensive view and outline of the best practices for future users of phytoscreening.

4.2 MATERIAL AND METHODS

A comparison between Spearman's coefficients (ρ) and non-detection rates (ND%) of literature and field data is given, through the visualization of graphs indicating the optimal conditions achieved through the two meta-analyses. Results are displayed through bidimensional graphs indicating under which specific conditions phytoscreening should be used either as a screening (low ND%) or a monitoring tool (high ρ). In addition, conditions for the unfeasible application of the technique are given (high ND% and low ρ).

Results are shown and discussed in terms of:

- Contaminant properties: molecular weight (M_w), water solubility (S_w), Henry's constant (H_c), and octanol-water partition coefficient ($logK_{ow}$);
- Hydrogeology and aquifer parameters: depth to water table (DWT), aquifer thickness (b), and hydraulic conductivity (K);
- Tree identity and anatomy: family, xylem type, and diameter at breast height (DBH);
- Sampling and analysis protocols: tree-core length (L), sampling height along the trunk (H), and analysis approach.

4.3 RESULTS AND DISCUSSION

4.3.1 Contaminant properties

Generally speaking, there is a good correspondence between the results obtained for the different compounds in literature and field studies (FIGURE 4.1). In both cases, PCE and cDCE data show a comparable ρ value (~ 0.4), while TCE data exhibit a different correlation trend (ρ ~ 0.4 and 0.6 in literature and field data, respectively). On the other hand, ND% value is highly consistent between literature and field data, with PCE being the compound with higher detectability potential, followed by TCE and cDCE. Moreover, the rare detection of VC in literature data can be compared to the non-correlation (*p*-value > 0.05) and high ND% value of VC in our field data. Finally, regardless of literature and field data, the total value of CEs concentration invariably displays low ND% (< 5%) and high ρ (> 0.6).

As stated in Section 3.2.1, we assume that the combination of low volatility (H_c = 0.265) and high tendency to sorption ($logK_{ow}$ = 2.61) of TCE is probably responsible for its higher ρ and low ND% value in field investigations. Moreover, the analysis of ND% value gave more straightforward results, with PCE being the most detectable among CEs in both literature and field data sets. It appears clear that its higher M_w and $logK_{ow}$, along with a lower value of S_w, affect favorably its detection in trees.

Preceding studies stated that heavier, larger molecules migrate more slowly through the wood matrix, resulting in less effective diffusion of the compounds (Baduru et al., 2008). Our analyses show that this slower diffusion might be the key to more effective detection of the compound in trees. Consistently to Schnoor et al. (1995) and Chiou et al. (2001), higher chlorinated compounds such as PCE are more eager to get attached to roots - and less eager to remain in soil water - due to their less aqueous-soluble (low S_w) nature, resulting in an active transport through plant membranes and consequent uptake and detection. Moreover, high sorption compounds (log K_{ow} > 3) were reported to tend to be absorbed primarily by root surfaces, resulting in less translocation to the xylem (Schnoor et al., 1995), but our data suggest this higher sorption results in a greater accumulation in the xylem for PCE (log K_{ow} = 3.40), allowing an easier detection.

The good matching obtained for the total concentration of CEs raises awareness of possible phytodegradation processes likely affecting the correlation and detectability of single compounds.

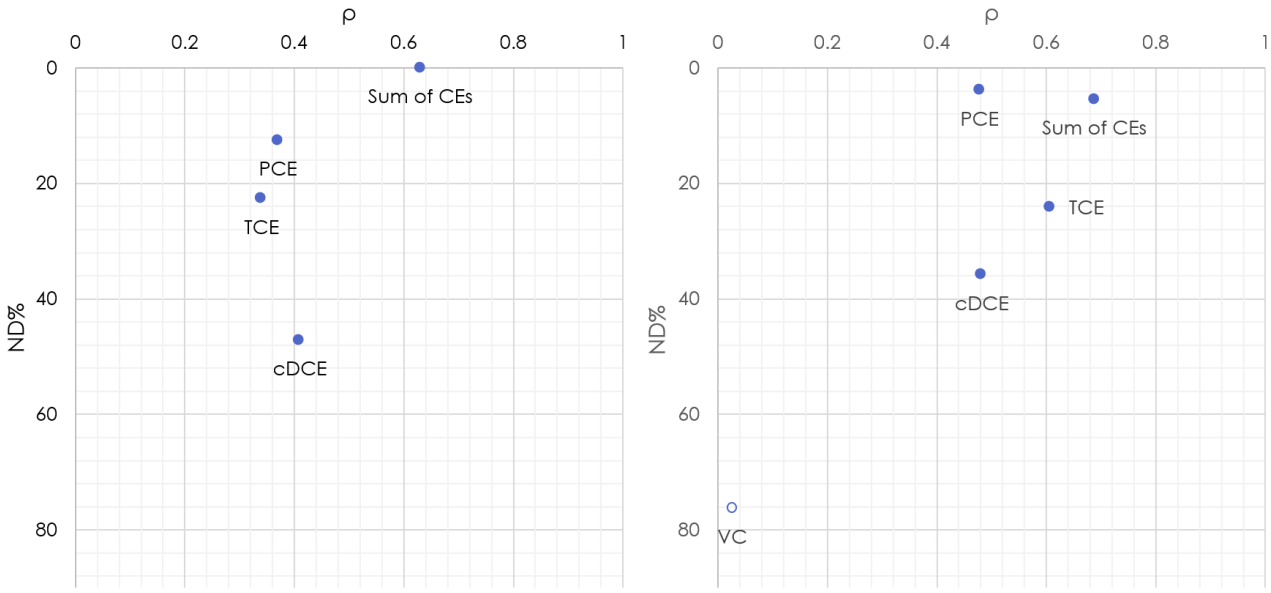

FIGURE 4.1. Comparison between literature (left) and field (right) results. Spearman's ρ (x-axis) and ND% (y-axis, values in inverse order) of compounds series. Blank symbols refer to as *p*-values>0.05. Solid symbols refer to as *p*-values≤0.05

4.3.2 Hydrogeology and aquifer parameters

In general, shallower aquifers obtained better correlation results in both literature and field data analyses (FIGURE 4.2). Since DWT in our field sites was never lower than 1 m b.g.l., an accurate comparison is to be done among the medium ($1 \leq DWT < 3$ m b.g.l.) and lower interval (< 3 m b.g.l.) for literature and field data, respectively. In literature data, this interval shows a ρ near 0.6, while in the field the same interval attains a value of 0.7. For DWT ≥ 3 m b.g.l., both literature and field data show a lower correlation than the latter ($\rho = 0.5$). Similarly, detectability potential is from higher to slightly higher in shallower aquifers (ND% value of 16 and 26% for literature and field data, respectively) than in deeper ones (ND% value of 17 and 38 %).

Literature and field data barely agree on results associated with the aquifer vertical extent. Indeed, correlation potential appears to have opposite trends in the two databases. The value of ρ is 0.3 for the literature's higher interval (b > 3.5 m) and near 0.6 for the field's higher interval (b ≥ 3 m). Oppositely, the lower b interval shows a ρ value of 0.7 and 0.4 for literature and field data, respectively. On the other hand, a similar trend is confirmed for the detectability potential, with an ND% value that decreases for thicker aquifers.

A more coherent comparison is observed for the aquifer hydraulic conductivity K, where the ρ value slightly differs among intervals and the ND% value is higher for the lower permeability interval in both literature and field data.

These results show that in shallower aquifers phytoscreening can be more effective in terms of both correlation and detectability potential, as also suggested by Duncan and Brusseau (2018). Studies on the maximum extent of tree roots (Canadell et al., 1996) confirm that, in temperate climates, most tree species have a rhizosphere that is limited to a maximum of 3 m b.g.l., thus explaining our findings. However, no previous authors investigated other aquifer parameters.

Our results on literature data suggest that aquifer thickness plays an important role in the detection of CEs in trees. This may be because CEs, in the majority of contaminant events, enter the subsoil as dense non-aqueous phase liquids (DNAPLs), which tend to sink towards deeper sections of the

aquifer, thus influencing the shape of dissolved contaminant plumes (e.g., Parker et al., 2003). In particular, the sinking of CEs could result in an increased distance of the dissolved contaminant plume from the root zone in thicker aquifers. Field data are however less clear in highlighting the role of the aquifer vertical extent, probably because our field database contains a much lower variability (b ranging from 1.75 to 4 m) than the literature database (b ranging from 0.9 to 6.6 m).

Aquifer conductivity results are clear in identifying that in more permeable aquifers the detectability potential of trees is increased. Coarser grained lithologies can indeed allow higher mobility of the contaminants in the aquifer, favoring their uptake by trees.

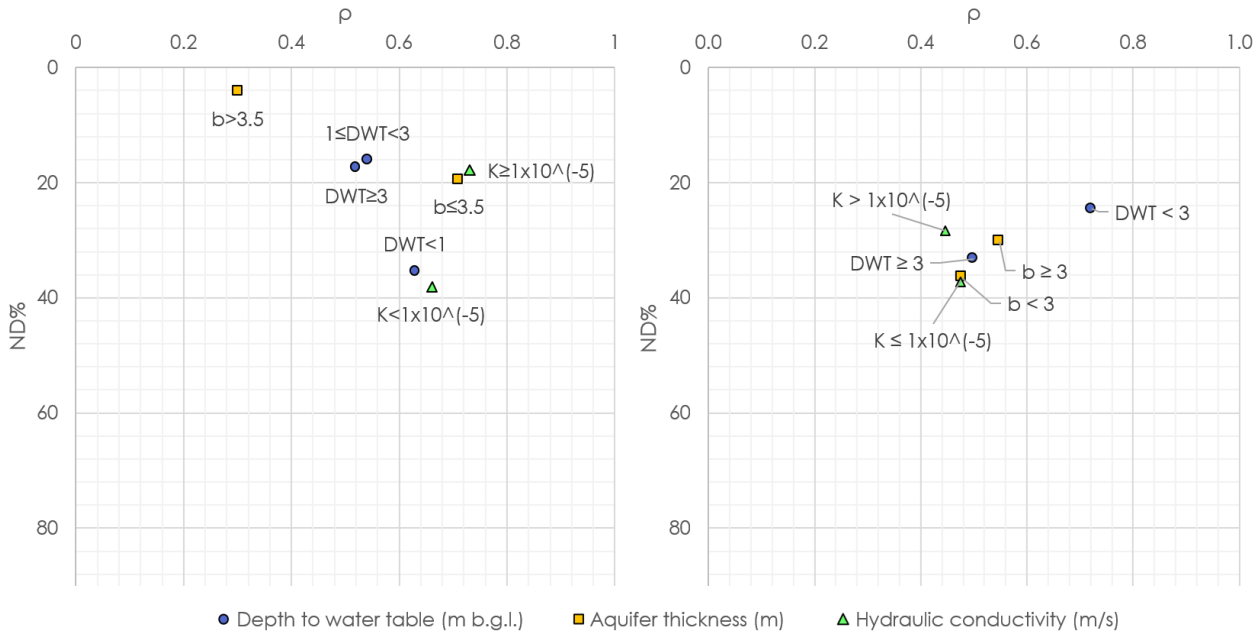

FIGURE 4.2. Comparison between literature (left) and field (right) results. Spearman's ρ (x-axis) and ND% (y-axis, values in inverse order) of each interval considered for the hydrogeological parameters.

4.3.3 Tree identity and anatomy

As for tree identity, only the analysis of literature data could give an insight into the differences among different families with the only exception of Salicaceae, for which we had a consistent number of field data to undergo statistical analysis. Nonetheless, this family showed contrasting results in terms of correlation potential among literature (*p*-value > 0.05) and field data (ρ = 0.54). Similarly, the overall high detectability potential differed widely between literature (3%) and field data (27%).

On the contrary, results obtained by clustering for xylem types were clearer: ring-porous trees showed low or no correlation and low detectability potential, while diffuse-porous trees exhibited moderate to high correlation and moderate to high detectability potential (FIGURE 4.3). Literature data also show a good correlation and detectability for conifers.

Although tree sizes were clustered differently among literature and field data, the intervals denoted opposite trends in terms of correlation potential. Literature data indeed put in evidence that smaller trees are more suited for quantifying contaminants concentrations, while field data seem to state the contrary. In terms of detectability potential, both databases agree that larger trunk diameter trees have a higher chance of detecting the investigated compounds.

The great difference among the results obtained for the various families analyzed in the literature review could be associated with the variability of roots depth, which is in turn related to DWT variation and it is species-specific (Stone and Kalisz, 1991). In both literature and field data, ring-porous trees show a scarce surveillance capacity on contamination. Diffuse-porous ones denote a high variability among families. In general terms, diffuse-porous trees show a good capacity for locating the contamination while they are less effective in determining its intensity. Conifers are more suited to quantifying the contamination according to literature data.

The reason for these differences must be associated with the different transport mechanisms among xylem types. The water flow is localized in the outermost growth ring in ring-porous trees, promoting phytovolatilization. Oppositely, xylem flow in diffuse-porous and coniferous trees is more equally distributed among rings (Ellmore and Ewers, 1986).

The analysis of trunk size exhibited contrasting results on the correlation potential while a clear advantage in terms of detectability is found when sampling large-diameter trunks (DBH > 40 cm). This is probably due to the higher extent of the rhizosphere of more mature trees, which ensures a higher probability of uptaking contaminants. Moreover, diffusional loss in large trunks occurs at a lower rate than in smaller ones due to the lower surface area to volume ratio of the last with a more

rapid depletion of the compound accumulated in the trunk (Schumacher et al., 2004; Struckhoff, 2003).

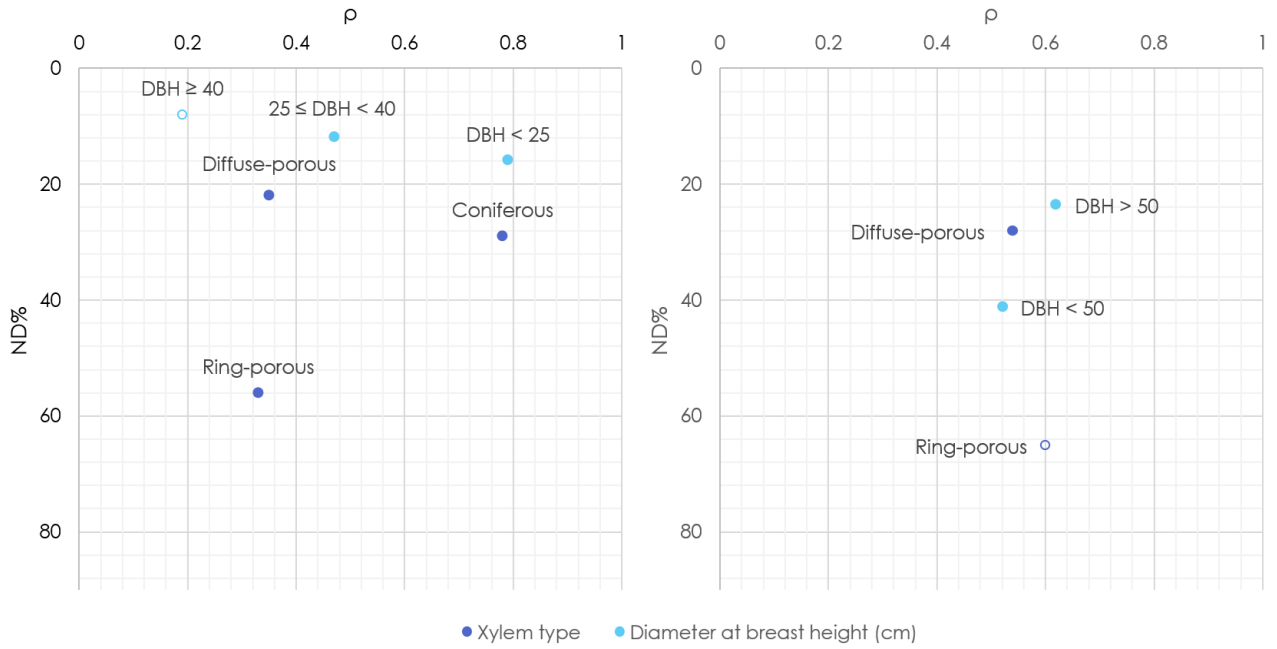

FIGURE 4.3. Comparison between literature (left) and field (right) results. Spearman's ρ (x-axis) and ND% (y-axis, values in inverse order) of each xylem structure and intervals for tree diameters. Blank symbols refer to as *p*-values>0.05. Solid symbols refer to as *p*-values≤0.05

4.3.4 Sampling and analysis protocols

A comparison of sampling and analysis protocols between literature and field meta-analyses is not possible but some inferences can be provided.

Sampling shorter tree-cores appeared to be unfavorable according to both databases, being the correlation low in literature data and having carried out unsuccessful surveys when sampling cores shorter than 6 cm in the field (see SECTION 3.3.1.7 G SITE).

Sampling at a lower height above ground level showed a higher detectability potential in the literature meta-analysis and higher concentrations in field data (see SECTION 3.3.1.6 F SITE) even if samples collected at ~ 100 cm a.g.l. showed concentrations that were in good correlation with gw.

Sampling and extraction in organic-free water seem to be the best protocol according to literature data results and the correlation and detectability obtained via this method in our field results confirm

this outcome. Moreover, *in planta* sampling with the PID showed consistent results, with a high correlation to tree-core concentrations that did not vary in the different seasons, as instead was observed with colorimetric vials.

REFERENCES

Canadell, J., Jackson, R.B., Ehleringer, J.R., Mooney, H.A., Sala, O.E., Schulze, E.-D., 1996. Maximum Rooting Depth of Vegetation Types at the Global Scale, Oecologia.

Chiou, C.T., Sheng, G., Manes, M., 2001. A Partition-Limited Model for the Plant Uptake of Organic Contaminants from Soil and Water. https://doi.org/10.1021/es0017561

Duncan, C.M., Brusseau, M.L., 2018. An assessment of correlations between chlorinated VOC concentrations in tree tissue and groundwater for phytoscreening applications. Sci. Total Environ. 616–617, 875–880. https://doi.org/10.1016/j.scitotenv.2017.10.235

Parker, B.L., Cherry, J.A., Chapman, S.W., Guilbeault, M.A., 2003. Review and Analysis of Chlorinated Solvent Dense Nonaqueous Phase Liquid Distributions in Five Sandy Aquifers. Vadose Zo. J. 2, 116–137. https://doi.org/10.2113/2.2.116

Schnoor, J.L., Licht, L.A., McCutcheon, S.C., Wolfe, N.L., Carreir, L.H., 1995. Phytoremediation of Organic and Nutrient Contaminants. Environ. Sci. Technol. 29, 318A-323A. https://doi.org/10.1021/es00007a747

Schumacher, J.G., Struckhoff, G.C., Burken, J.G., 2004. Assessment of subsurface chlorinated solvent contamination using tree cores at the front street site and a former dry cleaning facility at the Riverfront Superfund site, New Haven, Missouri, 1999-2003, U.S. Geological Survey Scientific Investigations Report 2004-5049. https://doi.org/https://doi.org/10.3133/sir20045049

Stone, E.L., Kalisz, P.J., 1991. On the maximum extent of tree roots. For. Ecol. Manage. 46, 59–102. https://doi.org/10.1016/0378-1127(91)90245-Q

Struckhoff, G., 2003. Uptake of vapor phase PCE by plants: impacts to phytoremediation. Masters

theses.

5
Conclusions

Although phytoscreening is still poorly accepted due to the general conclusion that it is only a qualitative technique, a multitude of benefits derives from using trees as sentinels to detect groundwater contamination. Conventionally, environmental contaminations are assessed directly with groundwater chemical analyses but the potentialities of phytoscreening could improve and enhance these assessments, for example by rendering viable an analysis in areas that are poorly accessible to heavy machinery for cost and logistic reasons. Indirect and sustainable measurements of contamination occurrence in the soil and environment are gaining ground in the field of characterization and monitoring of contaminated sites in recent years, such as the coupled use of s and accumulation chambers for tracking soil and shallow groundwater contamination. Similarly, trees could behave as biosentinels with the advantage of average contaminant concentrations temporally and spatially, with a higher relevance than single-shot point measurements. Moreover, phytoscreening has the clear advantage of being a low-cost technique that can contribute to a cheap and not invasive insight into groundwater contamination.

Phytoscreening potential advantages are although mitigated by its numerous technical limitations. For example, despite substantial progress in understanding the process of organic compound uptake by trees, for a variety of other compounds, it is challenging to overcome the barrier of the trees' transpiration stream due to factors that concern microbial degradation in the rhizosphere and redox conditions of the critical zone. Moreover, compounds that can be absorbed by the trees face other obstacles. As discussed in the literature and our work, factors like tree identity, trunk size, and seasonality can influence phytovolatilization and phytodegradation loss rates. Concerning sampling

methods, they need to be standardized on a global scale and sensitive analytical instrumentations are required to detect the contamination.

Even so, phytoscreening for chlorinated ethenes could provide meaningful and robust data and could represent a source of a valuable dataset to better assess contaminated sites.

The major outcomes finalized with this work, which analyzed over 800 tree-core concentration data from either literature or field investigations, are hereby synthesized together with their practical applications and implications on phytoscreening. It is to be noted that the majority of field sites were localized in temperate climates. Conceptual models derived from literature and field data are shown in FIGURE 5.1.

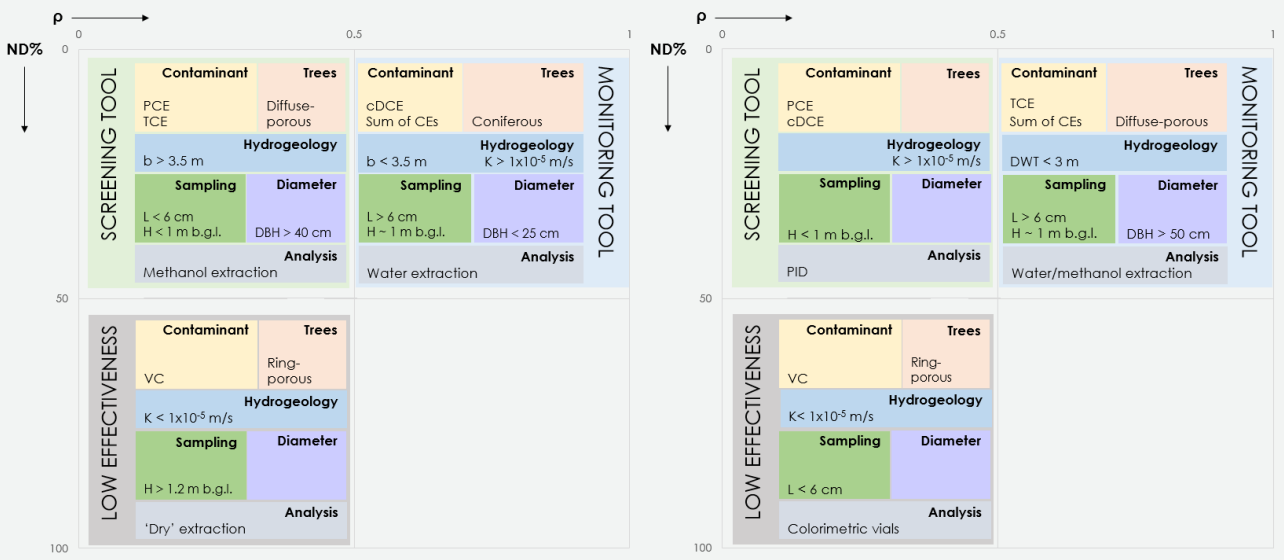

FIGURE 5.1. Comparison between literature (left) and field (right) results. Spearman's ρ (x-axis) and ND% (y-axis, values in inverse order) show an outline of the conditions that are more suitable for using phytoscreening as a screening tool (green quadrants) or as a monitoring tool (blue quadrant). Conditions that showed low effectiveness for phytoscreening applications are highlighted in the grey quadrant.

The aim was to evaluate the effect of various factors affecting the potentialities of the technique. Among the factors analyzed, we included physicochemical properties of CEs, hydrogeological conditions of the underlying contaminated aquifers, tree identity and anatomy, and sampling and extraction protocols.

The conclusions are thus portrayed by focalizing the use of the technique on specific site objectives: qualitative screening or quantitative monitoring of a contamination hydrogeological setting?

A final conceptual model of the results is given in FIGURE 5.2. Generally speaking, the detectability in trees is higher when factor conditions favor accumulation in the xylem and hinder volatilization loss through the bark. The correlation (quantitative monitoring potential) is higher when the hydrogeological dynamics promote direct uptake of contaminated gw, and the concentration is homogeneously distributed in the tree and the tree-core sample.

These being said, the best field protocol would generally be that of sampling systematically the same tree family, or trees with the same xylem structure, to have a more standardized view of the contamination setting.

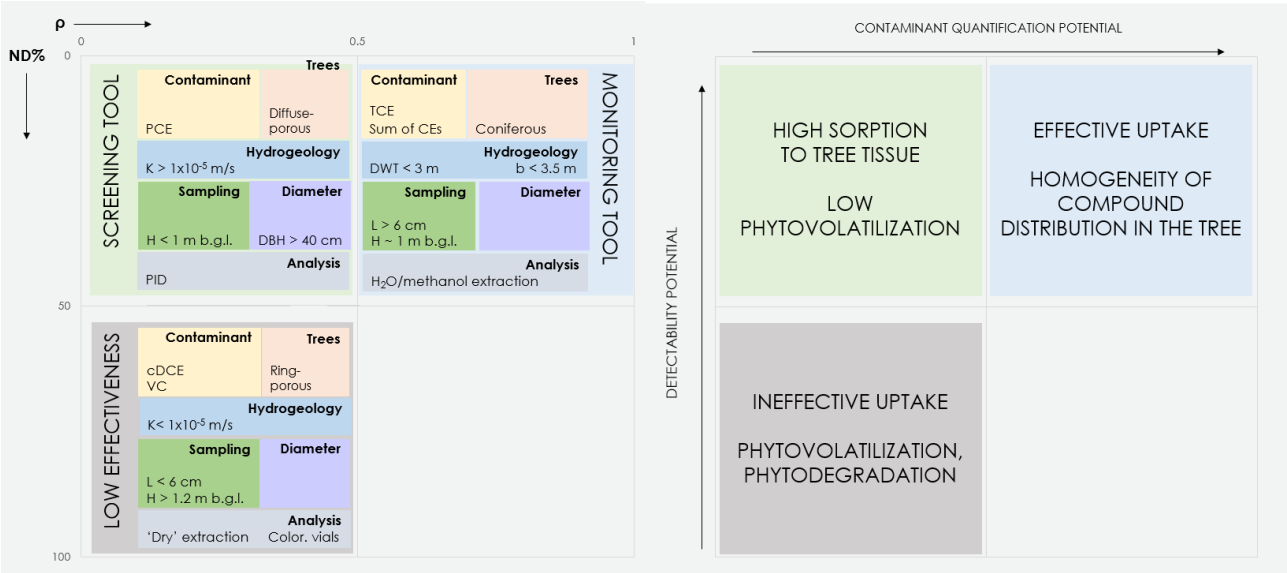

Figure 5.2. Left side: Spearman's ρ (x-axis) and ND% (y-axis, values in inverse order) show an outline of the conditions that are more suitable for using phytoscreening as a screening tool (green quadrants) or also as a monitoring tool (blue quadrant). Conditions that showed low effectiveness for phytoscreening applications are highlighted in the grey quadrant. Right side: physical causes for which factors fall in the different quadrants.

Screening tools

We have studied the rate of detection associated with different factors and the main findings suggest that the following conditions are recommended to qualitatively survey chlorinated ethenes-contaminated groundwaters via phytoscreening:

- The contamination should be mainly composed of parent compounds, namely PCE and TCE, since their higher sorption and molecular weight favor contaminant accumulation in the xylem. cDCE and VC are between two and four times less detectable than the parent compounds, respectively. VC, when detected, is probably associated with concentrations in groundwater that exceed hundreds of µg/L.
- The bulk saturated hydraulic conductivity should be higher than $1x10^{-5}$ m/s since a more effective uptake by tree roots is expected as they act like biopumps of compounds dissolved in groundwater.
- Diffuse-porous trees should be sampled, with a preference for poplars and willows (Salicaceae) due to their higher uptake rates. Trunks with diameters larger than 40 cm are to be preferred since their rhizosphere is expected to be more developed both vertically and horizontally in the ground.
- Core sampling should be carried out near the ground surface, at an approximate height of 0.5 m since phytovolatilization losses are reduced than higher up on the trunk.
- Samples should be preserved in organic-free water solutions since this seems to maximize contaminant extraction with the headspace analysis followed by GC/MS. Moreover, consistent results were achieved through *in planta* SPME and PID measurements, according to literature and field survey, respectively.

Monitoring tools

The analysis of Spearman's rank correlation coefficients of the investigated factors suggests that the following recommendations should be taken into account in order to accomplish the monitoring of groundwater contamination:

- The monitoring should be mainly focused on TCE since its combination of high sorption and low volatility appear to allow the attainment of an equilibrium of concentration inside the xylem.
- The water table should be localized within 3 m below the ground level since the roots of most tree species in temperate climates are located within this distance. Unconfined aquifers with a saturated zone's thickness lower than 3.5 m are to be preferred since the possible sinking of chlorinated ethenes could hinder uptake.
- Conifers are to be preferred as bio-sentinels, due to their more homogeneous distribution of pores and vessels.
- Tree-cores should exceed 6 cm in length since homogeneity of concentration in the sample is enhanced. Core sampling should be carried out at an approximate height of 1 m, where equilibrium of the compound concentration seems to be attained inside the xylem.
- Samples should be extracted in either methanol or organic-free water-filled vials.

Drawbacks

Phytoscreening was found to be less effective under the following conditions:

- The contamination is mainly composed of cDCE and VC. In this case, a low correlation with groundwater concentration is expected for cDCE due to its low sorption, while a low detectability and no correlation are expected for VC due to its high volatility and low sorption.

- The aquifer has a hydraulic conductivity lower than $1x10^{-5}$ m/s. In this case, trees are expected to show lower concentrations than gw since the mobility of the contaminants in the porous medium is hindered.
- Ring-porous trees are sampled. Results from oaks and elms (Fagaceae and Ulmaceae) showed no correlation at all and low detectability due to their particular xylem structure that can promote phytovolatilization.
- Tree-cores are sampled in lengths shorter than 6 cm and at a height higher than 1.2 m above ground level, which promotes phytovolatilization.
- Samples are placed in vials 'as is' or measurements are carried out with colorimetric vials. In this case, a strong dependence on weather conditions is expected.

Suggestions for future work

Despite the clarifications provided by our meta-analysis, several factors influencing phytoscreening effectiveness remain unexplored on a global scale. This is the case of meteorological conditions, such as precipitation and temperature, which in some field cases showed to be responsible for differential uptake and volatilization loss from the tree. Moreover, soil and vadose zone properties such as porosity, volumetric water content, and content of organic carbon could influence uptake, volatilization loss at the ground surface, and sorption to soil particles, respectively. Finally, compound degradation processes occurring inside the tree might hinder correlation with concentrations in groundwater, as demonstrated by the higher detectability and correlation obtained for the total sum of CEs rather than the single compounds. Specifically, Compound Specific Isotope Analysis should be performed to assess the degree of degradation of the compounds between groundwater and the tree. This could finally solve the issues related to the quantification of the contaminants in the trees. Future research should also be directed towards the fate of the most toxic and most undetectable (in trees) of these contaminants: VC.

Appendix

Supplementary Materials (SM) - Chapter 2

Supplementary Materials (SM) - Chapter 3

SM - Chapter 2

Values equal to 0 correspond to measures below limit of detection

Blank cells correspond to measures not available

A quantitative review and meta-analysis on phytoscreening applied to aquifers contaminated by chlorinated ethenes												
Carlotta Leoncini, Maria Filippini, Juri Nascimbene, Alessandro Gargini												
Department of Biological, Geological, and Environmental Sciences, Alma Mater Studiorum University of Bologna, via Zamboni 67, 40126 Bologna, Italy												
	Aquifer parameters			Tree identity and anatomy			Sampling and analysis protocols			Concentrations		
article	DWT	K	b	genus	xylem	DBH	extraction	H	L	compound	tree-core	gw
Larsen et al. (2008)	2.5	1.00E-04	3.0	Salix	diffuse-porous		dry	100		cDCE	741	140
Larsen et al. (2008)	2.5	1.00E-04	3.0	Pinus	coniferous		dry	100		cDCE	933	583
Larsen et al. (2008)	2.5	1.00E-04	3.0	Betula	diffuse-porous		dry	100		cDCE	220	583
Larsen et al. (2008)	2.5	1.00E-04	3.0	Quercus	ring-porous		dry	100		cDCE	14	63.8
Larsen et al. (2008)	2.5	1.00E-04	3.0	Alnus	diffuse-porous		dry	100		cDCE	0	63.8
Larsen et al. (2008)	2.5	1.00E-04	3.0	Alnus	diffuse-porous		dry	100		cDCE	0	63.8
Larsen et al. (2008)	2.5	1.00E-04	3.0	Betula	diffuse-porous		dry	100		cDCE	0	63.8
Larsen et al. (2008)	2.5	1.00E-04	3.0	Alnus	diffuse-porous		dry	100		cDCE	60	63.8
Larsen et al. (2008)	2.5	1.00E-04	3.0	Pinus	coniferous		dry	100		cDCE	13	19
Larsen et al. (2008)	2.5	1.00E-04	3.0	Populus	diffuse-porous		dry	100		cDCE	67	140
Larsen et al. (2008)	2.5	1.00E-04	3.0	Alnus	diffuse-porous		dry	100		cDCE	40	187
Larsen et al. (2008)	2.5	1.00E-04	3.0	Alnus	diffuse-porous		dry	100		cDCE	7	187
Larsen et al. (2008)	2.5	1.00E-04	3.0	Alnus	diffuse-porous		dry	100		cDCE	0	140
Larsen et al. (2008)	2.5	1.00E-04	3.0	Alnus	diffuse-porous		dry	100		cDCE	0	140

Larsen et al. (2008)	2.5	1.00E-04	3.0	Fagus	diffuse-porous		dry	100		cDCE	0	12
Larsen et al. (2008)	2.5	1.00E-04	3.0	Quercus	ring-porous		dry	100		cDCE	0	3.1
Larsen et al. (2008)	2.5	1.00E-04	3.0	Quercus	ring-porous		dry	100		cDCE	0	40.3
Vroblesky et al. (1999)	0.75	5.30E-06		Pinus	coniferous		dry	150	6.8	cDCE	110	150
Vroblesky et al. (1999)	0.75	5.30E-06		Pinus	coniferous		dry	150	6.8	cDCE	0	150
Vroblesky et al. (1999)	0.75	5.30E-06		Pinus	coniferous		dry	150	6.8	cDCE	0	150
Vroblesky et al. (1999)	0.75	5.30E-06		Pinus	coniferous		dry	150	6.8	cDCE	0	150
Vroblesky et al. (1999)	0.75	5.30E-06		Pinus	coniferous		dry	150	6.8	cDCE	0	150
Vroblesky et al. (1999)	0.75	5.30E-06		Pinus	coniferous		dry	150	6.8	cDCE	0	150
Vroblesky et al. (1999)	0.75	5.30E-06		Pinus	coniferous		dry	150	6.8	cDCE	0	125
Vroblesky et al. (1999)	0.75	5.30E-06		Pinus	coniferous		dry	150	6.8	cDCE	0	100
Vroblesky et al. (1999)	0.75	5.30E-06		Pinus	coniferous		dry	150	6.8	cDCE	0	125
Vroblesky et al. (1999)	0.75	5.30E-06		Pinus	coniferous		dry	150	6.8	cDCE	0	75
Vroblesky et al. (1999)	0.75	5.30E-06		Taxodium	coniferous		dry	150	6.8	cDCE	55	25
Vroblesky et al. (1999)	0.75	5.30E-06		Taxodium	coniferous		dry	150	6.8	cDCE	0	25
Vroblesky et al. (1999)	0.75	5.30E-06		Taxodium	coniferous		dry	150	6.8	cDCE	210	25
Vroblesky et al. (1999)	0.75	5.30E-06		Taxodium	coniferous		dry	150	6.8	cDCE	0	25
Vroblesky et al. (1999)	0.75	5.30E-06		Taxodium	coniferous		dry	150	6.8	cDCE	0	25
Vroblesky et al. (1999)	0.75	5.30E-06		Taxodium	coniferous		dry	150	6.8	cDCE	225	150
Vroblesky et al. (1999)	0.75	5.30E-06		Taxodium	coniferous		dry	150	6.8	cDCE	24	150
Vroblesky et al. (1999)	0.75	5.30E-06		Taxodium	coniferous		dry	900	6.8	cDCE	61	150
Vroblesky et al. (1999)	0.75	5.30E-06		Taxodium	coniferous		dry	150	6.8	cDCE	175	150
Vroblesky et al. (1999)	0.75	5.30E-06		Taxodium	coniferous		dry	150	6.8	cDCE	47	300
Vroblesky et al. (1999)	0.75	5.30E-06		Taxodium	coniferous		dry	150	6.8	cDCE	16	300
Vroblesky et al. (1999)	0.75	5.30E-06		Taxodium	coniferous		dry	180	6.8	cDCE	18	300
Vroblesky et al. (1999)	0.75	5.30E-06		Taxodium	coniferous		dry	150	6.8	cDCE	23	300
Vroblesky et al. (1999)	0.75	5.30E-06		Taxodium	coniferous		dry	150	6.8	cDCE	19	75
Vroblesky et al. (1999)	0.75	5.30E-06		Taxodium	coniferous		dry	150	6.8	cDCE	26	75
Vroblesky et al. (1999)	0.75	5.30E-06		Taxodium	coniferous		dry	150	6.8	cDCE	0	125
Vroblesky et al. (1999)	0.75	5.30E-06		Taxodium	coniferous		dry	150	6.8	cDCE	0	125
Vroblesky et al. (1999)	0.75	5.30E-06		Taxodium	coniferous		dry	150	6.8	cDCE	32	25
Vroblesky et al. (1999)	0.75	5.30E-06		Taxodium	coniferous		dry	300	6.8	cDCE	33	25
Vroblesky et al. (1999)	0.75	5.30E-06		Taxodium	coniferous		dry	150	6.8	cDCE	11	25
Vroblesky et al. (1999)	0.75	5.30E-06		Taxodium	coniferous		dry	150	6.8	cDCE	0	25
Vroblesky et al. (1999)	0.75	5.30E-06		Taxodium	coniferous		dry	150	6.8	cDCE	54	50
Vroblesky et al. (1999)	0.75	5.30E-06		Taxodium	coniferous		dry	150	6.8	cDCE	12	25
Vroblesky et al. (1999)	0.75	5.30E-06		Taxodium	coniferous		dry	180	6.8	cDCE	12	325
Vroblesky et al. (1999)	0.75	5.30E-06		Taxodium	coniferous		dry	150	6.8	cDCE	18	325

Vroblesky et al. (1999)	0.75	5.30E-06		Taxodium	coniferous		dry	150	6.8	cDCE	25	325
Vroblesky et al. (1999)	0.75	5.30E-06		Taxodium	coniferous		dry	150	6.8	cDCE	0	150
Vroblesky et al. (1999)	0.75	5.30E-06		Taxodium	coniferous		dry	150	6.8	cDCE	99	325
Vroblesky et al. (1999)	0.75	5.30E-06		Taxodium	coniferous		dry	150	6.8	cDCE	124	325
Vroblesky et al. (1999)	0.75	5.30E-06		Taxodium	coniferous		dry	150	6.8	cDCE	0	50
Vroblesky et al. (1999)	0.75	5.30E-06		Taxodium	coniferous		dry	150	6.8	cDCE	0	50
Vroblesky et al. (1999)	0.75	5.30E-06		Taxodium	coniferous		dry	150	6.8	cDCE	0	50
Vroblesky et al. (1999)	0.75	5.30E-06		Taxodium	coniferous		dry	150	6.8	cDCE	0	50
Vroblesky et al. (1999)	0.75	5.30E-06		Taxodium	coniferous		dry	180	6.8	cDCE	0	50
Vroblesky et al. (1999)	0.75	5.30E-06		Taxodium	coniferous		dry	150	6.8	cDCE	0	100
Vroblesky et al. (1999)	0.75	5.30E-06		Taxodium	coniferous		dry	150	6.8	cDCE	0	150
Vroblesky et al. (1999)	0.75	5.30E-06		Taxodium	coniferous		dry	180	6.8	cDCE	0	200
Vroblesky et al. (1999)	0.75	5.30E-06		Taxodium	coniferous		dry	150	6.8	cDCE	29	400
Vroblesky et al. (1999)	0.75	5.30E-06		Taxodium	coniferous		dry	150	6.8	cDCE	23	400
Vroblesky et al. (1999)	0.75	5.30E-06		Taxodium	coniferous		dry	150	6.8	cDCE	55	400
Vroblesky et al. (1999)	0.75	5.30E-06		Taxodium	coniferous		dry	150	6.8	cDCE	71	400
Vroblesky et al. (1999)	0.75	5.30E-06		Taxodium	coniferous		dry	150	6.8	cDCE	0	450
Vroblesky et al. (1999)	0.75	5.30E-06		Taxodium	coniferous		dry	150	6.8	cDCE	0	450
Vroblesky et al. (1999)	0.75	5.30E-06		Taxodium	coniferous		dry	150	6.8	cDCE	0	400
Vroblesky et al. (1999)	0.75	5.30E-06		Taxodium	coniferous		dry	150	6.8	cDCE	0	300
Vroblesky et al. (1999)	0.75	5.30E-06		Taxodium	coniferous		dry	150	6.8	cDCE	0	300
Vroblesky et al. (1999)	0.75	5.30E-06		Taxodium	coniferous		dry	150	6.8	cDCE	0	200
Vroblesky et al. (1999)	0.75	5.30E-06		Taxodium	coniferous		dry	150	6.8	cDCE	0	200
Vroblesky et al. (1999)	0.75	5.30E-06		Taxodium	coniferous		dry	150	6.8	cDCE	0	50
Vroblesky et al. (1999)	0.75	5.30E-06		Taxodium	coniferous		dry	150	6.8	cDCE	0	50
Vroblesky et al. (1999)	0.75	5.30E-06		Liquidambar	diffuse-porous		dry	150	6.8	cDCE	60	50
Vroblesky et al. (1999)	0.75	5.30E-06		Liquidambar	diffuse-porous		dry	150	6.8	cDCE	0	75
Vroblesky et al. (1999)	0.75	5.30E-06		Liquidambar	diffuse-porous		dry	150	6.8	cDCE	0	100
Vroblesky et al. (1999)	0.75	5.30E-06		Liquidambar	diffuse-porous		dry	150	6.8	cDCE	0	100
Vroblesky et al. (1999)	0.75	5.30E-06		Liquidambar	diffuse-porous		dry	150	6.8	cDCE	0	100
Vroblesky et al. (1999)	0.75	5.30E-06		Nyssa	diffuse-porous		dry	150	6.8	cDCE	56	300
Vroblesky et al. (1999)	0.75	5.30E-06		Nyssa	diffuse-porous		dry	180	6.8	cDCE	66	300

Vroblesky et al. (1999)	0.75	5.30E-06		Nyssa	diffuse-porous		dry	150	6.8	cDCE	42	300
Vroblesky et al. (1999)	0.75	5.30E-06		Nyssa	diffuse-porous		dry	150	6.8	cDCE	74	300
Vroblesky et al. (1999)	0.75	5.30E-06		Nyssa	diffuse-porous		dry	150	6.8	cDCE	23	300
Vroblesky et al. (1999)	0.75	5.30E-06		Nyssa	diffuse-porous		dry	150	6.8	cDCE	0	50
Vroblesky et al. (1999)	0.75	5.30E-06		Nyssa	diffuse-porous		dry	150	6.8	cDCE	0	50
Vroblesky et al. (1999)	0.75	5.30E-06		Platanus	diffuse-porous		dry	150	6.8	cDCE	0	100
Vroblesky et al. (1999)	0.75	5.30E-06		Platanus	diffuse-porous		dry	150	6.8	cDCE	0	125
Vroblesky et al. (1999)	0.75	5.30E-06		Quercus	ring-porous		dry	180	6.8	cDCE	0	100
Vroblesky et al. (1999)	0.75	5.30E-06		Quercus	ring-porous		dry	150	6.8	cDCE	0	100
Vroblesky et al. (1999)	0.75	5.30E-06		Quercus	ring-porous		dry	150	6.8	cDCE	0	100
Vroblesky et al. (1999)	0.75	5.30E-06		Quercus	ring-porous		dry	150	6.8	cDCE	40	125
Vroblesky et al. (1999)	0.75	5.30E-06		Quercus	ring-porous		dry	150	6.8	cDCE	0	125
Vroblesky et al. (1999)	0.75	5.30E-06		Quercus	ring-porous		dry	150	6.8	cDCE	70	150
Vroblesky et al. (1999)	0.75	5.30E-06		Quercus	ring-porous		dry	150	6.8	cDCE	90	150
Vroblesky et al. (1999)	0.75	5.30E-06		Quercus	ring-porous		dry	150	6.8	cDCE	0	150
Vroblesky et al. (1999)	0.75	5.30E-06		Quercus	ring-porous		dry	150	6.8	cDCE	0	175
Vroblesky et al. (1999)	0.75	5.30E-06		Quercus	ring-porous		dry	150	6.8	cDCE	0	100
Holm & Rotard (2011)	2.8		4.0	Betula	diffuse-porous	24	SPME	50	4	cDCE	0.31	2500
Holm & Rotard (2011)	1.5		4.0	Betula	diffuse-porous	24	SPME	50	4	cDCE	1419	2500
Holm & Rotard (2011)	1.7		4.0	Betula	diffuse-porous	53	SPME	50	4	cDCE	43040	5645
Holm & Rotard (2011)	3.5		4.0	Betula	diffuse-porous	35	SPME	50	4	cDCE	9261	2500
Holm & Rotard (2011)	1.2		4.0	Betula	diffuse-porous	47	SPME	50	4	cDCE	0	2500
Holm & Rotard (2011)	1.8		4.0	Betula	diffuse-porous	31	SPME	50	4	cDCE	0	5000
Holm & Rotard (2011)	2		4.0	Betula	diffuse-porous	48	SPME	50	4	cDCE	0	2500
Holm & Rotard (2011)	3.5		4.0	Betula	diffuse-porous	33	SPME	50	4	cDCE	721	2500

Holm & Rotard (2011)	1.5		4.0	Betula	diffuse-porous	28	SPME	50	4	cDCE	11022	2500
Holm & Rotard (2011)	1.6		4.0	Malus	diffuse-porous	18	SPME	50	4	cDCE	4819	10000
Holm & Rotard (2011)	1.8		4.0	Populus	diffuse-porous	27	SPME	50	4	cDCE	14.4	5645
Holm & Rotard (2011)	1.9		4.0	Salix	diffuse-porous	35	SPME	50	4	cDCE	54.2	11054
Holm & Rotard (2011)	2		4.0	Salix	diffuse-porous	102	SPME	50	4	cDCE	0.56	8000
Holm & Rotard (2011)	2		4.0	Salix	diffuse-porous	45	SPME	50	4	cDCE	3.11	7000
Holm & Rotard (2011)	2		4.0	Salix	diffuse-porous	29	SPME	50	4	cDCE	43.2	7000
Holm & Rotard (2011)	1.5		4.0	Salix	diffuse-porous	48	SPME	50	4	cDCE	9.75	7000
Holm & Rotard (2011)	2		4.0	Salix	diffuse-porous	57	SPME	50	4	cDCE	1.09	7000
Holm & Rotard (2011)	2		4.0	Salix	diffuse-porous	63	SPME	50	4	cDCE	0.26	7000
Holm & Rotard (2011)	2		4.0	Salix	diffuse-porous	28	SPME	50	4	cDCE	0.44	7000
Holm & Rotard (2011)	2		4.0	Salix	diffuse-porous	83	SPME	50	4	cDCE	2698	7000
Holm & Rotard (2011)	2		4.0	Salix	diffuse-porous	34	SPME	50	4	cDCE	14497	7000
Holm & Rotard (2011)	2		4.0	Salix	diffuse-porous	41	SPME	50	4	cDCE	24038	7000
Holm & Rotard (2011)	3		4.0	Quercus	ring-porous	22	SPME	50	4	cDCE	0.06	2500
Larsen et al. (2008)	2.5	1.00E-04	3.0	Salix	diffuse-porous		dry	100		PCE	14944	5813
Larsen et al. (2008)	2.5	1.00E-04	3.0	Pinus	coniferous		dry	100		PCE	12058	40571
Larsen et al. (2008)	2.5	1.00E-04	3.0	Betula	diffuse-porous		dry	100		PCE	5136	40571
Larsen et al. (2008)	2.5	1.00E-04	3.0	Quercus	ring-porous		dry	100		PCE	2644	3860
Larsen et al. (2008)	2.5	1.00E-04	3.0	Alnus	diffuse-porous		dry	100		PCE	2277	3860
Larsen et al. (2008)	2.5	1.00E-04	3.0	Alnus	diffuse-porous		dry	100		PCE	1852	3860

Larsen et al. (2008)	2.5	1.00E-04	3.0	Betula	diffuse-porous		dry	100		PCE	1475	3860
Larsen et al. (2008)	2.5	1.00E-04	3.0	Alnus	diffuse-porous		dry	100		PCE	687	3860
Larsen et al. (2008)	2.5	1.00E-04	3.0	Pinus	coniferous		dry	100		PCE	203	80.5
Larsen et al. (2008)	2.5	1.00E-04	3.0	Populus	diffuse-porous		dry	100		PCE	176	5813
Larsen et al. (2008)	2.5	1.00E-04	3.0	Alnus	diffuse-porous		dry	100		PCE	77	7146
Larsen et al. (2008)	2.5	1.00E-04	3.0	Alnus	diffuse-porous		dry	100		PCE	22	7146
Larsen et al. (2008)	2.5	1.00E-04	3.0	Alnus	diffuse-porous		dry	100		PCE	0	5813
Larsen et al. (2008)	2.5	1.00E-04	3.0	Alnus	diffuse-porous		dry	100		PCE	0	5813
Larsen et al. (2008)	2.5	1.00E-04	3.0	Fagus	diffuse-porous		dry	100		PCE	0	8.2
Larsen et al. (2008)	2.5	1.00E-04	3.0	Quercus	ring-porous		dry	100		PCE	0	4.1
Larsen et al. (2008)	2.5	1.00E-04	3.0	Quercus	ring-porous		dry	100		PCE	0	11.2
Duncan et al. (2017)	9.5	1.00E-03		Prosopis	diffuse-porous		methanol		7	PCE	5320	2
Duncan et al. (2017)	9.5	1.00E-03		Parkinsonia	diffuse-porous		methanol	150	7	PCE	1195	2
Duncan et al. (2017)	9.5	1.00E-03		Populus	diffuse-porous		methanol	150	7	PCE	588	2
Duncan et al. (2017)	9.5	1.00E-03		Ambrosia	diffuse-porous		methanol		7	PCE	385	2
Duncan et al. (2017)	26	1.00E-04	4.0	Eucalyptus	diffuse-porous		methanol	150	7	PCE	2790	10
Duncan et al. (2017)	27	5.00E-05		Populus	diffuse-porous		methanol	150	7	PCE	0	70
Struckhoff & Burken (2005)	6.8	1.00E-04	6.0				dry		6	PCE	2580	1086
Struckhoff & Burken (2005)	6.8	1.00E-04	6.0				dry		6	PCE	2274	1958
Struckhoff & Burken (2005)	6.8	1.00E-04	6.0				dry		6	PCE	1714	645
Struckhoff & Burken (2005)	6.8	1.00E-04	6.0				dry		6	PCE	793	32

Struckhoff & Burken (2005)	6.8	1.00E-04	6.0				dry		6	PCE	456	739
Struckhoff & Burken (2005)	6.8	1.00E-04	6.0				dry		6	PCE	211	51
Struckhoff & Burken (2005)	6.8	1.00E-04	6.0				dry		6	PCE	174	2895
Struckhoff & Burken (2005)	6.8	1.00E-04	6.0				dry		6	PCE	133	32
Struckhoff & Burken (2005)	6.8	1.00E-04	6.0				dry		6	PCE	33	109
Struckhoff & Burken (2005)	6.8	1.00E-04	6.0				dry		6	PCE	15	683
Struckhoff & Burken (2005)	6.8	1.00E-04	6.0				dry		6	PCE	9	2221
Struckhoff & Burken (2005)	6.8	1.00E-04	6.0				dry		6	PCE	7	280
Struckhoff & Burken (2005)	6.8	1.00E-04	6.0				dry		6	PCE	1	49
Struckhoff & Burken (2005)	6.8	1.00E-04	6.0				dry		6	PCE	1	197
Struckhoff & Burken (2005)	6.8	1.00E-04	6.0				dry		6	PCE	1	48
Struckhoff & Burken (2005)	6.8	1.00E-04	6.0				dry		6	PCE	1	1
Struckhoff & Burken (2005)	6.8	1.00E-04	6.0				dry		6	PCE	0	1
Struckhoff & Burken (2005)	6.8	1.00E-04	6.0				dry		6	PCE	0	1
Struckhoff & Burken (2005)	6.8	1.00E-04	6.0				dry		6	PCE	0	1
Struckhoff & Burken (2005)	7.8	1.00E-04	6.0				dry		6	PCE	5	258
Vroblesky et al. (2004)	3	7.00E-05	0.9	Juniperus	coniferous		dry	150	3.8	TCE	0	300
Vroblesky et al. (2004)	7.9	7.00E-05	0.9	Juniperus	coniferous		dry	150	3.8	TCE	11	500
Vroblesky et al. (2004)	7.9	7.00E-05	0.9	Juniperus	coniferous		dry	150	3.8	TCE	7	600
Vroblesky et al. (2004)	5	7.00E-05	0.9	Pinus	coniferous		dry	150	3.8	TCE	6	400
Vroblesky et al. (2004)	4	7.00E-05	0.9	Populus	diffuse-porous		dry	150	3.8	TCE	334	300
Vroblesky et al. (2004)	4	7.00E-05	0.9	Populus	diffuse-porous		dry	150	3.8	TCE	340	300

Vroblesky et al. (2004)	5	7.00E-05	0.9	Populus	diffuse-porous		dry	150	3.8	TCE	101	50
Vroblesky et al. (2004)	1	7.00E-05	0.9	Populus	diffuse-porous	74.8	dry	150	3.8	TCE	1392	100
Vroblesky et al. (2004)	1	7.00E-05	0.9	Populus	diffuse-porous	74.8	dry	150	3.8	TCE	995	100
Vroblesky et al. (2004)	1	7.00E-05	0.9	Populus	diffuse-porous	74.8	dry	150	3.8	TCE	788	100
Vroblesky et al. (2004)	1	7.00E-05	0.9	Populus	diffuse-porous	74.8	dry	150	3.8	TCE	724	100
Vroblesky et al. (2004)	4	7.00E-05	0.9	Salix	diffuse-porous		dry	150	3.8	TCE	278	300
Vroblesky et al. (2004)	4	7.00E-05	0.9	Salix	diffuse-porous		dry	150	3.8	TCE	255	300
Vroblesky et al. (2004)	5	7.00E-05	0.9	Carya	ring-porous		dry	150	3.8	TCE	44	400
Vroblesky et al. (2004)	1	7.00E-05	0.9	Celtis	ring-porous		dry	150	3.8	TCE	59	200
Vroblesky et al. (2004)	5.6	7.00E-05	0.9	Quercus	ring-porous		dry	150	3.8	TCE	494	250
Vroblesky et al. (2004)	5.6	7.00E-05	0.9	Quercus	ring-porous		dry	150	3.8	TCE	207	100
Vroblesky et al. (2004)	6	7.00E-05	0.9	Quercus	ring-porous		dry	150	3.8	TCE	176	1200
Vroblesky et al. (2004)	5.6	7.00E-05	0.9	Quercus	ring-porous		dry	150	3.8	TCE	11	300
Vroblesky et al. (2004)	7	7.00E-05	0.9	Quercus	ring-porous		dry	150	3.8	TCE	50	1000
Vroblesky et al. (2004)	7	7.00E-05	0.9	Quercus	ring-porous		dry	150	3.8	TCE	120	1100
Vroblesky et al. (2004)	1	7.00E-05	0.9	Ulmus	ring-porous		dry	150	3.8	TCE	26	50
Vroblesky et al. (2004)	5	7.00E-05	0.9	Ulmus	ring-porous		dry	150	3.8	TCE	106	500
Vroblesky et al. (2004)	2	7.00E-05	0.9				dry	150	3.8	TCE	12	150
Vroblesky et al. (2004)	0.5	1.00E-05	6.6	Populus	diffuse-porous	25	dry	150	3.8	TCE	2191	39
Vroblesky et al. (2004)	1	1.00E-05	6.6	Populus	diffuse-porous	25	dry	150	3.8	TCE	2255	100
Vroblesky et al. (2004)	8	1.00E-05	6.6	Populus	diffuse-porous	25	dry	150	3.8	TCE	99	200
Vroblesky et al. (2004)	0.5	1.00E-05	6.6	Populus	diffuse-porous	25	dry	150	3.8	TCE	320	300
Vroblesky et al. (2004)	0.5	1.00E-05	6.6	Populus	diffuse-porous	25	dry	150	3.8	TCE	548	300
Vroblesky et al. (2004)	3	1.00E-05	6.6	Populus	diffuse-porous	25	dry	150	3.8	TCE	267	39
Vroblesky et al. (2004)	0.5	1.00E-05	6.6	Populus	diffuse-porous	25	dry	150	3.8	TCE	552	29

Vroblesky et al. (2004)	0.5	1.00E-05	6.6	Populus	diffuse-porous	25	dry	150	3.8	TCE	1272	500
Vroblesky et al. (2004)	0.5	1.00E-05	6.6	Quercus	ring-porous	25	dry	150	3.8	TCE	295	300
Vroblesky et al. (2004)	3	4.00E-06	3.5	Pinus	coniferous	36.5	dry	150	3.8	TCE	8535	10000
Vroblesky et al. (2004)	3	4.00E-06	3.5	Pinus	coniferous	35	dry	150	3.8	TCE	54	500
Vroblesky et al. (2004)	3	4.00E-06	3.5	Pinus	coniferous	35	dry	150	3.8	TCE	54	500
Vroblesky et al. (2004)	3	4.00E-06	3.5	Pinus	coniferous	35	dry	150	3.8	TCE	97	1100
Vroblesky et al. (2004)	3	4.00E-06	3.5	Pinus	coniferous	35	dry	150	3.8	TCE	68	50
Vroblesky et al. (2004)	3	4.00E-06	3.5	Pinus	coniferous	35	dry	150	3.8	TCE	1052	500
Vroblesky et al. (2004)	3	4.00E-06	3.5	Pinus	coniferous	35	dry	150	3.8	TCE	291	10000
Vroblesky et al. (2004)	3	4.00E-06	3.5	Pinus	coniferous	35	dry	150	3.8	TCE	962	700
Vroblesky et al. (2004)	3	4.00E-06	3.5	Pinus	coniferous	35	dry	150	3.8	TCE	10190	10000
Vroblesky et al. (2004)	3	4.00E-06	3.5	Pinus	coniferous	35	dry	150	3.8	TCE	1446	900
Larsen et al. (2008)	2.5	1.00E-04	3.0	Salix	diffuse-porous		dry	100		TCE	429	96.2
Larsen et al. (2008)	2.5	1.00E-04	3.0	Pinus	coniferous		dry	100		TCE	536	330
Larsen et al. (2008)	2.5	1.00E-04	3.0	Betula	diffuse-porous		dry	100		TCE	86	330
Larsen et al. (2008)	2.5	1.00E-04	3.0	Quercus	ring-porous		dry	100		TCE	12	36.4
Larsen et al. (2008)	2.5	1.00E-04	3.0	Alnus	diffuse-porous		dry	100		TCE	0	36.4
Larsen et al. (2008)	2.5	1.00E-04	3.0	Alnus	diffuse-porous		dry	100		TCE	0	36.4
Larsen et al. (2008)	2.5	1.00E-04	3.0	Betula	diffuse-porous		dry	100		TCE	12	36.4
Larsen et al. (2008)	2.5	1.00E-04	3.0	Alnus	diffuse-porous		dry	100		TCE	0	36.4
Larsen et al. (2008)	2.5	1.00E-04	3.0	Pinus	coniferous		dry	100		TCE	45	5.9
Larsen et al. (2008)	2.5	1.00E-04	3.0	Populus	diffuse-porous		dry	100		TCE	0	96.2
Larsen et al. (2008)	2.5	1.00E-04	3.0	Alnus	diffuse-porous		dry	100		TCE	0	99
Larsen et al. (2008)	2.5	1.00E-04	3.0	Alnus	diffuse-porous		dry	100		TCE	0	99
Larsen et al. (2008)	2.5	1.00E-04	3.0	Alnus	diffuse-porous		dry	100		TCE	0	96.2
Larsen et al. (2008)	2.5	1.00E-04	3.0	Alnus	diffuse-porous		dry	100		TCE	0	96.2
Larsen et al. (2008)	2.5	1.00E-04	3.0	Fagus	diffuse-porous		dry	100		TCE	0	0.9

Larsen et al. (2008)	2.5	1.00E-04	3.0	Quercus	ring-porous		dry	100		TCE	0	0.3
Larsen et al. (2008)	2.5	1.00E-04	3.0	Quercus	ring-porous		dry	100		TCE	0	2.6
Duncan et al. (2017)	26	1.00E-04	4.0	Eucalyptus	diffuse-porous		methanol	150	7	TCE	22760	70
Duncan et al. (2017)	27	5.00E-05		Populus	diffuse-porous		methanol	150	7	TCE	50	170
Vroblesky et al. (1999)	0.75	5.30E-06		Pinus	coniferous		dry	150	6.8	TCE	730	1400
Vroblesky et al. (1999)	0.75	5.30E-06		Pinus	coniferous		dry	150	6.8	TCE	1742	1400
Vroblesky et al. (1999)	0.75	5.30E-06		Pinus	coniferous		dry	150	6.8	TCE	1241	1400
Vroblesky et al. (1999)	0.75	5.30E-06		Pinus	coniferous		dry	150	6.8	TCE	308	800
Vroblesky et al. (1999)	0.75	5.30E-06		Pinus	coniferous		dry	150	6.8	TCE	318	800
Vroblesky et al. (1999)	0.75	5.30E-06		Pinus	coniferous		dry	150	6.8	TCE	751	800
Vroblesky et al. (1999)	0.75	5.30E-06		Pinus	coniferous		dry	150	6.8	TCE	764	1200
Vroblesky et al. (1999)	0.75	5.30E-06		Pinus	coniferous		dry	150	6.8	TCE	2263	900
Vroblesky et al. (1999)	0.75	5.30E-06		Pinus	coniferous		dry	150	6.8	TCE	118	800
Vroblesky et al. (1999)	0.75	5.30E-06		Pinus	coniferous		dry	150	6.8	TCE	1131	1400
Vroblesky et al. (1999)	0.75	5.30E-06		Pinus	coniferous		dry	150	6.8	TCE	479	900
Vroblesky et al. (1999)	0.75	5.30E-06		Taxodium	coniferous		dry	150	6.8	TCE	220	327
Vroblesky et al. (1999)	0.75	5.30E-06		Taxodium	coniferous		dry	150	6.8	TCE	376	327
Vroblesky et al. (1999)	0.75	5.30E-06		Taxodium	coniferous		dry	150	6.8	TCE	100	327
Vroblesky et al. (1999)	0.75	5.30E-06		Taxodium	coniferous		dry	150	6.8	TCE	298	327
Vroblesky et al. (1999)	0.75	5.30E-06		Taxodium	coniferous		dry	150	6.8	TCE	0	327
Vroblesky et al. (1999)	0.75	5.30E-06		Taxodium	coniferous		dry	150	6.8	TCE	410	2400
Vroblesky et al. (1999)	0.75	5.30E-06		Taxodium	coniferous		dry	150	6.8	TCE	8590	1500
Vroblesky et al. (1999)	0.75	5.30E-06		Taxodium	coniferous		dry	150	6.8	TCE	3180	1500
Vroblesky et al. (1999)	0.75	5.30E-06		Taxodium	coniferous		dry	150	6.8	TCE	2093	1500
Vroblesky et al. (1999)	0.75	5.30E-06		Taxodium	coniferous		dry	900	6.8	TCE	35040	1500
Vroblesky et al. (1999)	0.75	5.30E-06		Taxodium	coniferous		dry	150	6.8	TCE	4370	1500
Vroblesky et al. (1999)	0.75	5.30E-06		Taxodium	coniferous		dry	150	6.8	TCE	780	2300
Vroblesky et al. (1999)	0.75	5.30E-06		Taxodium	coniferous		dry	150	6.8	TCE	283	2200
Vroblesky et al. (1999)	0.75	5.30E-06		Taxodium	coniferous		dry	180	6.8	TCE	119	2200
Vroblesky et al. (1999)	0.75	5.30E-06		Taxodium	coniferous		dry	150	6.8	TCE	174	2200
Vroblesky et al. (1999)	0.75	5.30E-06		Taxodium	coniferous		dry	150	6.8	TCE	362	750
Vroblesky et al. (1999)	0.75	5.30E-06		Taxodium	coniferous		dry	150	6.8	TCE	457	750
Vroblesky et al. (1999)	0.75	5.30E-06		Taxodium	coniferous		dry	150	6.8	TCE	106	900
Vroblesky et al. (1999)	0.75	5.30E-06		Taxodium	coniferous		dry	150	6.8	TCE	116	900
Vroblesky et al. (1999)	0.75	5.30E-06		Taxodium	coniferous		dry	150	6.8	TCE	296	900
Vroblesky et al. (1999)	0.75	5.30E-06		Taxodium	coniferous		dry	300	6.8	TCE	153	900
Vroblesky et al. (1999)	0.75	5.30E-06		Taxodium	coniferous		dry	150	6.8	TCE	824	850

Vroblesky et al. (1999)	0.75	5.30E-06		Taxodium	coniferous		dry	150	6.8	TCE	270	850
Vroblesky et al. (1999)	0.75	5.30E-06		Taxodium	coniferous		dry	150	6.8	TCE	310	600
Vroblesky et al. (1999)	0.75	5.30E-06		Taxodium	coniferous		dry	150	6.8	TCE	536	600
Vroblesky et al. (1999)	0.75	5.30E-06		Taxodium	coniferous		dry	150	6.8	TCE	0	300
Vroblesky et al. (1999)	0.75	5.30E-06		Taxodium	coniferous		dry	150	6.8	TCE	0	100
Vroblesky et al. (1999)	0.75	5.30E-06		Taxodium	coniferous		dry	180	6.8	TCE	415	2000
Vroblesky et al. (1999)	0.75	5.30E-06		Taxodium	coniferous		dry	150	6.8	TCE	221	2000
Vroblesky et al. (1999)	0.75	5.30E-06		Taxodium	coniferous		dry	150	6.8	TCE	430	2000
Vroblesky et al. (1999)	0.75	5.30E-06		Taxodium	coniferous		dry	150	6.8	TCE	1324	1400
Vroblesky et al. (1999)	0.75	5.30E-06		Taxodium	coniferous		dry	150	6.8	TCE	966	2000
Vroblesky et al. (1999)	0.75	5.30E-06		Taxodium	coniferous		dry	150	6.8	TCE	242	2000
Vroblesky et al. (1999)	0.75	5.30E-06		Taxodium	coniferous		dry	150	6.8	TCE	0	300
Vroblesky et al. (1999)	0.75	5.30E-06		Taxodium	coniferous		dry	150	6.8	TCE	0	400
Vroblesky et al. (1999)	0.75	5.30E-06		Taxodium	coniferous		dry	150	6.8	TCE	0	450
Vroblesky et al. (1999)	0.75	5.30E-06		Taxodium	coniferous		dry	150	6.8	TCE	0	500
Vroblesky et al. (1999)	0.75	5.30E-06		Taxodium	coniferous		dry	180	6.8	TCE	0	500
Vroblesky et al. (1999)	0.75	5.30E-06		Taxodium	coniferous		dry	150	6.8	TCE	28	700
Vroblesky et al. (1999)	0.75	5.30E-06		Taxodium	coniferous		dry	150	6.8	TCE	96	1000
Vroblesky et al. (1999)	0.75	5.30E-06		Taxodium	coniferous		dry	180	6.8	TCE	272	1400
Vroblesky et al. (1999)	0.75	5.30E-06		Taxodium	coniferous		dry	150	6.8	TCE	167	2000
Vroblesky et al. (1999)	0.75	5.30E-06		Taxodium	coniferous		dry	150	6.8	TCE	244	2000
Vroblesky et al. (1999)	0.75	5.30E-06		Taxodium	coniferous		dry	150	6.8	TCE	216	2000
Vroblesky et al. (1999)	0.75	5.30E-06		Taxodium	coniferous		dry	150	6.8	TCE	351	2500
Vroblesky et al. (1999)	0.75	5.30E-06		Taxodium	coniferous		dry	150	6.8	TCE	46	2000
Vroblesky et al. (1999)	0.75	5.30E-06		Taxodium	coniferous		dry	150	6.8	TCE	310	2500
Vroblesky et al. (1999)	0.75	5.30E-06		Taxodium	coniferous		dry	150	6.8	TCE	49	2000
Vroblesky et al. (1999)	0.75	5.30E-06		Taxodium	coniferous		dry	150	6.8	TCE	249	1800
Vroblesky et al. (1999)	0.75	5.30E-06		Taxodium	coniferous		dry	150	6.8	TCE	128	1800
Vroblesky et al. (1999)	0.75	5.30E-06		Taxodium	coniferous		dry	150	6.8	TCE	219	1750
Vroblesky et al. (1999)	0.75	5.30E-06		Taxodium	coniferous		dry	150	6.8	TCE	213	1750
Vroblesky et al. (1999)	0.75	5.30E-06		Taxodium	coniferous		dry	150	6.8	TCE	71	1500
Vroblesky et al. (1999)	0.75	5.30E-06		Taxodium	coniferous		dry	150	6.8	TCE	63	1500
Vroblesky et al. (1999)	0.75	5.30E-06		Taxodium	coniferous		dry	150	6.8	TCE	78	1300
Vroblesky et al. (1999)	0.75	5.30E-06		Taxodium	coniferous		dry	150	6.8	TCE	31	1300
Vroblesky et al. (1999)	0.75	5.30E-06		Taxodium	coniferous		dry	150	6.8	TCE	25	1300
Vroblesky et al. (1999)	0.75	5.30E-06		Taxodium	coniferous		dry	150	6.8	TCE	0	1000
Vroblesky et al. (1999)	0.75	5.30E-06		Taxodium	coniferous		dry	150	6.8	TCE	44	900
Vroblesky et al. (1999)	0.75	5.30E-06		Liquidambar	diffuse-porous		dry	150	6.8	TCE	0	200

Vroblesky et al. (1999)	0.75	5.30E-06		Liquidambar	diffuse-porous		dry	150	6.8	TCE	0	200
Vroblesky et al. (1999)	0.75	5.30E-06		Liquidambar	diffuse-porous		dry	150	6.8	TCE	230	1200
Vroblesky et al. (1999)	0.75	5.30E-06		Liquidambar	diffuse-porous		dry	150	6.8	TCE	60	1000
Vroblesky et al. (1999)	0.75	5.30E-06		Liquidambar	diffuse-porous		dry	150	6.8	TCE	0	1000
Vroblesky et al. (1999)	0.75	5.30E-06		Liquidambar	diffuse-porous		dry	150	6.8	TCE	74	1300
Vroblesky et al. (1999)	0.75	5.30E-06		Nyssa	diffuse-porous		dry	150	6.8	TCE	1469	2200
Vroblesky et al. (1999)	0.75	5.30E-06		Nyssa	diffuse-porous		dry	180	6.8	TCE	1021	2200
Vroblesky et al. (1999)	0.75	5.30E-06		Nyssa	diffuse-porous		dry	150	6.8	TCE	1149	2200
Vroblesky et al. (1999)	0.75	5.30E-06		Nyssa	diffuse-porous		dry	150	6.8	TCE	426	2100
Vroblesky et al. (1999)	0.75	5.30E-06		Nyssa	diffuse-porous		dry	150	6.8	TCE	1033	2100
Vroblesky et al. (1999)	0.75	5.30E-06		Nyssa	diffuse-porous		dry	150	6.8	TCE	0	600
Vroblesky et al. (1999)	0.75	5.30E-06		Nyssa	diffuse-porous		dry	150	6.8	TCE	0	600
Vroblesky et al. (1999)	0.75	5.30E-06		Platanus	diffuse-porous		dry	150	6.8	TCE	0	750
Vroblesky et al. (1999)	0.75	5.30E-06		Platanus	diffuse-porous		dry	150	6.8	TCE	130	800
Vroblesky et al. (1999)	0.75	5.30E-06		Quercus	ring-porous		dry	180	6.8	TCE	0	700
Vroblesky et al. (1999)	0.75	5.30E-06		Quercus	ring-porous		dry	150	6.8	TCE	0	700
Vroblesky et al. (1999)	0.75	5.30E-06		Quercus	ring-porous		dry	150	6.8	TCE	0	700
Vroblesky et al. (1999)	0.75	5.30E-06		Quercus	ring-porous		dry	150	6.8	TCE	0	1200
Vroblesky et al. (1999)	0.75	5.30E-06		Quercus	ring-porous		dry	150	6.8	TCE	0	1200
Vroblesky et al. (1999)	0.75	5.30E-06		Quercus	ring-porous		dry	150	6.8	TCE	0	1400
Vroblesky et al. (1999)	0.75	5.30E-06		Quercus	ring-porous		dry	150	6.8	TCE	0	1400
Vroblesky et al. (1999)	0.75	5.30E-06		Quercus	ring-porous		dry	150	6.8	TCE	0	1400
Vroblesky et al. (1999)	0.75	5.30E-06		Quercus	ring-porous		dry	150	6.8	TCE	0	1500
Vroblesky et al. (1999)	0.75	5.30E-06		Quercus	ring-porous		dry	150	6.8	TCE	69	900
Holm & Rotard (2011)	2.8		4.0	Betula	diffuse-porous	24	SPME	50	4	TCE	66.1	5000

Holm & Rotard (2011)	1.5		4.0	Betula	diffuse-porous	24	SPME	50	4	TCE	841	6000
Holm & Rotard (2011)	1.7		4.0	Betula	diffuse-porous	53	SPME	50	4	TCE	20.9	115574
Holm & Rotard (2011)	3.5		4.0	Betula	diffuse-porous	35	SPME	50	4	TCE	10.5	5000
Holm & Rotard (2011)	1.2		4.0	Betula	diffuse-porous	47	SPME	50	4	TCE	37.1	5000
Holm & Rotard (2011)	1.8		4.0	Betula	diffuse-porous	31	SPME	50	4	TCE	14.4	20000
Holm & Rotard (2011)	2		4.0	Betula	diffuse-porous	48	SPME	50	4	TCE	0.31	5000
Holm & Rotard (2011)	3.5		4.0	Betula	diffuse-porous	33	SPME	50	4	TCE	1.77	5000
Holm & Rotard (2011)	1.5		4.0	Betula	diffuse-porous	28	SPME	50	4	TCE	32.8	5000
Holm & Rotard (2011)	1.6		4.0	Malus	diffuse-porous	18	SPME	50	4	TCE	11.1	70000
Holm & Rotard (2011)	1.8		4.0	Populus	diffuse-porous	27	SPME	50	4	TCE	2730	115574
Holm & Rotard (2011)	1.9		4.0	Salix	diffuse-porous	35	SPME	50	4	TCE	155	75501
Holm & Rotard (2011)	2		4.0	Salix	diffuse-porous	102	SPME	50	4	TCE	91.4	60000
Holm & Rotard (2011)	2		4.0	Salix	diffuse-porous	45	SPME	50	4	TCE	3.7	50000
Holm & Rotard (2011)	2		4.0	Salix	diffuse-porous	29	SPME	50	4	TCE	2059	50000
Holm & Rotard (2011)	1.5		4.0	Salix	diffuse-porous	48	SPME	50	4	TCE	0.17	50000
Holm & Rotard (2011)	2		4.0	Salix	diffuse-porous	57	SPME	50	4	TCE	0.78	50000
Holm & Rotard (2011)	2		4.0	Salix	diffuse-porous	63	SPME	50	4	TCE	21.5	50000
Holm & Rotard (2011)	2		4.0	Salix	diffuse-porous	28	SPME	50	4	TCE	4181	50000
Holm & Rotard (2011)	2		4.0	Salix	diffuse-porous	83	SPME	50	4	TCE	5.67	50000
Holm & Rotard (2011)	2		4.0	Salix	diffuse-porous	34	SPME	50	4	TCE	55.2	50000

Holm & Rotard (2011)	2		4.0	Salix	diffuse-porous	41	SPME	50	4	TCE	21.8	50000
Holm & Rotard (2011)	3		4.0	Quercus	ring-porous	22	SPME	50	4	TCE	661	5000
Cox (2002)	9	1.00E-03	1.0	Pseudotsuga	coniferous	30	dry	120	6	TCE	0	72
Cox (2002)	9	1.00E-03	1.0	Pseudotsuga	coniferous	20	dry	120	6	TCE	0	72
Cox (2002)	9	1.00E-03	1.0	Pseudotsuga	coniferous	30	dry	120	6	TCE	0	72
Cox (2002)	9	1.00E-03	1.0	Pseudotsuga	coniferous	24	dry	120	6	TCE	0	7.2
Cox (2002)	9	1.00E-03	1.0	Pseudotsuga	coniferous	36	dry	120	6	TCE	0	47
Cox (2002)	9	1.00E-03	1.0	Pseudotsuga	coniferous	24	dry	120	6	TCE	0	20
Cox (2002)	9	1.00E-03	1.0	Pseudotsuga	coniferous	20	dry	120	6	TCE	0	1.3
Cox (2002)	9	1.00E-03	1.0	Pseudotsuga	coniferous	30	dry	120	6	TCE	0	14
Cox (2002)	9	1.00E-03	1.0	Pseudotsuga	coniferous	36	dry	120	6	TCE	0	7.2
Cox (2002)	9	1.00E-03	1.0	Pseudotsuga	coniferous	24	dry	120	6	TCE	0	72
Cox (2002)	9	1.00E-03	1.0	Quercus	ring-porous	16	dry	120	6	TCE	0	10
Cox (2002)	9	1.00E-03	1.0	Quercus	ring-porous	24	dry	120	6	TCE	0	30
Cox (2002)	9	1.00E-03	1.0	Quercus	ring-porous	30	dry	120	6	TCE	0	10
Cox (2002)	9	1.00E-03	1.0	Quercus	ring-porous	18	dry	120	6	TCE	0	72
Wittinglerova et al. (2013)	0.75	1.10E-04	3.0	Alnus	diffuse-porous	24	water	100	12.5	Sum of CEs	8489	9873
Wittinglerova et al. (2013)	0.6	1.10E-04	3.0	Alnus	diffuse-porous	24	water	100	12.5	Sum of CEs	2545	9361
Wittinglerova et al. (2013)	0.75	1.10E-04	3.0	Alnus	diffuse-porous	24	water	100	12.5	Sum of CEs	3578	8103
Wittinglerova et al. (2013)	1	1.10E-04	3.0	Alnus	diffuse-porous	24	water	100	12.5	Sum of CEs	3171	11610
Wittinglerova et al. (2013)	1	1.10E-04	3.0	Alnus	diffuse-porous	24	water	100	12.5	Sum of CEs	449	7185
Wittinglerova et al. (2013)	1	1.10E-04	3.0	Alnus	diffuse-porous	24	water	100	12.5	Sum of CEs	2626	10666
Wittinglerova et al. (2013)	1	1.10E-04	3.0	Alnus	diffuse-porous	24	water	100	12.5	Sum of CEs	1368	7864
Wittinglerova et al. (2013)	1.05	1.10E-04	3.0	Alnus	diffuse-porous	24	water	100	12.5	Sum of CEs	1068	6579
Wittinglerova et al. (2013)	0.95	1.10E-04	3.0	Alnus	diffuse-porous	24	water	100	12.5	Sum of CEs	5614	4842
Wittinglerova et al. (2013)	0.9	1.10E-04	3.0	Alnus	diffuse-porous	24	water	100	12.5	Sum of CEs	1188	5128
Wittinglerova et al. (2013)	0.6	1.10E-04	3.0	Alnus	diffuse-porous	24	water	100	12.5	Sum of CEs	8130	8103

Wittinglerova et al. (2013)	0.75	1.10E-04	3.0	Alnus	diffuse-porous	24	water	100	12.5	Sum of CEs	2106	6126
Wittinglerova et al. (2013)	0.57	1.10E-04	3.0	Populus	diffuse-porous	36	water	100	12.5	Sum of CEs	1786	1173
Wittinglerova et al. (2013)	0.35	1.10E-04	3.0	Populus	diffuse-porous	36	water	100	12.5	Sum of CEs	2901	699
Wittinglerova et al. (2013)	0.57	1.10E-04	3.0	Populus	diffuse-porous	36	water	100	12.5	Sum of CEs	1265	1103
Wittinglerova et al. (2013)	0.92	1.10E-04	3.0	Populus	diffuse-porous	36	water	100	12.5	Sum of CEs	1501	651
Wittinglerova et al. (2013)	0.94	1.10E-04	3.0	Populus	diffuse-porous	36	water	100	12.5	Sum of CEs	1027	506
Wittinglerova et al. (2013)	0.99	1.10E-04	3.0	Populus	diffuse-porous	36	water	100	12.5	Sum of CEs	1708	945
Wittinglerova et al. (2013)	0.99	1.10E-04	3.0	Populus	diffuse-porous	36	water	100	12.5	Sum of CEs	1691	633
Wittinglerova et al. (2013)	0.99	1.10E-04	3.0	Populus	diffuse-porous	36	water	100	12.5	Sum of CEs	782	742
Wittinglerova et al. (2013)	0.87	1.10E-04	3.0	Populus	diffuse-porous	36	water	100	12.5	Sum of CEs	2851	175
Wittinglerova et al. (2013)	0.77	1.10E-04	3.0	Populus	diffuse-porous	36	water	100	12.5	Sum of CEs	2088	435
Wittinglerova et al. (2013)	0.48	1.10E-04	3.0	Populus	diffuse-porous	36	water	100	12.5	Sum of CEs	2671	978
Wittinglerova et al. (2013)	0.54	1.10E-04	3.0	Populus	diffuse-porous	36	water	100	12.5	Sum of CEs	648	3093
Wittinglerova et al. (2013)	1.66	1.10E-04	3.0	Pinus	coniferous	11	water	100	12.5	Sum of CEs	648	3009
Wittinglerova et al. (2013)	1.64	1.10E-04	3.0	Pinus	coniferous	11	water	100	12.5	Sum of CEs	461	3470
Wittinglerova et al. (2013)	1.82	1.10E-04	3.0	Pinus	coniferous	11	water	100	12.5	Sum of CEs	147	3581
Wittinglerova et al. (2013)	1.84	1.10E-04	3.0	Pinus	coniferous	11	water	100	12.5	Sum of CEs	582	2960
Wittinglerova et al. (2013)	1.82	1.10E-04	3.0	Pinus	coniferous	11	water	100	12.5	Sum of CEs	651	2108
Wittinglerova et al. (2013)	1.8	1.10E-04	3.0	Pinus	coniferous	11	water	100	12.5	Sum of CEs	822	2203
Wittinglerova et al. (2013)	1.76	1.10E-04	3.0	Pinus	coniferous	11	water	100	12.5	Sum of CEs	431	2059
Wittinglerova et al. (2013)	1.85	1.10E-04	3.0	Pinus	coniferous	11	water	100	12.5	Sum of CEs	380	2792
Wittinglerova et al. (2013)	1.86	1.10E-04	3.0	Pinus	coniferous	11	water	100	12.5	Sum of CEs	1174	1881
Wittinglerova et al. (2013)	1.71	1.10E-04	3.0	Pinus	coniferous	11	water	100	12.5	Sum of CEs	714	3049
Wittinglerova et al. (2013)	1.46	1.10E-04	3.0	Pinus	coniferous	11	water	100	12.5	Sum of CEs	971	3272
Wittinglerova et al. (2013)	1.54	1.10E-04	3.0	Pinus	coniferous	11	water	100	12.5	Sum of CEs	639	4628
Wittinglerova et al. (2013)	2.66	1.10E-04	3.0	Pinus	coniferous	25	water	100	12.5	Sum of CEs	24135	130495
Wittinglerova et al. (2013)	2.8	1.10E-04	3.0	Pinus	coniferous	25	water	100	12.5	Sum of CEs	33481	120653

Wittinglerova et al. (2013)	2.92	1.10E-04	3.0	Pinus	coniferous	25	water	100	12.5	Sum of CEs	22815	26653
Wittinglerova et al. (2013)	2.83	1.10E-04	3.0	Pinus	coniferous	25	water	100	12.5	Sum of CEs	22566	230624
Wittinglerova et al. (2013)	2.74	1.10E-04	3.0	Pinus	coniferous	25	water	100	12.5	Sum of CEs	29717	54115
Wittinglerova et al. (2013)	2.65	1.10E-04	3.0	Pinus	coniferous	25	water	100	12.5	Sum of CEs	22615	24808
Wittinglerova et al. (2013)	2.75	1.10E-04	3.0	Pinus	coniferous	25	water	100	12.5	Sum of CEs	17706	22093
Wittinglerova et al. (2013)	1.33	1.10E-04	3.0	Pinus	coniferous	25	water	100	12.5	Sum of CEs	66251	5122
Wittinglerova et al. (2013)	2.6	1.10E-04	3.0	Pinus	coniferous	25	water	100	12.5	Sum of CEs	36123	25980
Wittinglerova et al. (2013)	1.75	1.10E-04	3.0	Pinus	coniferous	25	water	100	12.5	Sum of CEs	36422	4623
Wittinglerova et al. (2013)	2.55	1.10E-04	3.0	Pinus	coniferous	25	water	100	12.5	Sum of CEs	16710	51523
Wittinglerova et al. (2013)	2.66	1.10E-04	3.0	Betula	diffuse-porous	21	water	100	12.5	Sum of CEs	8785	130495
Wittinglerova et al. (2013)	2.8	1.10E-04	3.0	Betula	diffuse-porous	21	water	100	12.5	Sum of CEs	9358	120653
Wittinglerova et al. (2013)	2.92	1.10E-04	3.0	Betula	diffuse-porous	21	water	100	12.5	Sum of CEs	8012	26653
Wittinglerova et al. (2013)	2.83	1.10E-04	3.0	Betula	diffuse-porous	21	water	100	12.5	Sum of CEs	4199	230624
Wittinglerova et al. (2013)	2.74	1.10E-04	3.0	Betula	diffuse-porous	21	water	100	12.5	Sum of CEs	16834	54115
Wittinglerova et al. (2013)	2.65	1.10E-04	3.0	Betula	diffuse-porous	21	water	100	12.5	Sum of CEs	8087	24808
Wittinglerova et al. (2013)	2.75	1.10E-04	3.0	Betula	diffuse-porous	21	water	100	12.5	Sum of CEs	7016	22093
Wittinglerova et al. (2013)	1.33	1.10E-04	3.0	Betula	diffuse-porous	21	water	100	12.5	Sum of CEs	83795	5122
Wittinglerova et al. (2013)	2.6	1.10E-04	3.0	Betula	diffuse-porous	21	water	100	12.5	Sum of CEs	5146	25980
Wittinglerova et al. (2013)	1.75	1.10E-04	3.0	Betula	diffuse-porous	21	water	100	12.5	Sum of CEs	5720	4623
Wittinglerova et al. (2013)	2.55	1.10E-04	3.0	Betula	diffuse-porous	21	water	100	12.5	Sum of CEs	19177	51523

SM – Chapter 3

Values equal to 0 correspond to measures below limit of detection

Blank cells correspond to measures not available/not measured

Site A

survey	ID	species	diameter (cm)	L (cm)	H (cm)	colorimetric vials		PID (ppm)	Tree-core concentration (µg/kg)							
						compound	measure (ppm)		PCE	TCE	cDCE	VC	Benzene	Styrene	1,1,2,2-TCA	Naphthalene
1 - 29/06/2020	A1_SP22	Acer saccharinum	30	5.5	100	Benzene	0		0	0	0	0	0	0	0	0
1 - 29/06/2020	A2_SP22	Quercus sp	64	11.5	100	Benzene	0		0	0	0	0	9.9	0	0	0
1 - 29/06/2020	A_PB11	Acer campestris	75	11.5	100				0	0	0	0	0	0	0	0
1 - 29/06/2020	A_PB1	Tilia sp	47	11.5	100	PCE and TCE	0		1.4	0.7	0	0	0	22.69	5	0
1 - 29/06/2020	A_SI08	Alnus sp	66	11.5	100	TCE	0		0	0	0	0	0	0	0	0
1 - 29/06/2020	Bianco	Tilia sp	37	11.5	100		0		0	0	0	0	0	43.8	0	0
1 - 29/06/2020	A_SP22	Tilia sp	30	11.5	100	Benzene	0		0	0	0	0	0	27.9	0	24
2 - 15/04/2021	A_PB11	Acer campestris	75	12	100	Benzene	0	0	0	0	0	0	0	0	0	
2 - 15/04/2021	A_PB11	Acer campestris	75	12	50	Benzene	0	0	0	0	0	0	0	0	0	
2 - 15/04/2021	A_SP22	Tilia sp	30	12	100	Benzene	0	0	0	0	0	0	0	0	0	
2 - 15/04/2021	A_SP22	Tilia sp	30	12	50	Benzene	0	0	0	0	0	0	0	0	0	
2 - 15/04/2021	A2_SP22	Quercus sp	64	12	100	Benzene	0	0	0	0	0	0	5.2	0	0	
2 - 15/04/2021	A2_SP22	Quercus sp	64	12	50	Benzene	0	0	0	0	0	0	6.4	0	0	
2 - 15/04/2021	A_PB1	Tilia sp	47	11	100	PCE and TCE	0	0	0.8	0	0	0	0	3	14.4	
2 - 15/04/2021	A_PB1	Tilia sp	47	12.5	50	PCE and TCE	0	0	1	0	0	0	0	4.6	19.8	

2 - 15/04/2021	APB11_b	Populus nigra	128	12	100	Benzene	0	0.1	0	0	0	0	0	6	0	

B site

survey	ID	species	diameter (cm)	L (cm)	H (cm)	colorimetric vials		PID (ppm)	Tree-core concentration (µg/kg)			
						compound	measure (ppm)		PCE	TCE	cDCE	VC
1 - 03/09/2020	AC2	Tilia sp	59	11.5	100	PCE	1.2	0.4	436	1050	0	0
				11.5	100	TCE	0	0.3				
1 - 03/09/2020	AC8	Populus nigra	46	12.5	100	PCE	0	0.6	7300	2.2	0	0
				12	100	TCE	saturation	1.3				
1 - 03/09/2020	AC6	Populus nigra	94	11.5	100	PCE	0.2	0.8	970	8.7	3.8	0
				11.5	100	TCE		0.5				
1 - 03/09/2020	AC3	Quercus robur	43	11.5	100	PCE	0	0	41	0	0	0
				12	100	TCE	0	0				
1 - 03/09/2020	AC10B	Populus alba	87	11.5	100	PCE	0	0.1	222	0	0	0
				12	100	TCE	0	0.2				
1 - 03/09/2020	AC10	tilia sp	73	12	100	PCE	0	0	343	0	0	0
				12	100	TCE	0	0				
1 - 03/09/2020	BIANCO	Ulmus sp	37	12	100	PCE	0	0.4	0	0	0	0
				12	100	TCE	0	0.1				
2 - 04/11/2020	AC2	Tilia sp	59	12	100	PCE	0.2	0.3	48.6	721.4	1.1	0
				12	100	TCE	3	0				

2 - 04/11/2020	AC8	Populus nigra	46	12	100	PCE	0.5	0.4	2750	0	0	0
				12	100	TCE	1	0.3				
2 - 04/11/2020	AC6	Populus alba	94	12	100	PCE	0	0.1	77.8	24	4.9	
				12	100	TCE	0	0.2				
2 - 04/11/2020	AC3	Quercus robur	43	12	100	PCE	0	0	2.3	0	0	0
				12	100	TCE	0	0				
2 - 04/11/2020	AC10B	Populus alba	87	12	100	PCE	0	0	4.3	0	0	0
				12	100	TCE	0	0				
2 - 04/11/2020	AC10	Tilia sp	73	11	100	PCE	0	0	37.9	0	0	0
				12	100	TCE	0	0				
2 - 04/11/2020	BIANCO	Ulmus sp	37	12	100	PCE	0	0.3	0	0	0	0
				12.5	100	TCE	0	0				
2 - 04/11/2020	AC8b	Aesculus hippocastanum	31	12	100	PCE	0	0	0	0	0	0
				12	100	TCE	0	0				

survey	ID pz	elevation (m a.s.l.)	depth (m b.g.l.)	filtered interval (m b.g.l.)	DWT (m b.g.l.)	gw concentration (µg/L)						
						PCE	TCE	cDCE	VC			
1- 14/10/2020	C8	86.48	11.4	3.4-11.4	8.9	36.4	0.3	0	0			
1- 14/10/2020	C6	86.16	12.6	3.6-12.6	8.48	60.9	2.8	1.4	0			
1- 14/10/2020	C10		10	6-10	5.97	216	4.8	0.8	0			
1- 14/10/2020	C9		9.4	2.4-9.4	6.82	125	3.3	0.4	0			
1- 14/10/2020	C3	85.07	11.7	2.7-11.7	7.69	187	3.1	1.3	0			
1- 14/10/2020	C2	87.76	15	3.4-11.4	10.12	2.1	0	0	0			

C site

survey	ID	species	diameter (cm)	L (cm)	H (cm)	colorimetric vials		PID (ppm)	Tree-core concentration (µg/kg)			
						compound	measure (ppm)		PCE	TCE	cDCE	VC
1- 09/09/2020	APZPARCO	Populus nigra	189	10.5	100	PCE		0.5	1.2	0	0	0
				11.5	100	TCE		0.1				
1- 09/09/2020	APZPIAVE12	Tilia sp	128	11.5	100	PCE	0	0.2	0	0	0	0
				11.5	100	TCE	0	0				
1- 09/09/2020	AMM1	Populus alba	200	12	100	PCE	0	0.5	0.5	0	0	0
				12	100	TCE	0	0.1				
1- 09/09/2020	AMM2	Aesculus Hippocastanus	160	12	100	PCE	0	0	0	0	0	0
				12	100	TCE	0	0				
2-01/12/2020	APZPARCO	Populus nigra	189	12.5	100	PCE		0.3	0	0	0	0
				12	100	TCE		0.4				
2-01/12/2020	AMM1	Populus alba	200	12.5	100	PCE		0.1	0	0	0	0
				12	100	TCE		0				
2-01/12/2020	AGOR2	Platanus sp	156	12	100	PCE		0	0	0	0	0
				12	100	TCE		0				
2-01/12/2020	AGOR1	Platanus sp	190	12	100	PCE		0	1.4	0	0	0
				12	100	TCE		0				
2-01/12/2020	AMM4	Tilia sp	198	12	100	PCE		0	0.5	0	0	0
				12	100	TCE		0				
2-01/12/2020	AMM3	Celtis sp	210	12	100	PCE		0	25.6	0	0	0
				12	100	TCE		0				

D site

survey	ID	species	diameter (cm)	L (cm)	H (cm)	colorimetric vials		PID (ppm)	Tree-core concentration (µg/kg)			
						compound	measure (ppm)		PCE	TCE	cDCE	VC
1-10/01/2020	Blank	Populus nigra	25	12	100				0	0	0	0
1-10/01/2020	A_PZ1	Populus alba	38	12	100				0	0	0	0
1-10/01/2020	A_PZ5 (source)	Platanus occidentalis	48	12	100				4300	0	0	0
1-10/01/2020	A_PZ12	Fraxinus excelsior	19	9.5	100				3.1	0	0	0
1-10/01/2020	A_PZ3	Populus alba	54	13.5	100				450	3.9	11	0
1-10/01/2020	A_PZ13	Fraxinus excelsior	27	12	100				160	0	0	0
1-10/01/2020	A_PZ10	Populus alba	45	12	100				1000	0	0	0
1-10/01/2020	A_PZ9	Populus nigra	57	12	100				236	5.1	0	0
1-10/01/2020	A_PZ7	Celtis occidentalis	32	12	100				41	0	0	0
2-30/06/2020	Blank	Populus nigra	25	12	100				0	0	0	0
				12	100							
2-30/06/2020	A_P5 (source)	Platanus occidentalis	48	12	100	PCE	0.5		4080	1.1	2.6	0
				12	100	TCE	4					
2-30/06/2020	A_PZ12	Fraxinus excelsior	19	10	100	PCE	0		6.6	0	0	0
				10	100							
2-30/06/2020	A_PZ3	Populus alba	54	13	100	PCE	0.2		1550	3	18.9	0
				13	100	TCE	1					
2-30/06/2020	A_PZ13	Fraxinus excelsior	27	12	100	PCE	0		310	0	0	0
				12	100							
2-30/06/2020	A_PZ10	Populus alba	45	12.5	100	PCE	0.5		1670	10.3	8.1	0
				12.5	100	TCE	0.3					
2-30/06/2020	A_PZ9	Populus nigra	57	12.5	100	PCE	0		280	10.4	7.9	0
				12.5	100	TCE	0					
2-30/06/2020	A_PZ7	Celtis occidentalis	32	11.5	100	PCE	0		190	0	0	0
				11.5	100							

2-30/06/2020	A_PZ7b	Populus alba (?)	51	12	100	PCE	1		2270	0	0	0
				12	100	TCE	0.8					
3-23/11/2020	Blank	Populus nigra	25	12	100				0	0	0	0
				12	100							
3-23/11/2020	A_PZ5 (source)	Platanus occidentalis	48	12	100	PCE	0.7	0.5	3700	1.4	0	0
				12	100	TCE	0.9	0.2				
3-23/11/2020	A_PZ12	Fraxinus excelsior	19	9	100	PCE	0	0.1	2.5	0	0	0
				10	100	TCE	0	0.1				
3-23/11/2020	A_PZ3	Populus alba	54	12	100	PCE	0	0.4	2260	3.5	0	0
				11	100	TCE	0	0.2				
3-23/11/2020	A_PZ13	Fraxinus excelsior	27	12	100	PCE	0	0.2	187.6	0	1.3	0
				12	100	TCE	0.5	0				
3-23/11/2020	A_PZ10	Populus alba/deltoides	45	12	100	PCE	0.2	0.1	1750	16.4	12.3	0
				12	100	TCE	0	0.1				
3-23/11/2020	A_PZ9	Populus Nigra	57	12	100	PCE	0	0.1	77.7	7.9	4.9	0
				11.5	100	TCE	0	0				
3-23/11/2020	A_PZ7	Celtis occidentalis	32	11.5	100	PCE	0	0	109.4	0	0	0
				12	100	TCE	0	0				
3-23/11/2020	A_PZ7b	Populus alba	51	12	100	PCE	0.1	0.6	1660	0	0	0
				12	100	TCE	0	0.4				

survey	ID pz	DWT (m b.g.l.)	gw concentration (µg/L)									
			PCE	TCE	cDCE	VC						
1-14/02/2020	Pz1	2.91	9.17	0.252	0	0						
1-14/02/2020	Pz2	3	0.177	0	0	0						
1-14/02/2020	Pz3	2.69	61.7	11.3	66.7	0.646						
1-14/02/2020	Pz6	3.66	4.74	0.298	0.611	0						
1-14/02/2020	Pz7	3.44	49.6	0.485	0.889	0						

1-14/02/2020	Pz9	3.45	13.1	1.11	1.01	0						
1-14/02/2020	Pz12		94.66	1.4	7.35	0						
1-14/02/2020	Pz13		264.62	4.37	63.81	2.32						
3-1/10/2020	Pz3	2.81	318	8.9	36.1	1.2						
3-1/10/2020	Pz7	3.57	85.1	0.2	0.8	0						
3-1/10/2020	Pz9	3.4	12.2	2.1	1.5	0						
3-1/10/2020	Pz12	2.9	74.3	0.9	2.4	0						
3-1/10/2020	Pz13	3	1060	6.3	23.6	3.9						
3-1/10/2020	P5	2.75	1431	49.5	84.5	4.4						
3-1/10/2020	Pz10	3.39	221	1	5.7	0						

E site

survey	ID	species	diameter (cm)	L (cm)	H (cm)	tree-core concentration (µg/kg)				gw concentration (µg/L)				colorimetric vials (ppb)		
						PCE	TCE	cDCE	VC	PCE	TCE	cDCE	VC	PCE	TCE	VC
1-30/11/2018	A_PB3	Populus alba	55	11.5	100	417	1051	238	0.5	420	4500	13938	0.56	1890	800	2250
1-30/11/2018	A_PB3b	Populus alba	76	11.5	100	2230	1918	489	0	420	4500	13938	0.56	1.48	270	750
1-30/11/2018	A_MW1	Populus nigra	35	17	100	0	0	0	0	7	1.66	0.26	0	0	0	
1-30/11/2018	A_MW2b	Populus alba	46	10	100	3	0	0	0	2.02	38	2923	750			
1-30/11/2018	A_MW2	Populus alba	58	12	100	1348	1429	686	0.5	2.02	38	2923	750	1350	1990	1500
1-30/11/2018	A_PB2	Populus alba	47	11.5	100	9023	634	75	0	420	4500	13938	0.56	1350	1860	300

1-30/11/2018	Blank	Populus nigra	42	11.5	100	1	0	2	0							
2-26/03/2019	A_MW2b	Populus alba	46	11	100	6	0.6	0	0	610	4200	7662	1120			
2-26/03/2019	A_MW2	Populus alba	58	11.5	100	120	1480	1580	0	11.2	59	2602	1410	546	546	
2-26/03/2019	A_PB2	Populus alba	47	12.5	100	16300	2230	560	2	7900	14100	10280	1320	2183	2183	546
2-26/03/2019	A_PB3	Populus alba	55	14	100	4130	4850	1340	0	16000	44000	12418	1640	1637	2728	218
2-26/03/2019	A_PB3b	Populus alba	76	11.5	100	6870	3340	1490	0	16000	44000	12418	1640	2074	764	-
2-26/03/2019	A_P1PZ1	Populus alba	51	12.5	100	9900	4550	31	0	19.1	1080	1030	171.16	2183	4911	546
2-26/03/2019	A_MW1b	Populus nigra	64	11.5	100	0	0	0	0	7.7	5.8	9.847	0.28			
2-26/03/2019	Blank	Populus alba	43	11.5	100	0.8	0	6	0							
3-30/10/2019	A_MW1blank	Populus nigra			100	0	0	0	0							
3-30/10/2019	A_MW2b	Populus alba			100	5.3	0	0	0	302	502	7867	6910			
3-30/10/2019	A_MW2	Populus alba			100	200	1060	820	0	7.4	54.3	3210	4129			
3-30/10/2019	A_MS1	Populus alba			100	720	16900	1230	0	302	502	7867	6910			

3-30/10/2019	A_PB3	Populus alba			100	3320	2800	660	0							
3-30/10/2019	A_PB3b	Populus alba			100	2760	1990	1090	0							
3-30/10/2019	A_PB2	Populus alba			100	9770	1040	61.4	0	1955	1563	15977	7105			
3-30/10/2019	A_P1PZ1b	Populus alba			100	5150	3280	262	0							
3-30/10/2019	A_MW3	Populus nigra			100	64.9	23.4	74.5	0							
3-30/10/2019	A_MW3b	Populus alba			100	1620	1350	393	0							
4-09/06/2020	A_MW1bia	Populus nigra	65	12	100	0	0	0	0							
4-09/06/2020	A_MW2b	Populus alba	46	12	100	3.6	0	0	0	1150	6100	8300	870			
4-09/06/2020	A_MW2	Populus alba	59	12	100	45.6	605.6	467.6	0	35	370	8000	1320			
4-09/06/2020	A_MS1	Populus alba	64	12	100	1380	11200	1080	0							
4-09/06/2020	A_PB3	Populus alba	56	12	100	2070	630	96.8	0	3029.9	4085.1	6856	2495.5			
4-09/06/2020	A_PB3b	Populus alba	76	12	100	1060	2900	2100	0	3029.9	4085.1	6856	2495.5			
4-09/06/2020	A_PB2	Populus alba	47	12	100	18400	1490	53.2	0	10799	5175	9987	3776			
4-09/06/2020	A_P1PZ1b	Populus alba	59	12	100											

4-09/06/2020	A_MW3	Populus nigra	45	12	100	31	23.8	45.2	0	771	149	650	26.9			
4-09/06/2020	A_MW3b	Populus alba	58	12	100											

F site

survey	ID	species	diameter (cm)	L (cm)	H (cm)	colorimetric vials		PID (ppm)	Tree-core concentration (µg/kg)						
						compound	measure (ppm)		PCE	TCE	DCE	VC	1.2DCA	CF	1.1.1-TCA
1-10/09/2020	Apz3	Populus alba	62	12	100	PCE and TCE	0		1.5	12.3	7.7	0			
1-10/09/2020	BIANCO	Populus alba	73	12	100	PCE and TCE	0		4	6.9	0.8	0			
1-10/09/2020	A_2	Populus alba	34	12	100	PCE and TCE	0		0	1.4	0	0			
1-10/09/2020	A_3	Populus alba	32	12	100	PCE and TCE	0		0	0	0	0			
1-10/09/2020	A_4	Populus alba	33	12	100	PCE and TCE	0		3.7	0	0	0			
1-10/09/2020	Apm4	Populus alba	51	12	100	PCE and TCE	0		0	0	0	0			
2-11/05/2021	Apm4	Populus alba	51	12	100	PCE	0	0	2.5	0	0	0	1	0	0
2-11/05/2021	Apm1	Populus alba	80	12	100	PCE	0	2.5	0.9	0.7	0	0	0	5.9	0
2-11/05/2021	Apz3	Populus alba	62	12	100	PCE	0	0	0	2.1	1.5	0	0	0	0
2-11/05/2021	Apm8	Populus alba	48	12	100	PCE	0	0	0	0	0	0	0	0	0
2-11/05/2021	Apz4	Populus alba	64	12	100	PCE	0	0	0	0	0	0	0	0	4.6
2-11/05/2021	Apm4	Populus alba	51	12	50	PCE	0	0	3.2	0	0	0	1.8	0.6	0
2-11/05/2021	Apm1	Populus alba	80	12	50	PCE	0	2.9	1.1	0.7	0	0	0	9.4	0

2-11/05/2021	Apz3	Populus alba	62	12	50	PCE	0	0.3	0.9	3.1	1.7	0	0	0	0
2-11/05/2021	Apm8	Populus alba	48	12	50	PCE	0	0	0	0	0	0	0	0	0
2-11/05/2021	Apz4	Populus alba	64	12	50	PCE	0	0	0	0	0	0	0	0	4.5

survey	ID pz	elevation (m a.s.l.)	DWT (m b.g.l.)	gw concentration (µg/L)										
				PCE	TCE	DCE	VC	1,2-DCA	CF	1,1,1-TCA				
2-24/02/2021	pm4	14.12	3.08		0.354	0.473	0	0.194	0	0				
2-24/02/2021	pm1	14.21	3.42		0.154	5.57	0	0.843	0	0				
2-24/02/2021	pz3	14.08	3.15		1.35	184	3.96	0.943	0.02	0				
2-24/02/2021	pm8	13.88	2.77		0	0.183	0.562	0	0.05	0				
2-24/02/2021	pz4	13.75	2.89		0	0	0	2.77	0	0.275				

G site

survey	ID	species	diameter (cm)	L (cm)	H (cm)	Tree-core concentration (µg/kg)				gw concentration (µg/L)			
						PCE	TCE	DCE	VC	PCE	TCE	cDCE	VC
0-16/07/2018	1B	Acer burgerianum	14	4	100	0	0	0	0	24	45	3500	30400
0-16/07/2018	2B	Pyrus communis	22	3	100	0	0	0	0	24	45	3500	15200
0-16/07/2018	3B	Acer saccharinum	13	4.3	100	0	0	0	0	37650	20490	167500	22900
0-16/07/2018	4B	Liriodendron tulipifera	23	4	100	0	0	0	0	100	120	1420	150
0-16/07/2018	1A	Celtis australis	10	4.5	100	0	0	0	0	0.07	0	1.44	39.6
0-16/07/2018	2A	Celtis australis	11	3.7	100	0	0	0	0	24	45	3500	40.6
0-16/07/2018	3A	Celtis australis	43	4	100	0	0	0	0	23.9	12.9	0	40.6

0-16/07/2018	4A	Acer negundo	28	7	100	0	0	0	0	1	1	0.8	26.2
0-16/07/2018	5A	Acer negundo	40	4	100	0	0	0	0	1.2	1.5	0.5	26.2
0-16/07/2018	Blank	Tilia cordata	18	9	100	0	0	0	0	0	0	0	0
	ID	Depth (m b.g.l.) and H (cm a.g.l.)	species	diameter (cm)	L (cm)	Tree-core concentration (µg/kg)				gw concentration (µg/L)			
						PCE	TCE	DCE	VC	PCE	TCE	cDCE	VC
1-22/05/2019	*A1_MS2*	100	Populus nigra	59	12	*11*	*74*	*5200*	*33*				
1-22/05/2019	*A2_MS2*	100	Populus nigra	46	12	*3*	*7*	*1160*	*0*				
1-22/05/2019	MS2	-1.05											
1-22/05/2019	MS2	-2.06								0.55	2.1	3335	1373
1-22/05/2019	MS2	-3.06								154	1129	23200	7181
1-22/05/2019	MS2	-4.07								13	121	4500	3550
1-22/05/2019	MS2	-5.03								4.4	15	1650	5900
1-22/05/2019	MS2	-6.03											
1-22/05/2019	MS2	-7.04								3.9	19	2750	13250
1-22/05/2019	MS2	-8.04								0.7	6.8	450	2350
2-11/10/2019	A1_MS2	100	Populus nigra	59	12	9	62	7220	13				
2-11/10/2019	A2_MS2	100	Populus nigra	46	12	4	21	1310	3				
2-11/10/2019	MS2	-1.05											
2-11/10/2019	MS2	-2.06											
2-11/10/2019	MS2	-3.06								23.7	284	3146	584

2-11/10/2019	MS2	-4.07								3.34	22	212	110
2-11/10/2019	MS2	-5.03								0.61	3.02	28.3	1649
3-24/06/2020	A1_MS2	100	Populus nigra	t1_MS2	12	6.5	27.9	3150	19.7				
3-24/06/2020	A2_MS2	100	Populus nigra	t2_MS2	12	1.8	1.1	540	1.6				
3-24/06/2020	MS2	-1.05											
3-24/06/2020	MS2	-2.06											
3-24/06/2020	MS2	-3.06								130	120	1650	800
3-24/06/2020	MS2	-4.07								1	4.79	96.5	164
3-24/06/2020	MS2	-5.03								0.37	1.82	52.5	2230
4-24/09/2020	A1_MS2	100	Populus nigra	59	12	8.6	36.6	5280					
4-24/09/2020	A2_MS2	100	Populus nigra	46	12	4.3	7.6	860					
4-24/09/2020	MS2	-1.05											
4-24/09/2020	MS2	-2.06											
4-24/09/2020	MS2	-3.06								9.5	175	2116	274
4-24/09/2020	MS2	-4.07								4.9	28	276	119
4-24/09/2020	MS2	-5.03								0.72	3.3	36	1529

H site

survey	ID	species	diameter (cm)	L (cm)	H (cm)	tree-core concentration (µg/kg)				gw concentration (µg/L)				colorimetric vials (ppb)	
						PCE	TCE	DCE	VC	PCE	TCE	cDCE	VC	PCE	TCE
1-20/11/2018	A_MW20	Catalpa speciosa	73	11.5	100	400	2770	49	0	380	2200	220	0.18	2760	11020
1-20/11/2018	A_PB4	Catalpa speciosa	48	11.5	100	110	1020	20	0	680	6300	730	0	11050	2760
1-20/11/2018	A_MW24B	Juglans regia	41	11.5	100	0	0	0	0	1.2	690	2600	3.3		
1-20/11/2018	A-MW21	Tilia cordata	60	11.5	100	0	0	0	0	0.06	2.7	1.1	0		
1-20/11/2018	Blank	Juglans regia	-	11.5	100	0	0	0	0						
2-14/10/2019	A_MW20	Catalpa Speciosa	73	11.5	100	1690	10950	116	0	380	2200	220	0.18		
2-14/10/2019	A_PB4	Catalpa Speciosa	48	11.5	100	77	2460	36	0	680	6300	730	0		
2-14/10/2019	A_MW24B	Juglans Regia	41	11.5	100	0	0	0	0	1.2	690	2600	3.3		
2-14/10/2019	A-MW21	Tilia Cordata	60	11.5	100	0	0	0	0	0.06	2.7	1.1	0		
2-14/10/2019	A_MW23	Populus Alba	57	11.5	100	0	0	0	0	0.26	150	4.5	0		
2-14/10/2019	A_MW36b	Carpinus Betulus	35	11.5	100	0	0	0	0	14	0.048	0	0.03		
2-14/10/2019	A_P11	Acer pseudoplanus	32	11.5	100	0	0	0	0	3.13	20.74	7.5	0		

2-14/10/2019	A_MW27b	Acer platanoides	29	11.5	100	0	0	0	0	49	1400	220	0		
2-14/10/2019	A_MW18b	Quercus robur	37	11.5	100	0	0	0	0	120	3300	530	0.4		